3/5 1/18/80

DR. 614

SAN-1604-4

SOLAR CENTRAL RECEIVER PROTOTYPE HELIOSTAT

Interim Technical Report

MASTER

April 5, 1978

Work Performed Under Contract No. EG-77-C-03-1604

Boeing Engineering & Construction
Division of The Boeing Company
Seattle, Washington

U.S. Department of Energy

Solar Energy

DISCLAIMER

Available from the National Technical Information Service, U. S. Department of Commerce, Springfield, Virginia 22161.

Price: Paper Copy $9.00
Microfiche $3.00

SAN-1604-4
Distribution Category UC-62

TECHNICAL PROGRESS REPORT

(INTERIM)

SOLAR CENTRAL RECEIVER PROTOTYPE HELIOSTAT

5 April, 1978

Prepared For

UNITED STATES

DEPARTMENT OF ENERGY

By

Boeing Engineering and Construction
a Division of The Boeing Company
Seattle, Washington

FORWORD

This document is the Interim Technical Report of work performed under DOE Contract EG-77-C-03-1604, "Solar Central Receiver Prototype Heliostats." The primary objective of this study is to develop a preliminary design of heliostats which is consistent with production quantities and rates projected for future commercial utilization of solar energy. Work under this Phase I contract was initiated on October 1, 1977, and is scheduled for completion on June 30, 1978. This report complies with the Contract Reporting Requirements Checklist.

TABLE OF CONTENTS

1.0 INTRODUCTION

Boeing Engineering and Construction (BEC) submits herein the Interim Technical Progress Report of work performed under DOE Contract EG-77-C-03-1604. This report describes the accomplishments of the first six months of this nine month Phase I study contract.

The objective of this project is to support the Solar Central Receiver Power Plant research, development and demonstration effort by:

- Establishment of a heliostat design, with associated manufacturing, assembly, installation and maintenance approaches, that, in quantity production will yield significant reductions in capital and operating costs over an assumed 30 year plant lifetime as compared with existing designs.

- Identification of needs for near term and future research and development in heliostat concept, materials, manufacture, installation, maintenance, and other areas, where successful accomplishment and application would offer significant payoffs in the further reduction of the cost of electrical energy from Solar Central Receiver Power Plants.

- Definition of a Phase II program which will:
  1) Provide detail design, fabrication and testing of one or more prototype heliostats.
  2) Provide preliminary design of processes, tooling and equipment for commercial level production and utilization of heliostats.
  3) Provide a refined estimation of heliostat life cycle cost.

The Phase I study will define a low-cost heliostat preliminary design and the conceptual design of a heliostat manufacturing/installation plan which will result in low life cycle cost when produced and installed at high rate and large quantities for commercial Solar Central Receiver Power Plants.

The study will develop the annualized life cycle cost and the performance of heliostats for a 30 year plant life, for each of three rates of continuous production and installation. The three specified rates are 25,000, 250,000, and 1,000,000 heliostats per year. The analysis of these varying production rates, requiring highly automated tooling and installation equipment concepts, will define the economies of large scale not realizable on Pilot Plant or Demonstration Plant installations.

The study is structured primarily to develop the low-cost heliostat preliminary design, manufacture, installation and maintenance concept rather than to optimize a heliostat field geometry for a specific power output. The end products of this study are:

1) A low-cost heliostat design compatible with high-rate production/installation and low maintenance cost to achieve a minimized 30 year life cycle cost.
2) A conceptual design of critical high production rate tooling.
3) A conceptual design of the required manufacturing/assembly facilities for commercial high rate production.
4) A conceptual design of the installation processes and equipment.
5) A definition of the heliostat field maintenance required and conceptual design of special maintenance equipment.
6) A definition of the thermal energy incident on the specified receiver for each of three specified heliostat locations within the field for each of four specified days.
7) Annualized life cycle cost per heliostat for an assumed 30 year plant life.
8) A program plan for the Phase II follow-on.
9) Identification of further research and development which, where successful, would offer significant payoffs in further reduction of the cost of electrical energy from Solar Central Receiver Power Plants.

The figure of merit for relative evaluation of design concepts is the Cost Performance Ratio (CPR). This study will provide a level of depth in cost/performance estimates never before achieved for definition of large commercial utilization of solar electric power. A detailed justification will be provided to verify the soundness of design and completeness of realistic cost/performance estimates. To this end, this Interim Technical Progress Report describes the design/performance/cost trades conducted to date.

This study is based upon the heliostat concept demonstrated under ERDA Contract EY-76-C-03-1111.

Figure 1.0-1 is a picture of the research heliostats installed at the Boardman, Oregon test facility. Figure 1.0-2 is the preliminary baseline design with which this study was entered. The selected configuration developed by this study (see Figure 1.0-3) is similar but incorporates detailed feature changes as a result of the optimization process to minimize life cycle cost. Two principal changes as a result of study to date are:

1) Foundation - the foundation and basewall design was recognized as a high cost item of the heliostat design. The current configuration utilizes augered piling which offers the least material and a high installation rate with minimum labor. The base ring with stanchions and the one-piece formed dish offer high rate, minimum labor and automated production, with the features of low leak rate, ability to factory or field assemble the complete heliostat, and rapid installation on site.

2) Enclosure - the current configuration of a one-piece thermoformed enclosure has been demonstrated by thermoforming small scale domes with Boeing funding. Development effort has been proposed for full-scale enclosures. The economic payoff is significant by elimination of gore cutting, seaming and assembly.

The baseline size (9.69 m diameter enclosure) remains unchanged as a result of a size/cost trade study. All trade studies and detail design optimizations are described in Sections 2.0 and 3.0 of this report.

The study has been conducted as planned and shown by the Program Logic Flow Network (Figure 1.0-4) and the Master Schedule (Figure 1.0-5). All effort is now within schedule. Material screening test were completed approximately six weeks behind schedule because of delays in receipt of candidate materials from plastic film manufacturers. This delay did not significantly impact key mile-

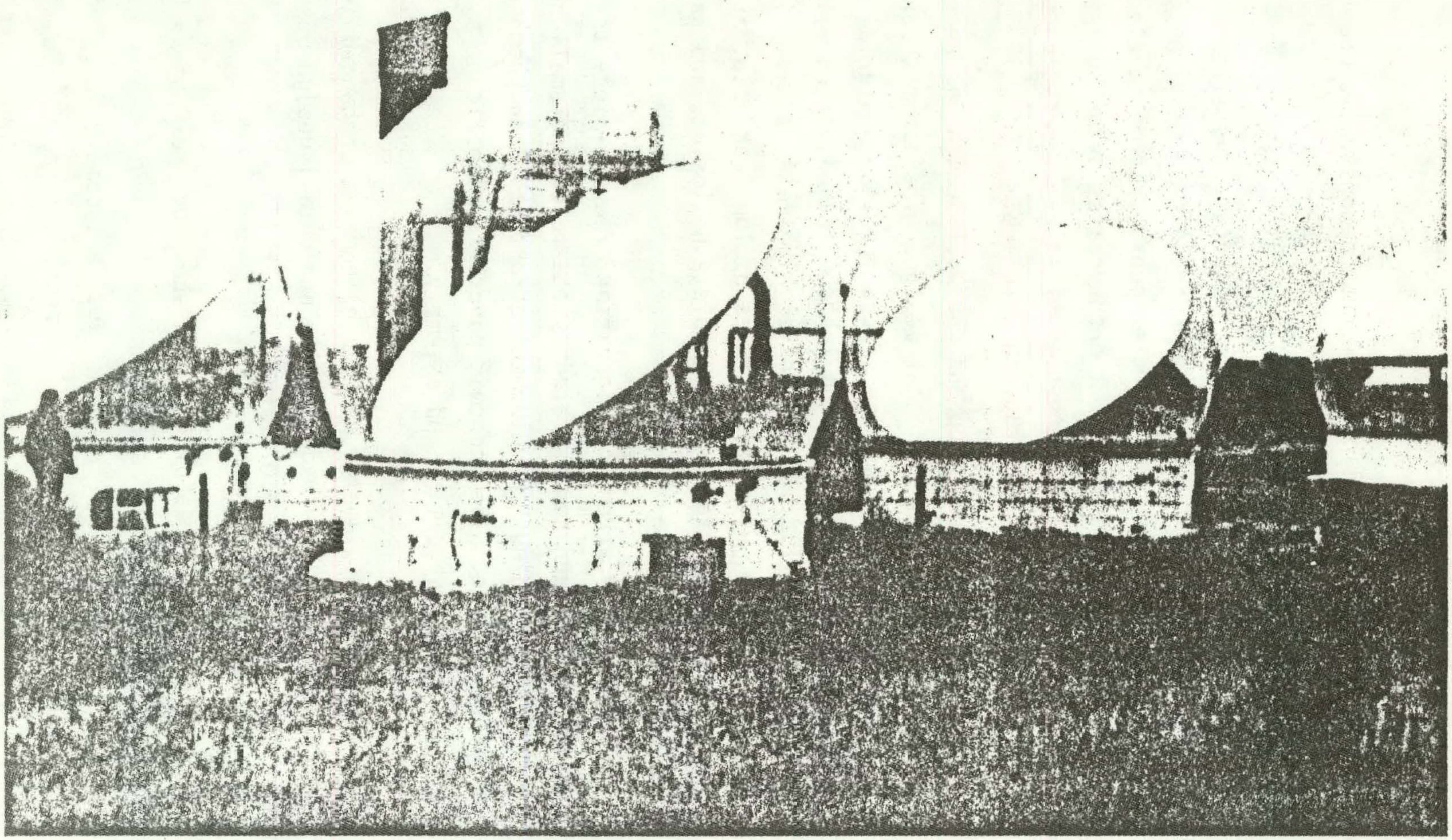

Figure 1.0-1. Boardman Photo

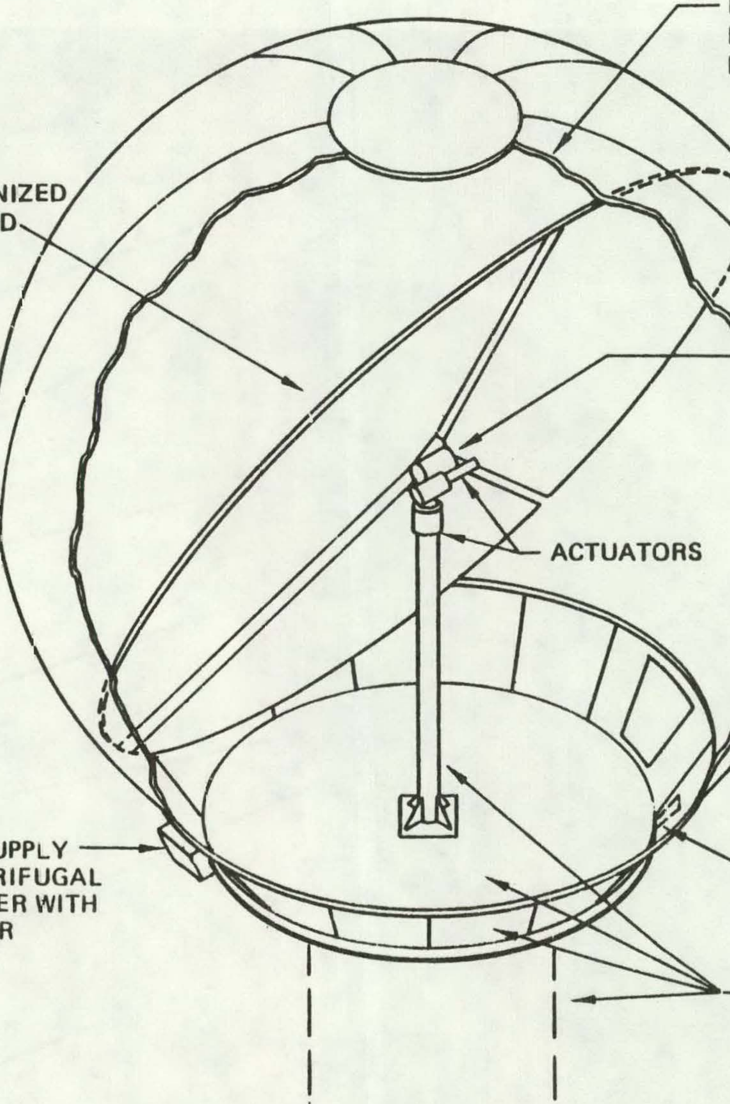

Figure 1.0-2. Preliminary Baseline of the Prototype Heliostat

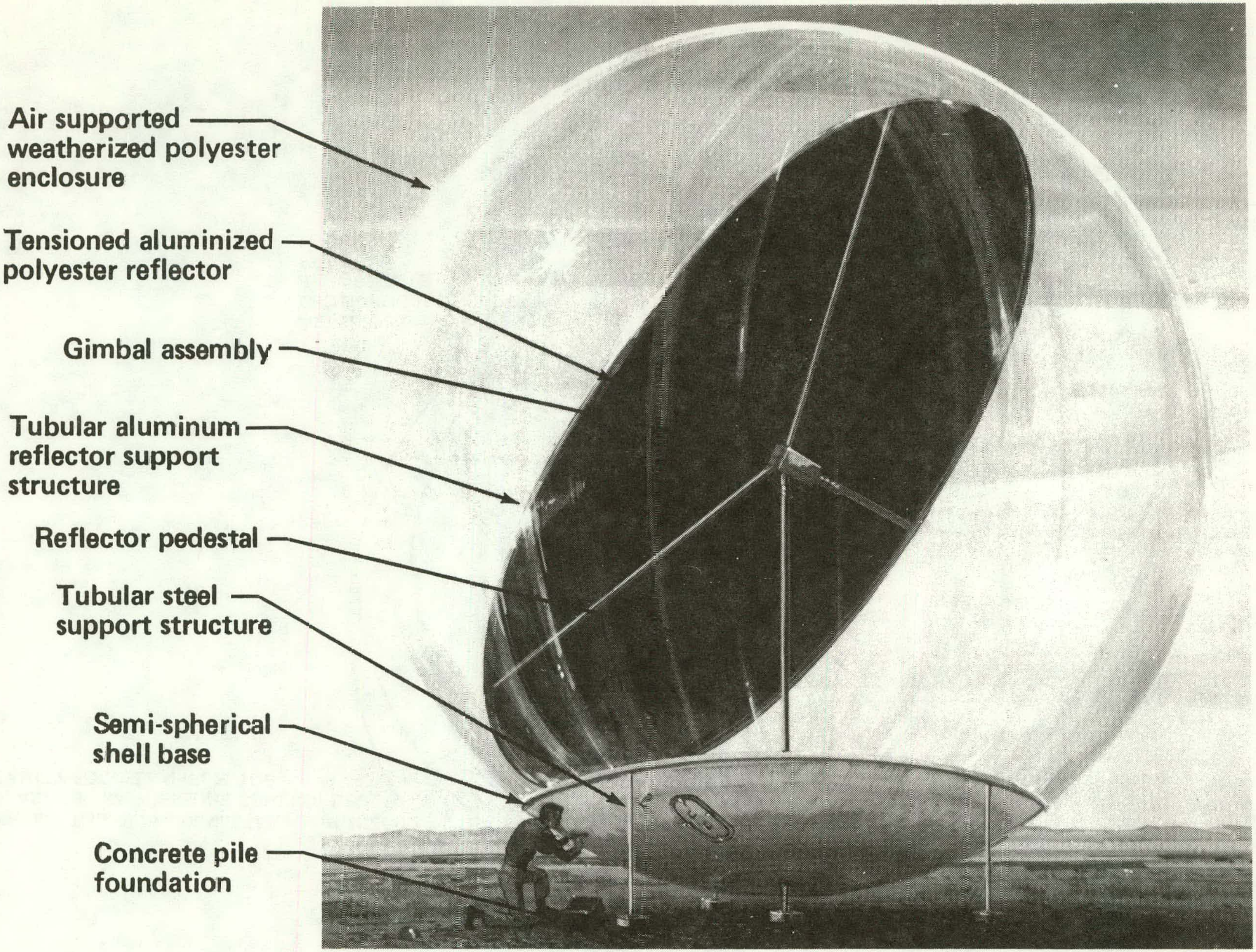

Figure 1.0-3. Selected Configuration

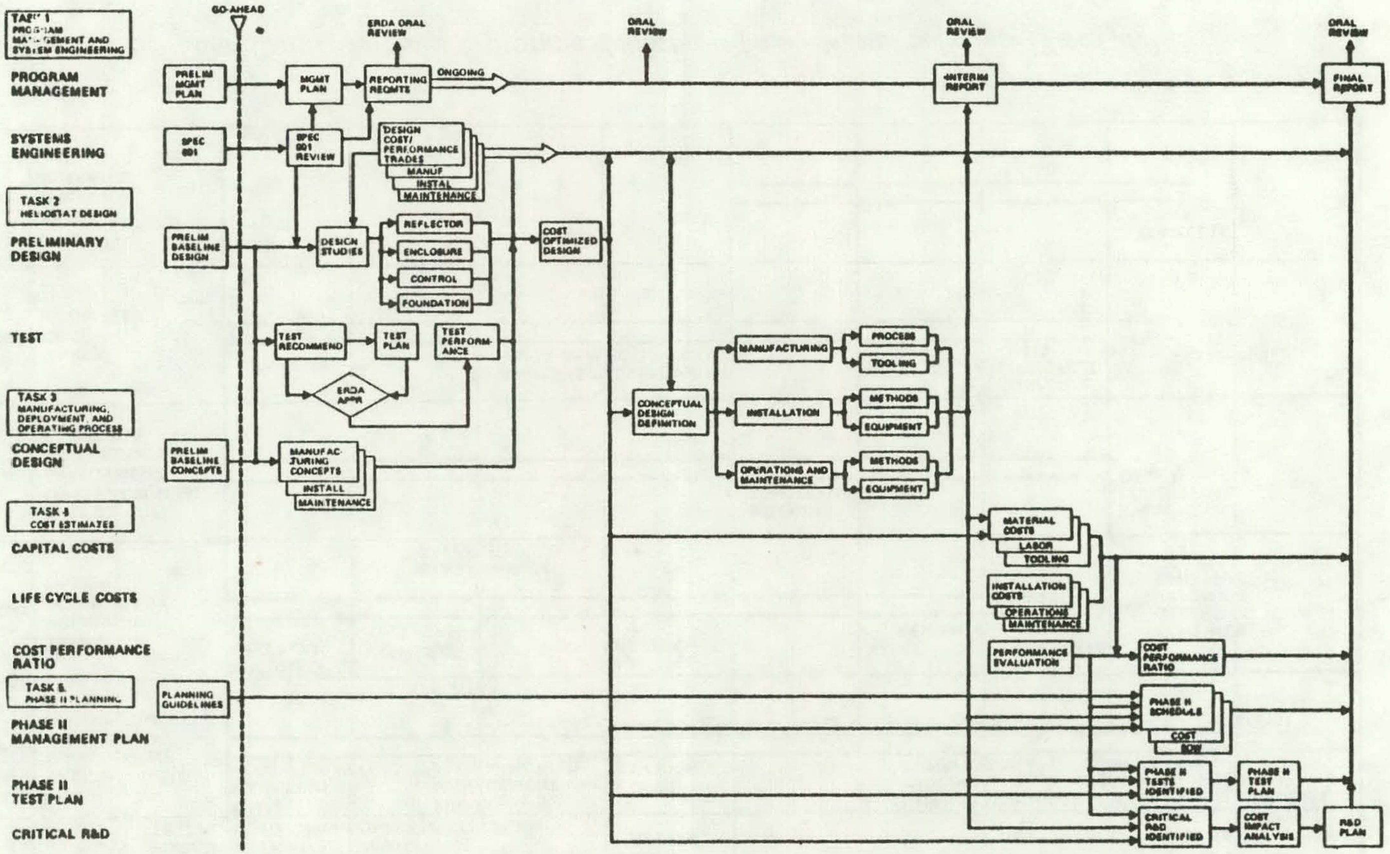

Figure 1.0-4. Program Logic Flow Network

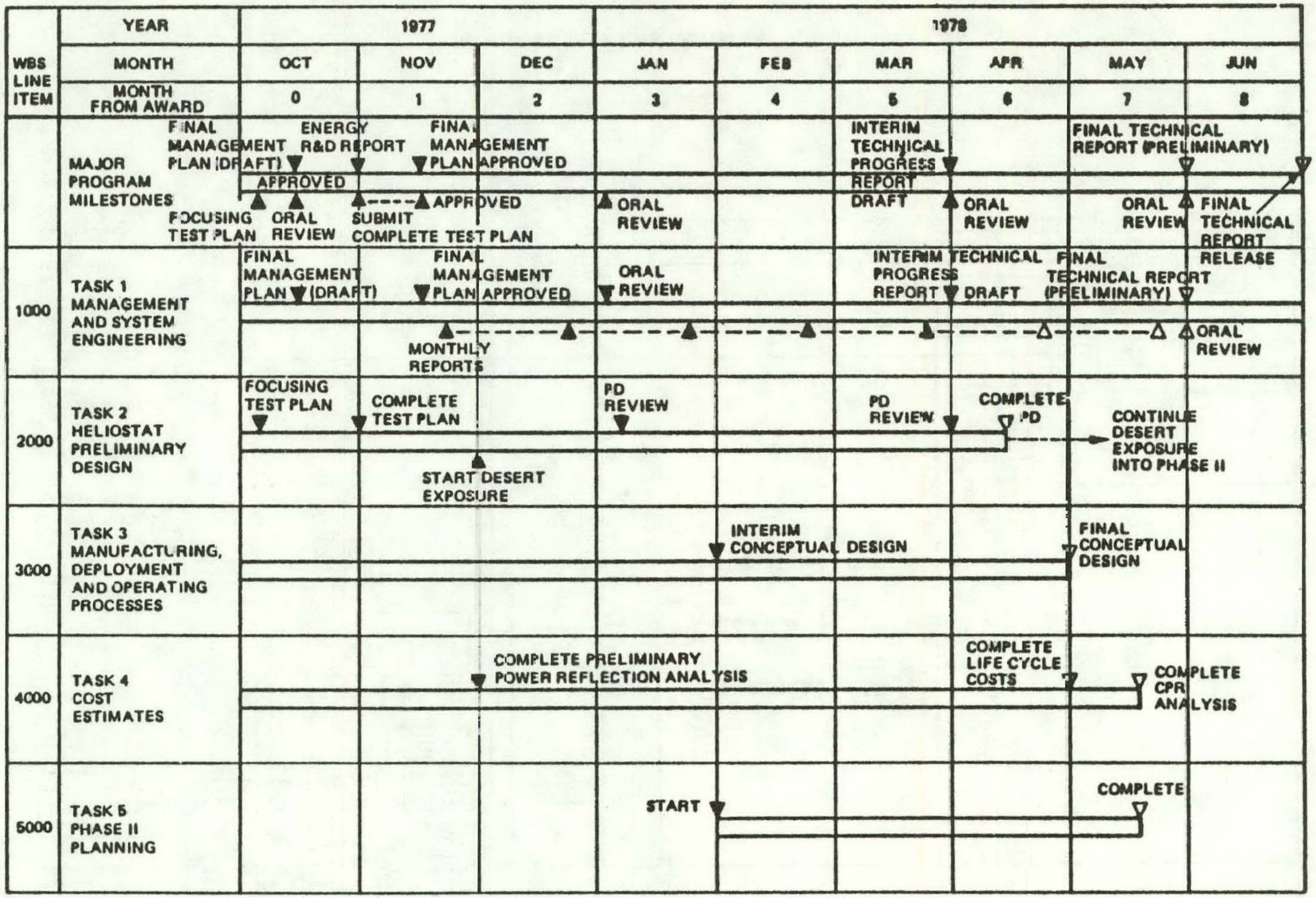

Figure 1.0-5. Solar Central Receiver Prototype Heliostat—Phase I Master Schedule (Tier I and II)

stone decisions. Excellent progress has been made in heliostat design optimization, manufacturing plans, installation concepts, and maintenance procedures. These data will provide a firm base for the primary remaining tasks of cost/performance definition, Phase II program planning and the identification of further critical R&D.

Section 5.0 is a summary plan providing scope and schedule for the Phase II effort. The plan including fabrication and test of full sized heliostats at the STTF will achieve maximum benefit in furtherance of solar heliostat development.

2.0 HELIOSTAT PRELIMINARY DESIGN

2.1 KEY DESIGN REQUIREMENTS/SPECIFICATIONS

The design requirements of Specification 001 together with the design response indicating design compliance is summarized in Table 2.1-1.

TABLE 2.1-1 SPECIFICATION COMPLIANCE

SPEC. PARA.	SUBJECT	REQUIREMENT SUMMARY	DESIGN RESPONSE
3.1.1.1	Availability	Maximize for daylight hours	High reliability - off operating hours maintenance
3.1.1.2	Interchange-ability	Major components shall be interchangeable	All components interchangeable throughout field.
3.1.1.3	Electrical Transients	Equipment shall not be adversely affected by specified transients. Normal operating - voltage ± 10% - frequency ± 0.1% Startup or shutdown - voltage +10% -25% with recovery within 5 cycles at 60 Hz Emergency - momentary total loss of power	Power regulation to accept plant power supply transients.
		Lightning - Effective protection on a cost-risk basis.	Lightning protection prevents damage propogating to adjacent heliostats.
3.1.2.1.2	Wind - Operational limit	Max operation wind speed consistent with min. cost of electricity production.	Operate to 90 mph (40 m/s)
3.1.2.1.3	Wind - Stowage initiation	Stow wind speed selected on tradeoff between loss of direct beam insolation and heliostat cost.	Reflector protected by enclosure. Stowage not required. Enclosure survives 40 m/s wind.
3.1.2.1.4	Wind Rise Rate	Rise rate = .01 m/s^2. Withstand 25 m/s wind at any reflector orientation.	Reflector protected by enclosure. Withstands 40 m/s wind.
3.1.2.1.5	Survival Wind	Survive 40 m/s (90 mph) without damage.	Enclosure survives 90 mph and enclosure deflection does not interfere with mirror at any orientation. 15% margin yield at 132°F.
3.1.2.1.6	Wind Profile	Varies exponentially with height to 0.15 power. Reference height is 10 m.	Profile used for enclosure load/deflection analysis. Wind tunnel verification of loads.

SPEC. PARA.	SUBJECT	REQUIREMENT SUMMARY	DESIGN RESPONSE
3.1.2.1.7	Dust Devils	Dust devils with wind speed to 17 m/s survived without damage	No apparent structural or optical damage. (Criteria not definitive)
3.1.2.2	Temperature	Operate in ambient range from - 30°C to 50°C	No problems at 50°C. Must evaluate possible cost penalty at -30°C.
3.1.2.3	Earthquake	Survive seismic zone 3. Realignment allowed.	Design for g loads.
3.1.2.4	Snow Environment	Survive 250 pascals (5 lb/sq. ft.)	Enclosure internal pressure is 14 lb/sq. ft. Orient reflector if deflections interfere.
3.1.2.5	Rain Environment	Average annual = 30 inches Max. 24 hour = 3 inches	No detrimental effects.
3.1.2.6	Ice Environment	Survive deposited ice layer 2 inches thick	Approximately 55% margin if ice deposited in cosine distribution over upper hemisphere of enclosure. (No ice on reflector)

SPEC. PARA.	SUBJECT	REQUIREMENTS SUMMARY	DESIGN RESPONSE
3.1.2.7	Hail	25 mm (lin.) dia. at 23 m/s (75 fps) Specific gravity = 0.9	Hailstone tests verify no structural failure. Negligible optical degradation over 15 yr. period.
3.12.B	Sandstorm	Survive tests per Mil. Std. 810B Method 510	Critical components protected by enclosure. Possible degradation of enclosure optical properties should be quantitatively assessed.
3.1.2.9	Lightning	Protection optimized on cost-risk basis	Lightning protection prevents damage from propogating to adjacent heliostats or to field controllers.
3.2	Performance	Optimize to achieve highest level of cost effectiveness,	Design with reflector size, contour accuracy, pointing accuracy, focusing, and material properties to achieve cost effectiveness.
3.2.1	Operational Periods	Performance rated for specified hours of four specified days.	Calculated power intercept at the receiver will be the integrated average for each specified period based on 950 w/m^2 insolation times all efficiency factors.

SPEC. PARA.	SUBJECT	REQUIREMENTS SUMMARY	DESIGN RESPONSE
3.2.2	Targets	Performance assessment for one of 3 specified target options	Design for surface receiver specified by para. 3.2.2.1
3.2.2.1	Target	Vertical cylinder 17m diameter by 25 m high. Center elevation 250 m above ground level.	Used for heliostat design and performance analysis.
3.2.3.1	Field Positions	Performance satisfied from 3 field positions: Position — N of Tower — S of Tower A — 1200 m — 430 m B — 800 m — 860 m C — -400 m — 430 m	Used for heliostat design and performance analysis.
3.2.4	Reflectivity	Maximum consistent with cost-optimized production of power.	To be satisfied by optimization studies of enclosure and reflector.
3.2.5	Reflective Area	Area selected consistent with cost-optimized production of power.	To be cost optimized within constraints of enclosure material strength

SPEC. PARA.	SUBJECT	REQUIREMENTS SUMMARY	DESIGN RESPONSE
3.3	Drive & Control	See following requirements:	
3.3.1	General	See following requirements:	
3.3.1.1	Availability	Fail-safe operation during power outage and electrical transients	Redundant power and signal systems with power regulation and protection for electrical transients.
3.3.1.2	Power Input	TBD	Minimize power usage during operational and non-operational periods.
3.3.1.3	Limit Controls	Provide as necessary to protect equipment or personnel.	Electro-mechanical travel limit switches.
3.3.2	Normal Operations	See following requirements:	
3.3.2.1	Tracking	Control tracking accuracy	Open loop control system with pointing accuracy cost optimized
3.3.2.2	Acquisition (beam-on)	Beam-on of groups of heliostats (less than 10% of field) on command from central control within 180 seconds	4 field controllers with 4 data busses each. 6.25% of field.

SPEC. PARA.	SUBJECT	REQUIREMENTS SUMMARY	DESIGN RESPONSE
3.3.2.3	Synthetic Tracking	Continuous tracking during cloudy periods	Software controlled tracking.
3.3.2.4	Offset Pointing	Capability to orient portions of array towards different locations on target to control flux levels and distribution	Incorporated in software.
3.3.2.5	Normal Shutdown	Orient groups of heliostats to safe stowage on command from central control within TBD minutes.	Programmed in software TBD will be established based on system considerations.
3.3.2.6a	Receiver/Stowage -Traverse	Reflected energy shall not impinge on tower during startup and shutdown.	Programmed to go to standby orientation prior to start-up or shutdown.
3.3.2.6b		All beams E of tower move one direction and all beams W of tower move in opposite direction when moved on or off receiver.	See 3.3.2.6c Can be accommodated by software if requirement is valid. Requires further study.
3.3.2.6c		Beams shall move in a controlled manner to avoid unsafe flux concentrations in the airspace.	Software controlled such that beams move first to standby, forming a toroid about the receiver. Then groups of beams moved in a controlled manner to stowage.
3.3.2.6d		Provide safe stowage to minimize environmental degradation.	All beams parallel and contained within field.

SPEC. PARA.	SUBJECT	REQUIREMENTS SUMMARY	DESIGN RESPONSE
3.3.3	Maintenance	Control features provided for maintenance purposes.	See subparagraphs
3.3.3.1	Manual Control	Provide at heliostat for maintenance and checkout purposes.	Manual control capability at each heliostat locks out central control and provides AZ and EL step pulses.
3.3.3.2	Calibration and Checkout	Provide orientation accuracy check from Central Control	Software programmed such that individual heliostat can be directed to alignment laser with position feed back to central control.
3.3.4	Abnormal Operations	Procedures shall be provided for abnormal conditions in any individual heliostat.	See subparagraphs
3.3.4.1	Failure Indication	Indication provided by local control to plant central control	Failure to correctly respond to programmed commands is communicated to central control. Individual heliostat controller automatically orients heliostat to stow. Other failure modes such as change in pressure is communicated to central control.

SPEC. PARA.	SUBJECT	REQUIREMENTS SUMMARY	DESIGN RESPONSE
3.3.4.2	Emergency Shutdown	On command from central control, individual heliostat radiation on receiver reduced to 3% of initial value within TBD seconds.	Central control can command individual heliostat to standby at slew rate 0.135 deg. per second.
3.4	Foundation	Maintain heliostat performance while operating in environments.	Foundation resists overturn from wind loads, and protects reflector components from environment.
3.4.1	Site Characteristics	Angle of internal friction is 30° $E = \beta (h + z)$ β = 18.1 MPa/m	Foundation design parameters
3.5	Physical Characteristics	See following requirements	
3.5a		Heliostat configuration and field spacing must permit access by service vehicles, wiring, and maintenance personnel.	Heliostat design and field spacing permits access. Airlock provides maintenance access to inside of enclosure.

SPEC. PARA.	SUBJECT	REQUIREMENTS SUMMARY	DESIGN RESPONSE
3.5.b		Provide for safe stow positions during maintenance, storms, or emergency shutdown.	Individual heliostats, groups or total field commanded to stow either from central control or from manual controllers at heliostat or field controllers.
3.5 c		Subsystems and components easily removed to facilitate maintenance.	All internal components can be easily removed thru the airlock except reflector and pedestal. Enclosure reflector and pedestal easily removed with mobile maintenance vehicle.
3.5d		Lifetime = 30 years with maintenance and replacement where necessary.	Select components for lifetime consistent with minimizing cost of electric power production.
3.6	Reliability	Achieve high reliability	Use high reliability components consistent with minimizing cost. Safety is prime consideration. Evaluate FMEA

SPEC. PARA.	SUBJECT	REQUIREMENTS SUMMARY	DESIGN RESPONSE
3.7	Maintenance		
3.7a		Provide easy cleaning without excessive degradation	Eliminate requirement to clean reflector and inside of enclosure, except when domes are replaced. Provide capability to clean (water rinse) reflector. Mobile maintenance vehicle for cleaning exterior of enclosure using water, air, solvents as necessary.
3.7b		Components subject to wear or damage, shall be capable of being inspected, serviced or replaced.	30 year life with minimum maintenance is a design goal. Requirements for periodic inspection, repair or replacement will be evaluated. Spares requirements will be defined.
3.7c		Components serviceable by personnel of normal skills. Special equipment for servicing shall be identified.	Special design consideration to simplify electronics trouble shooting and repair. Simple patching procedure to repair damage to enclosures. Identify field repair versus depot repair.

SPEC. PARA.	SUBJECT	REQUIREMENTS SUMMARY	DESIGN RESPONSE
3.8	Materials, Processes and Parts	Use standard materials and processes.	Utilize common materials, known processes and off-the-shelf components where cost effective. Be innovative where appropriate. At 30 years of continuous high rate production, a new material or process becomes standard.
3.9	Electrical Transients	See 3.1.1.3 and 3.1.2.9	
3.10	Workmanship	Use best modern practices consistent with cost and performance requirements.	Component manufacturing to be highly automated. Maximize factory assembly. Installation by crews trained for single repetitive functions.
3.11	Interchange-ability	Permit interchangeability	Design with tolerances such that all parts are interchangeable for every heliostat. Only software is unique per heliostat.

SPEC. PARA.	SUBJECT	REQUIREMENTS SUMMARY	DESIGN RESPONSE
3.12	Safety		See paragraphs 3.3, 3.5 and 3.6
a			
b			
c			
d			
e			
f			
3.13	Documentation	For planning purposes only during Phase I study	
4.0	Quality Assurance Provisions	For planning purposes only during Phase I study	

2.2 INTERFACE REQUIREMENTS

Heliostat component/component interface requirements are defined in pertinent sections of this document. The interface definitions below are those between the heliostat and other related elements of the Solar Central Receiver Power Plant.

Interface	Requirement Definition
Receiver	. Cylindrical surface receiver as specified in paragraph 3.2.2.1 of specification 001
Control System	
Data Bus	. Transmission Line Serial Digital Data Bi-Phase Manchester Code 10V P to P (optional)
Data Transfer	. Information to Heliostat Controller . 49 BIT word . Update Rate - 5 sec . Heliostat address or master address . Heliostat mode . Shutdown . Standby . Track . Align . Data request . Current position . Time . Alignment position . Heliostat status . Power status . Data identifier . Position commands . Reference time . Cycle time . Position data: Align, shutdown . Power modes: On/Off . Data variable format-defined by data identifier field . Other functions . Time sync (single or master) . Motor power (single or master) . Idle . Data load . Manual control . Error in received message

- <u>Information From Heliostat Controller</u>
    - 49 BIT word
    - Update Rate - 5 sec
    - Heliostat Controller Address
    - Heliostat Mode Response
        - Shutdown
        - Standby
        - Track
        - Align
    - Data identifier
        - Current position
        - Time
        - Alignment positions
        - Power status
        - Heliostat detailed status
    - Data variable format-defined by data identifier field
    - Received parity error
    - Other functions
        - Time sync
        - Motor power
        - Idle
        - Data load
        - Manual control
        - Error in received message

Field Cabling	. Power & signal wiring and associated equipment throughout the field, stubbed to J Box at each heliostat.
Alignment System	. Provision for attachment of hardware to tower.
	. 230/115V single phase power at tower interface point.
	. Data transmission cabling from tower interface to central control.
	. Surveyed monuments in field (two min.).
Site	. Rough graded and compacted
	. Vegetation removed.
	. Survey for heliostat locations
	. 14 foot chain link fence at perimeter of plant with 50% porosity.
	. Site security
	. Area and layout TBD

Plant Utility Power	. Control system - each heliostat operation 34 watts 115VAC 60 ~ shutdown 4.5 watts 115VAC 60 ~ . Blower TBD 115VAC 60 ~
Plant Utility Water	. TBD gallons per day with water reclamation facility to support cleaning maintenance.
Manufacture/Assembly Facility	. TBD acres adjacent to power "Park"
Transportation Facilities	. Access roads from public highway to manufacturing/assembly facility. . Rail spur to manufacture/assembly. . Inter-plant roads within the power "park" . TBD acres for parking.
Other Utilities	. Water and sewer to support TBD man factory and field work force. . Location for field controllers in or near central control facility. . Location for emergency generator and associated equipment. . Provision for spares and support equipment storage. . Maintenance equipment repair shop. . Office space for operations/maintenance personnel.

2.3 PROTOTYPE HELIOSTAT CONFIGURATION

The heliostat configuration (see Figure 2.3-1) is designed to achieve the objective of low-cost when produced in the large quantities and at the high production rates for commercial utilization of solar electric power.

The design satisfies all the requirements of Specification 001. The primary features of the design which provide cost/performance effectiveness are:

- Enclosure - An air-supported spherical enclosure thermoformed from weatherized oriented polyester film protects the reflector assembly from the environment. The polyester film is selected over the fluorocarbon materials on the basis of least material cost while providing high specular transmittance. Thermoforming of the one-piece spherical enclosure is compatible with high rate production and eliminates manufacturing costs associated with cutting and seaming of gores.

- Reflector - The reflector is a 2 mil Mylar membrane biaxially tensioned on a lightweight frame support structure. The aluminized membrane is weatherized for U/V protection, providing long life and a high specular reflectance.

- Base/Foundation - The base foundation provides support for the reflector and the enclosure. It consists of the following components:

  Pedestal - The pedestal is a standard pipe section selected to provide torsional and bending stiffness to react gravity and inertia loads of the gimbal/actuator driven reflector. The pedestal is mounted on a reinforced concrete piling, providing isolation from the remaining heliostat support structure.

  Base - The base structure provides the interface (retention) to the enclosure and transmits wind loadings from the enclosure to the ground. A standard pipe ring designed by stiffness to limit deflections transmits lift and drag wind loads through three pipe stanchions to three reinforced concrete pilings. A steel dish welded to the ring completes the pressurized spherical enclosure. Press-forming of the dish is compatible with low-cost

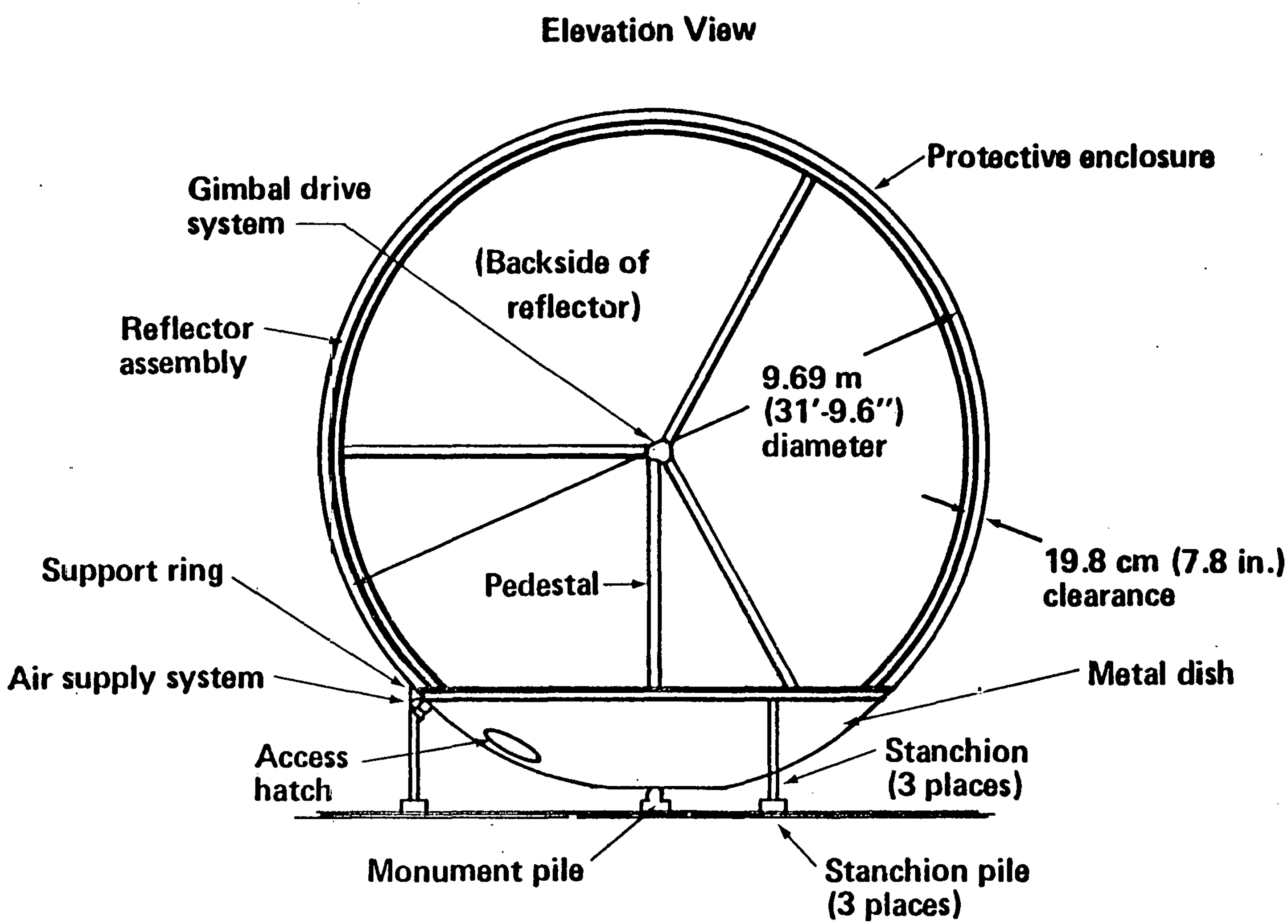

Figure 2.3-1 Heliostat Configuration

high-rate production and assembly. Study, discussed in Section 2.3.3, has shown the reinforced piling concept to be the least materials and least installation cost for high rate automated installation techniques.

Air Supply System - The blower/filter system is designed to maintain the internal pressure at 0.5 cm Hg (0.1 psig) above ambient pressure. The low leak rate of the heliostat, estimated at 0.006 m^3/min (0.2 CFM), results in a low flow blower requiring a minimum of power.

- Control System - An open-loop computer based control system provides tracking and mode control inputs to stepper motors driving the reflector through the two axis (azimuth and elevation) gimbal. The heliostat controller electronics and the reflector drive system are located within the protective enclosure. Components are selected to maximize MTBF to provide for minimum maintenance.

- Special Design Features - Some of the more important features of the design are:

  1) The protective enclosure allows the concept of the lightweight membrane reflector. This compounds to a lightweight gimbal, pedestal, and piling plus small drive motors with low power requirements. The base design concept also optimizes for least use of materials. A weight breakdown is provided in Table 2.3-1.

  2) The tightly sealed low air flow with air filtering negates dust degradation of the reflector. Under normal conditions, the reflector will not be cleaned until replacement of the enclosure. Enclosure replacement is provided during the period from 15 to 24 years.

  3) The heliostat is operable throughout all environmentally specified maximum conditions providing 100 percent availability except for planned and unplanned maintenance.

4) The design of all components have been optimized on the basis of life cycle cost. Special consideration has been given to achieving a design compatible with low-cost high-rate production and installation with minimum maintenance cost. The design is also compatible with complete assembly in the clean factory environment. It is then transported to the site and installed on the pre-positioned piling with a minimum of field labor.

TABLE 2.3-1

WEIGHT BREAKDOWN

	LB	LB/M^2
Base Structure	1655	25.2
Pedestal	270	4.1
Gimbal & Drives	65	1.0
Reflector	255	3.9
Enclosure	50	0.8
Electronics	30	0.5
Pressurization	15	0.2
subtotal	2340	35.6
Concrete and Embeds	4400	67.0
TOTAL	6740	102.6

2.3.1 Optical Performance Analysis

2.3.1.1 Ground rules and Methodology

The optical performance was calculated for each of the three specified heliostats for each of the four specified periods. The specified heliostats and the specified periods are as provided in Table 2.3.1.1-1. The performance is calculated using the Boeing HACSM optical ray trace program. The optical performance is defined as the thermal energy received within the target geometry as specified in Table 2.3.1.1-2. The average daily direct insolation was 950 watts per meter squared. The reflectivity and the enclosure transmissivity as a function of the incidence angle is as shown in Figures 2.3.1.1-1 and 2.3.1.1-2.

A further performance parameter affecting image size at the receiver is the diffusion effects due to both the mirror surface quality and the enclosure material. These scattering affects are input to the HACSM computer program as a one sigma conical angle spreading of each ray. The amount of this spreading is difficult to predict. Therefore, image power density maps, from actual tests at Livermore, California, were correlated with the HACSM program data to determine the proper scattering angle input to the computer program. The results of this correlation are shown in Figure 2.3.1.1-3 for a vacuum focused reflector. The scattering angle in the range of 0.05 to 0.10 degrees correlates with the actual test data. This correlation is for a 4 mil Tedlar enclosure. The particular batch of Tedlar used in the Livermore enclosure exhibited a relatively high scattering up to a cone angle of 0.6 degrees, as shown in Figure 2.3.1.1-4. Other candidate materials such as Melinex "O" and Celanar 4000 exhibit very little scattering above a cone angle of about 0.1 degrees as illustrated in the figure. It can therefore be assumed that a polyester material would cause less scattering. The initial optical performance analysis assumed a scattering cone angle effect of 0.12 degrees, however, 0.05 degrees will be used in a final analysis. Figure 2.3.1.1-5 illustrates this effect of scattering cone angle on capture efficiency.

TABLE 2.3.1.1-1

SPECIFIED HELIOSTATS AND PERFORMANCE PERIODS

HELIOSTAT	LOCATION		SLANT RANGE
	NORTH	EAST	
A	1200 M	430 M	1300 M
B	800 M	860 M	1200 M
C	-400 M	430 M	640 M

PERIOD	DAY	HOURS
Spring Equinox	March 21	8:00 A.M to 4:00 P.M.
Summer Solstice	June 22	6:00 A.M. to 6:00 P.M.
Fall Equinox	September 23	8:00 A.M. to 4:00 P.M.
Winter Solstice	December 22	9:00 A.M. to 3:00 P.M.

TABLE 2.3.1.1-2

SPECIFIED TARGET RECEIVER

Type	Cylindrical Surface
Diameter	17 meter
Height	25 meter
Elevation	250 meter (to center)

Figure 2.3.1.1-1. Mirror Optical Characteristics

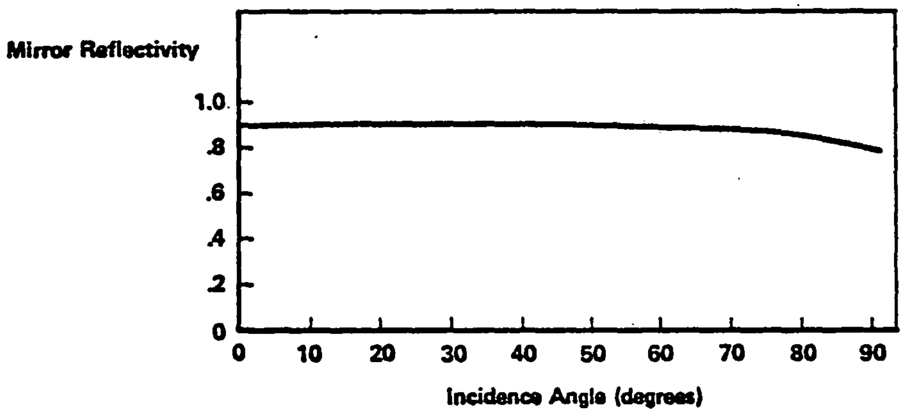

Figure 2.3.1.1-2. Enclosure Optical Characteristics

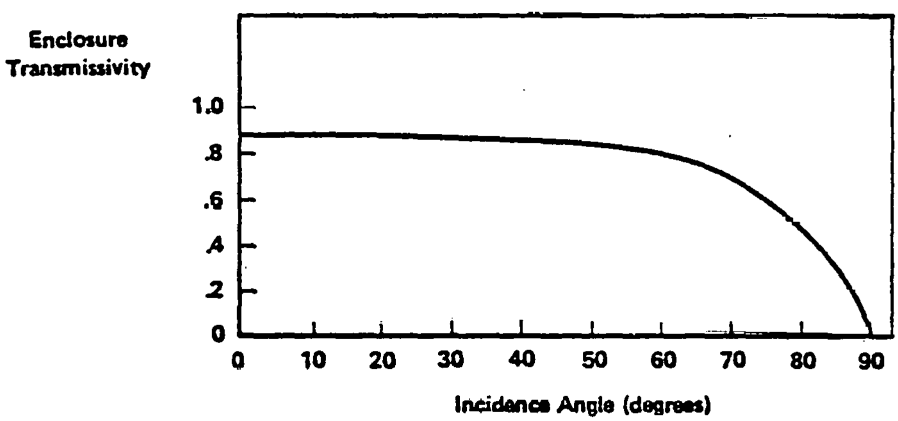

Figure 2.3.1.1.-3. Beam Scattering Correlation with Image Scan Measurement

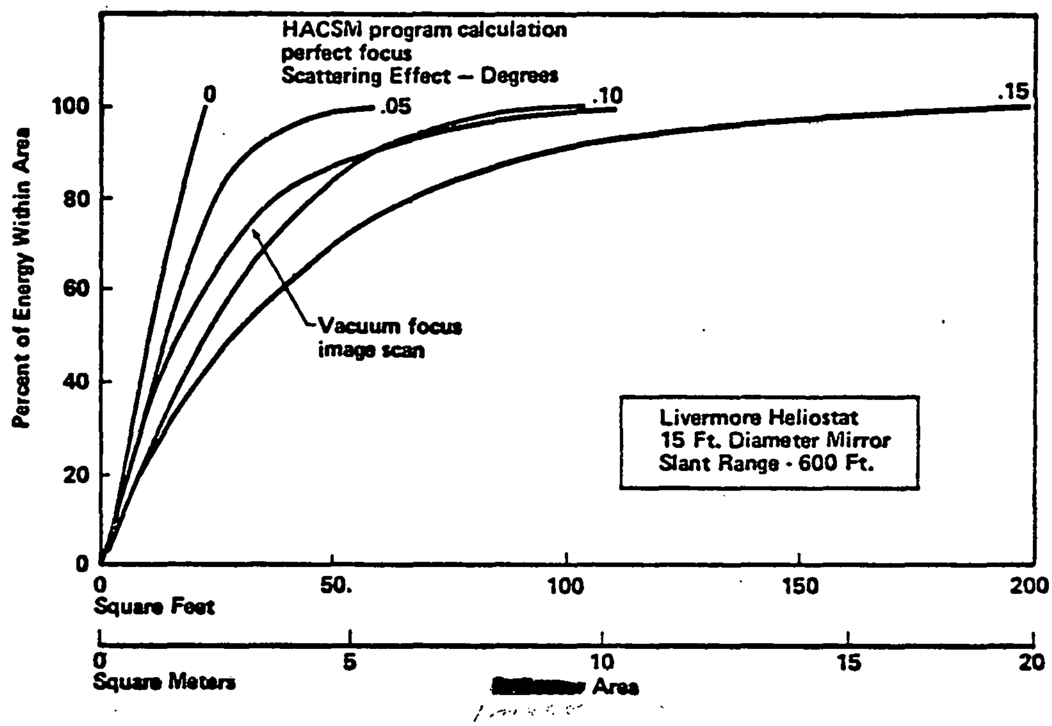

Figure 2.3.1.1.-4. Enclosure Optical Transmittance

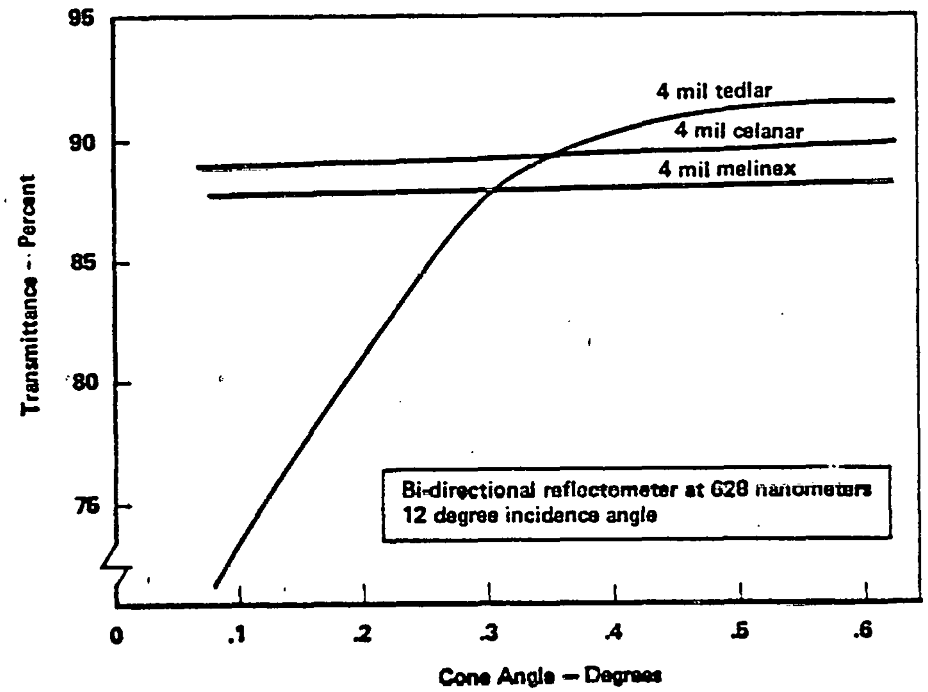

Figure 2.3.1.1.-5. Effect of Dome Material Scattering on Capture Efficiency

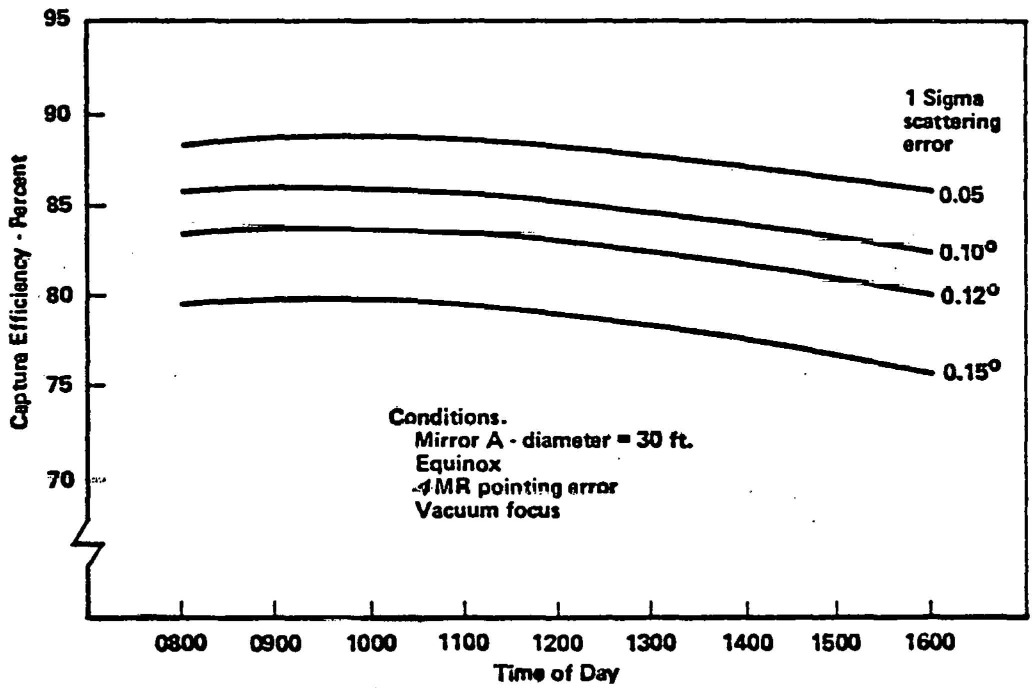

2.3.1.2 Performance Optimization

The optical performance analysis is combined with design and cost analysis in developing the selected configuration. The following discusses the primary trade studies as depicted in Figure 2.3.1.2-1. As shown, the matrix of focusing concepts was combined with each beam pointing accuracy for a range of reflector sizes. This matrix of parameter variations was evaluated using the HACSM optical ray trace program.

The first issue in the trades is to evaluate and select the focusing concept for the recommended configuration. The membrane reflector has an inherent ability to provide some focusing due to gravity sag of the membrane. Control of the sag (gravity focusing) can be achieved by the membrane tension applied during manufacture. For this study, the best calculated tension is established for the far field heliostat and not varied for heliostats in a near field zone. The membrane reflector can also be focused by mechanically pulling the center of the mirror or by applying a reflector back surface membrane and pulling a slight vacuum (vacuum focus). This concept is further enhanced by controlling the vacuum through the electronics and software to provide best focus for each mirror at all times. This is termed active-smart focus. A schematic of vacuum focusing and control is shown in Figure 2.3.1.2-2.

The focusing capabilities have been demonstrated with the heliostat installed at the Sandia Laboratories, Livermore, California. A schematic of the test setup is shown in Figure 2.3.1.2-3. Figure 2.3.1.2-4 shows the heliostat directing energy to the target board. Figure 2.3.1.2-5 shows that vacuum focusing significantly reduces the image size compared to the partial gravity focused image.* These images were mapped and the concentration of energy due to vacuum focusing is illustrated in Figure 2.3.1.2-6. It should be noted that the photographic film sensitivity does not provide an adequate measure of the image size at the target. The mapping shows that the image intensity ratio of about 0.13 is the background level of diffuse light at the target. The visual image as shown by the photograph is much less area than the area of the mapped image. The low intensity energy outside the visual image accounts for approximately 20 percent of the total energy.

* The Livermore reflector was fabricated with 1,000 psi tension. For the reflector tilt angle involved, this would produce a focal length in excess of 4,000 ft., compared to the target board distance of 600 ft.

Figure 2.3.1.2.-1. Design/Cost/Performance Optimization

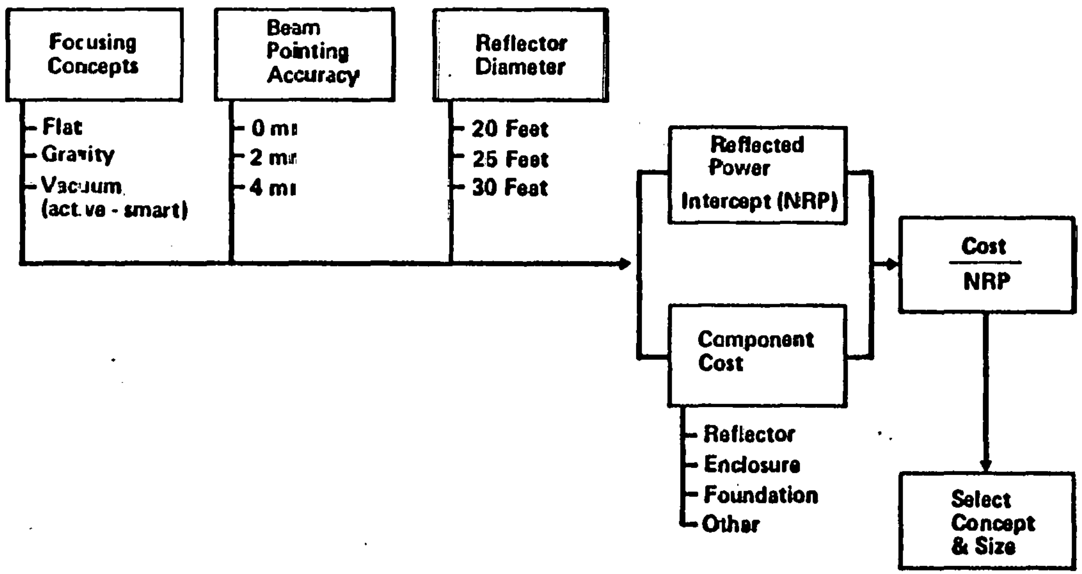

Figure 2.3.1.2.-2. Focus Control

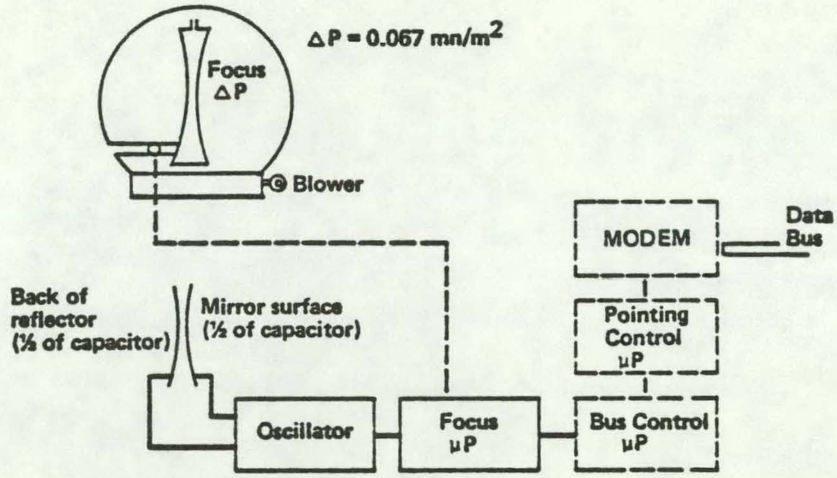

Figure 2.3.1.2.-3. Vacuum Focusing Test Schematic

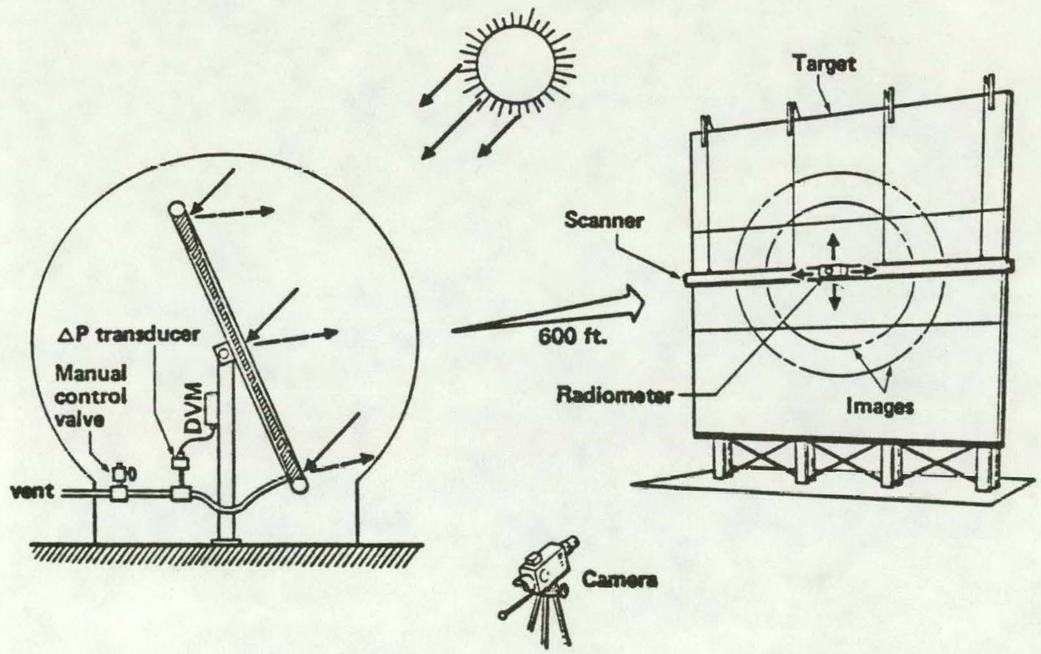

Figure 2.3.1.2.-4. Focusing Test at Livermore

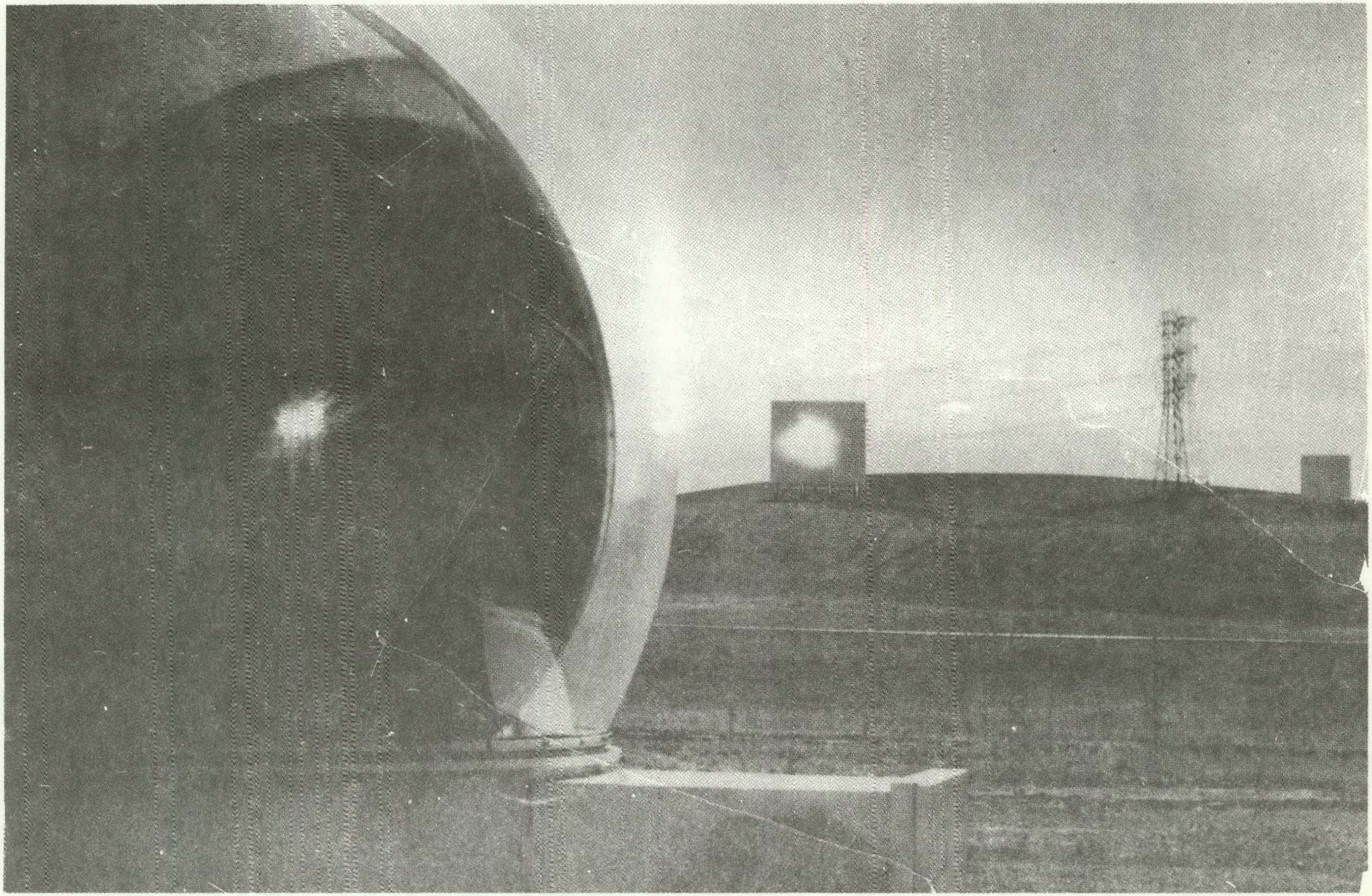

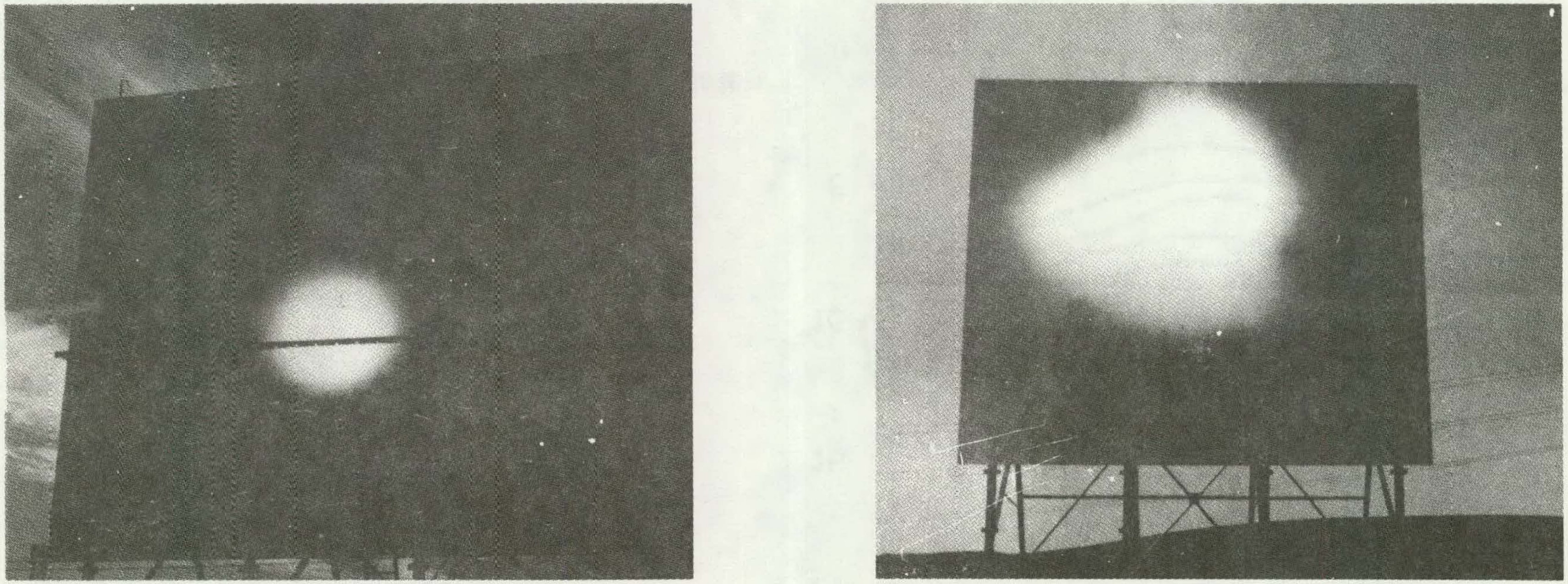

Vacuum Focusing **Partial Gravity Focusing**

Figure 2.3.1.2.-5. Visual Images at 600 ft Distance

Figure 2.3.1.2.-6. Image Power Density Distribution

Livermore Heliostat Tests
15 ft. diameter mirror
600 ft. slant range

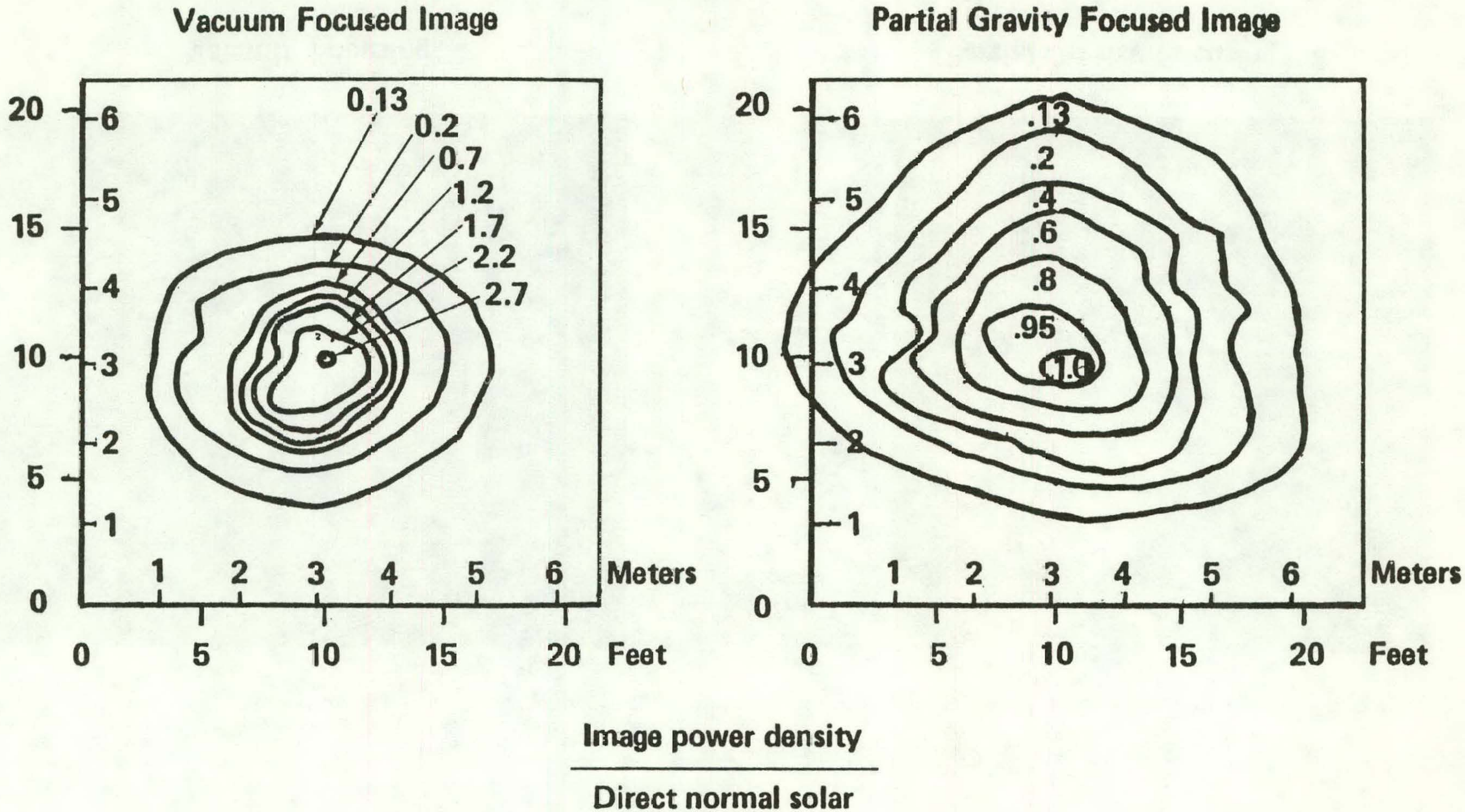

It was concluded from the tests that vacuum focusing significantly reduces image size. However, the question remained, does vacuum focusing improve performance over optimized gravity focusing? The answer from performance analyses is that vacuum focusing does not significantly improve optical performance over gravity focusing. This conclusion was reached by an integrated system study which evaluated total incident energy and capture efficiency at the target for the various focusing concepts, a range of beam pointing errors, a range of mirror sizes, for each specified heliostat, and for each specified day.

Figure 2.3.1.2-7 is a typical plot for a far field mirror (heliostat A) which illustrates that beam pointing error is the most significant parameter in performance optimization. The total energy on the target and capture efficiency is high for perfect pointing (0 MR pointing error). Significant losses occur as the pointing error increases. The total energy on target is essentially proportional to the reflector area and it is shown that, within the size range studied for the specified target, the mirror size has a negligible affect on spillage at the target. Figure 2.3.1.2-8 is a typical plot which summarizes the performance of each specified mirror for each specified day. Note that the near field mirror (heliostat C) has essentially a 100 percent capture efficiency. For this near field mirror (heliostat C) the vacuum focused mirror offers negligible performance gain over a worst case flat mirror. For the far field heliostats the difference between the best vacuum focus (active-smart) and the flat mirror is approximately three percent. The thin membrane mirror has the inherent gravity focus capability which, as shown by Figure 2.3.1.2-9, provides essentially the same optical performance as the active vacuum focused mirror. It is obvious that any small capital cost to provide vacuum focusing (plus consideration of reliability/maintenance) is not warranted. The selected configuration is, therefore, the simple membrane mirror with its gravity focusing capability.

The next issue in the trade study was to optimize and select the beam pointing accuracy. As discussed and shown previously, it is very significant to minimize the beam pointing error within any overriding cost constraint. A target

Figure 2.3.1.2.-7. Significance of Beam Pointing Error and Mirror Size

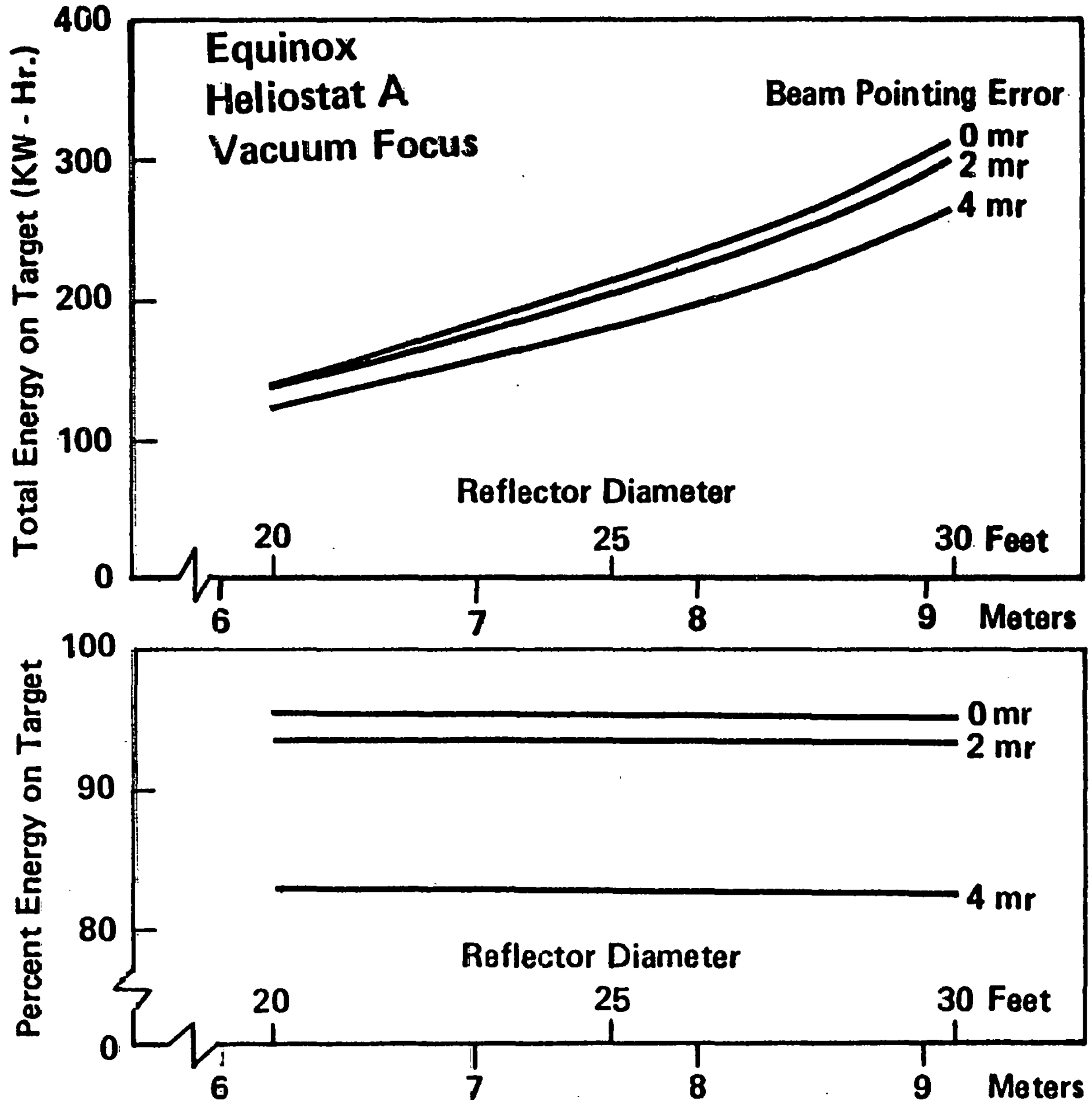

Figure 2.3.1.2.-8. Focusing Evaluation

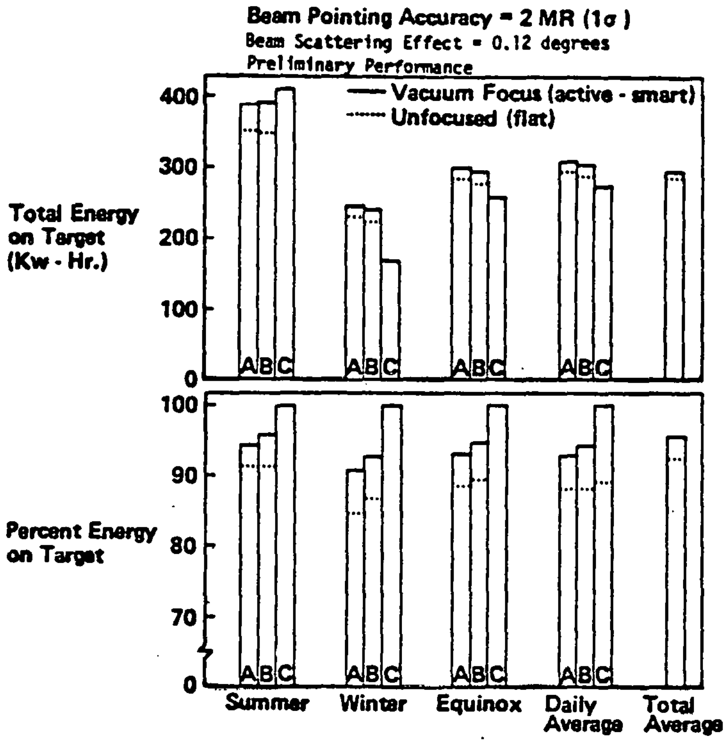

Figure 2.3.1.2.-9 Focusing Evaluation

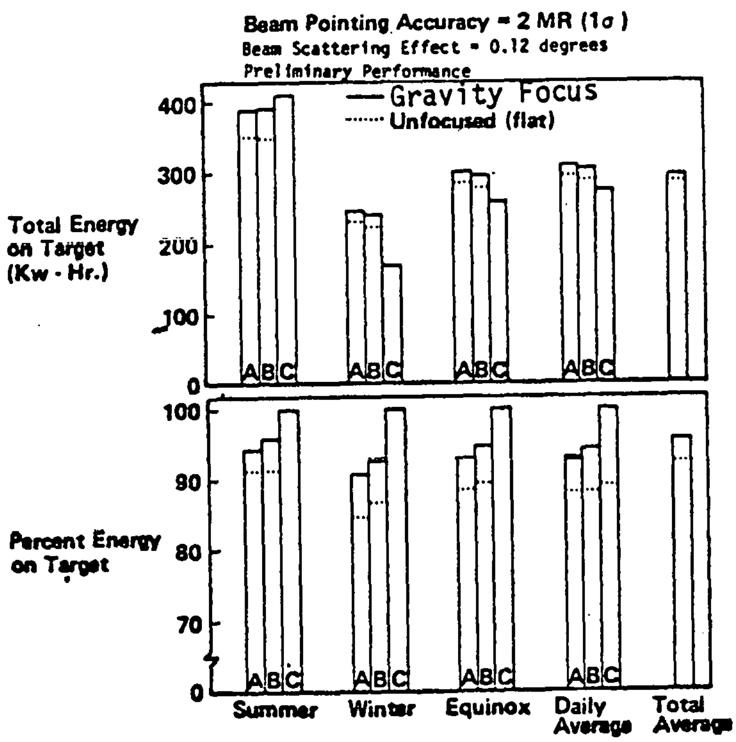

allocation for the beam pointing error budget is provided in Table 2.3.1.2-1. The gimbal/actuator system accuracy is being studied by two subcontract specialist firms. The cost optimized design/accuracy has not yet been established. In parallel, the study of alignment procedures which can provide a software input to correct gimbal orthogonal errors is being evaluated.

As of this time, it is believed that a 2 mr (1σ) beam pointing error is achievable and will be used for performance calculation. Due to the importance of this parameter, it is proposed that a Phase II tracking test be performed using a prototype heliostat at the STTF to verify system capability.

Table 2.3.1.2-1

BEAM POINTING ACCURACY ERROR BUDGET

Source	Budget Allocation (1σ)
Gimbal Actuator	
. Gimbal Actuator Error Cone	0.04 degrees
. Encoder Accuracy	0.0334
. Encoder Repeatability	0.0334
. Step resolution vs time (± ½ step)	0.0077
RSS	0.06238 degrees (1.0886 mr)
Control System	
. Ephemeris Data	0.0060 degrees
. Angle Calculation	0.0036
. Clock Resolution	0.0010
. Alignment	0.0746
RSS	0.07494 degrees (1.3078 mr)
TOTAL STATIC	0.0975 degrees (1.702 mr)
Pedestal, Actuator, Mirror Dynamics	0.0308 degrees
Total Errors RSS	0.10224 degrees (1.7844 mr)

The third issue in the performance trade study is the optimum size of the reflector. As shown earlier (see Figure 2.3.1.2-7), the thermal performance is nearly proportional to mirror area for the size range evaluated (6 meter to 12 meter diameter mirrors). The optimum size is, therefore, that which achieves minimum cost per mirror area. Preliminary cost/scaling size relationships were established for all heliostat components. Figure 2.3.1.2-10 shows the component scaling and Figure 2.3.1.2-11 shows that a reflector of approximately 12 meter diameter would provide minimum cost per reflector area. The size of 9.29 meter reflector diameter was selected based on the following:

1) Near optimum

2) Above 30 feet diameter, the capture efficiency at the target will reduce due to image size. Therefore, the CPR would increase faster than the cost/m^2.

3) The smaller size is more compatible with factory space, tooling, transportation and handling.

2.3.1.3 Results of Thermal Performance Analysis

Final thermal performance will be calculated based on the configuration resulting from the optimization studies. Performance will be based on:

1) A gravity focused reflector.

2) An effective reflector area of 65.7 sq. meters (9.29 foot diameter)

3) A reflectance of 0.91

4) A transmissivity of 0.88

5) An enclosure scattering cone computer correlation factor of 0.05 degrees, and

6) A beam pointing error of 2 Mr (1 σ).

The parasitic power requirements for the controls and pressurization blower will be approximately 40 watts electrical during operation and 10 watts electrical during shutdown. These values at 1 electrical equals 5 thermal will be subtracted from the thermal performance at the receiver. The net power performance will be presented as shown in Table 2.3.1.3-1. The capture efficiency will be presented as shown in Table 2.3.1.3-2.

Figure 2.3.1.2.-10. Heliostat Size/Cost Optimization

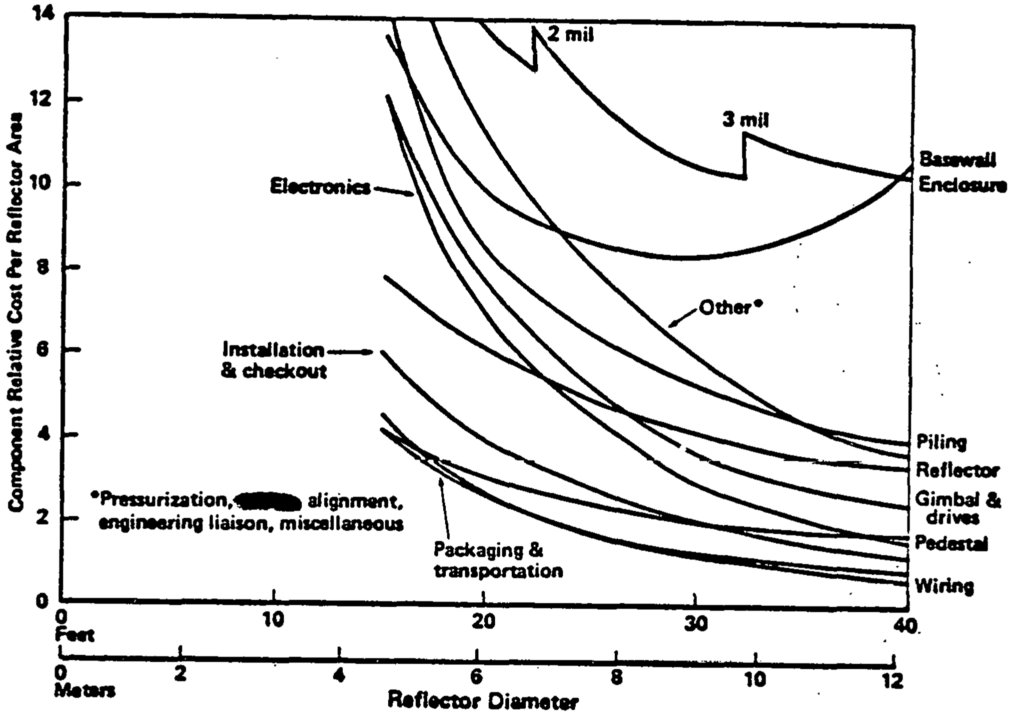

Figure 2.3.1.2.-11. Heliostat Size/Cost Optimization

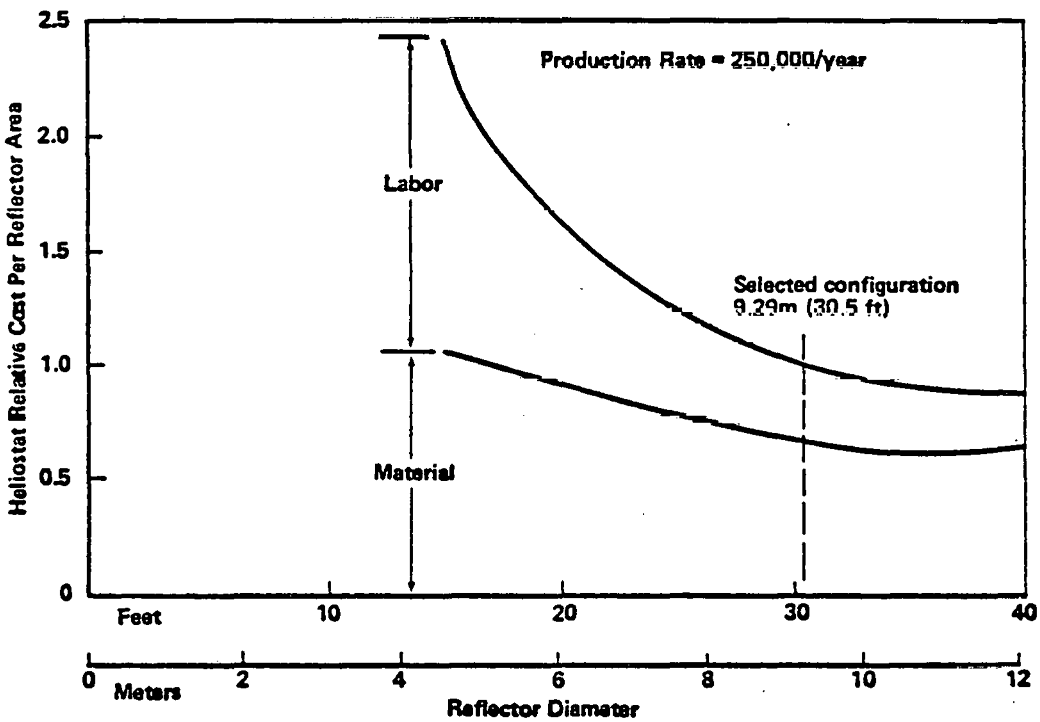

TABLE 2.3.1.3-1

HELIOSTAT OPTICAL PERFORMANCE

NET INCIDENT ENERGY ON RECEIVER (KW-HR)

PERIOD	HELIOSTAT		
	A	B	C
Spring & Fall Equinox	TBD	TBD	TBD
Summer Solstice	TBD	TBD	TBD
Winter Solstice	TBD	TBD	TBD

TABLE 2.3.1.3-2

HELIOSTAT OPTICAL PERFORMANCE

PERCENT REFLECTED ENERGY ON TARGET

PERIOD	HELIOSTAT		
	A	B	C
Spring & Fall Equinox	TBD	TBD	TBD
Summer Solstice	TBD	TBD	TBD
Winter Solstice	TBD	TBD	TBD

2.3.2 Protective Enclosure

2.3.2.1 Configuration

The protective enclosure (Figure 2.3.2.1-1) is a transparent weatherized polyester material thermoformed to a spherical shape. The spherical enclosure is truncated at a 45^0 angle from the spherical center to interface with an attachment fitting at the base support ring.

The diameter of 9.69 m (31.8 ft.) provides a clearance of 19.8 cm (7.8 inches) from the reflector support ring. This clearance accommodates assembly and installation tolerances plus enclosure deflection due to the maximum design winds.

The enclosure is thermoformed from an 0.5 cm (0.020 in.) thick weatherized polyester film. The thermoforming results in a finished dome with a minimum film thickness of 0.008 cm (0.003 inches).

The enclosure interfaces with the base/foundation at a retention fitting which provides the tension load path and a positive air pressure seal. The design objectives for the retention fitting are:

1) Positive pressure seal
2) Adequate load path
3) Ease of assembly (minimum labor)
4) Ease of disassembly (minimum labor)
5) Minimum cost of materials
6) Long life

Several configurations of the retention device are currently being evaluated. Six candidate configurations are shown in Figures 2.3.2.1-2 and 2.3.2.1-3. One of the more promising configurations at this time is the "Clip Wrapped Joint" which is discussed in the following paragraphs.

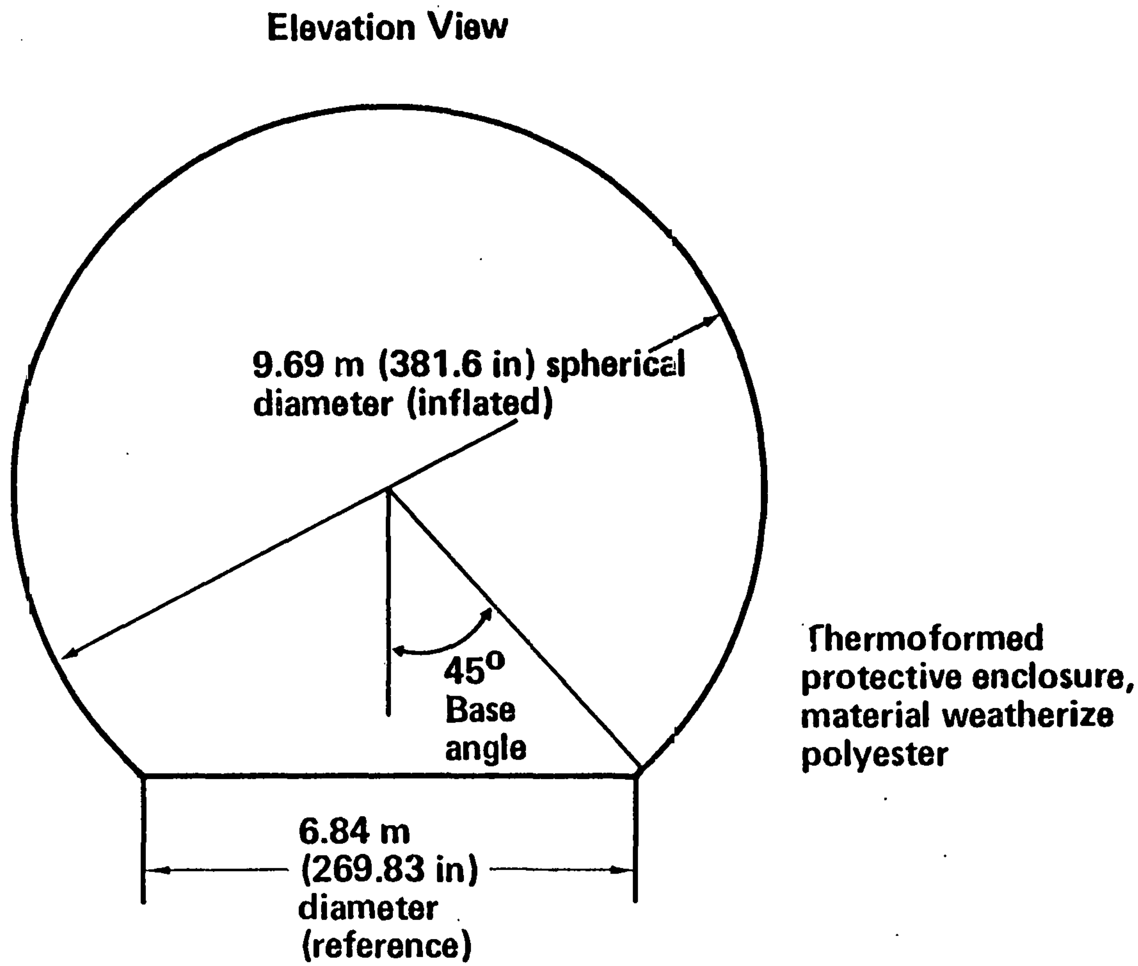

Figure 2.3.2.1-1. Protective Enclosure Envelope—Elevation View

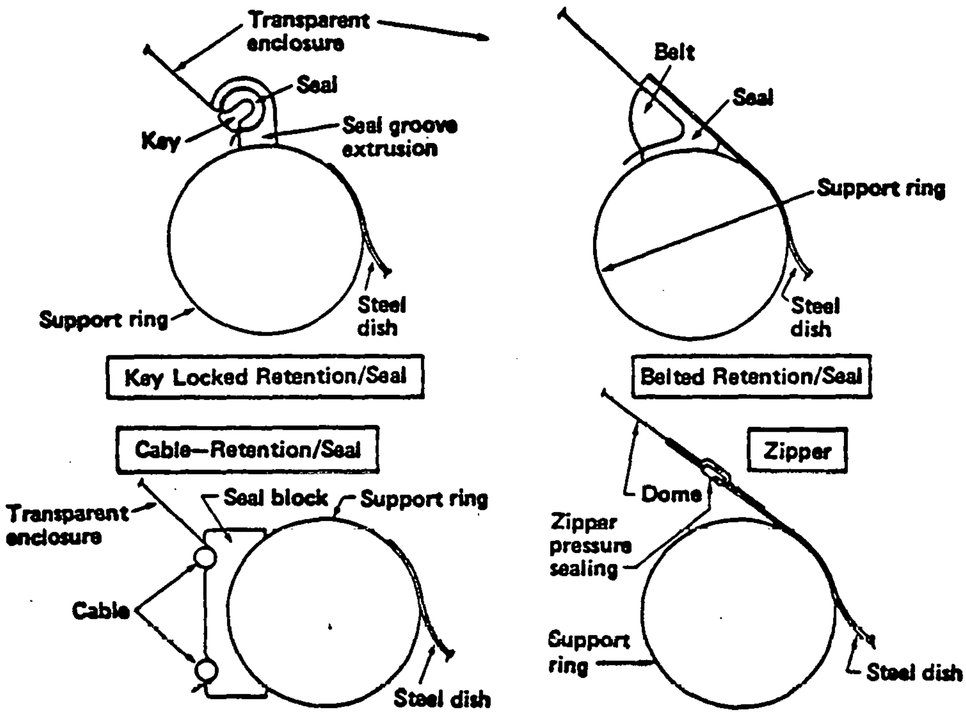

Figure 2.3.2.1-2. Interface Concepts (Non-energizing)

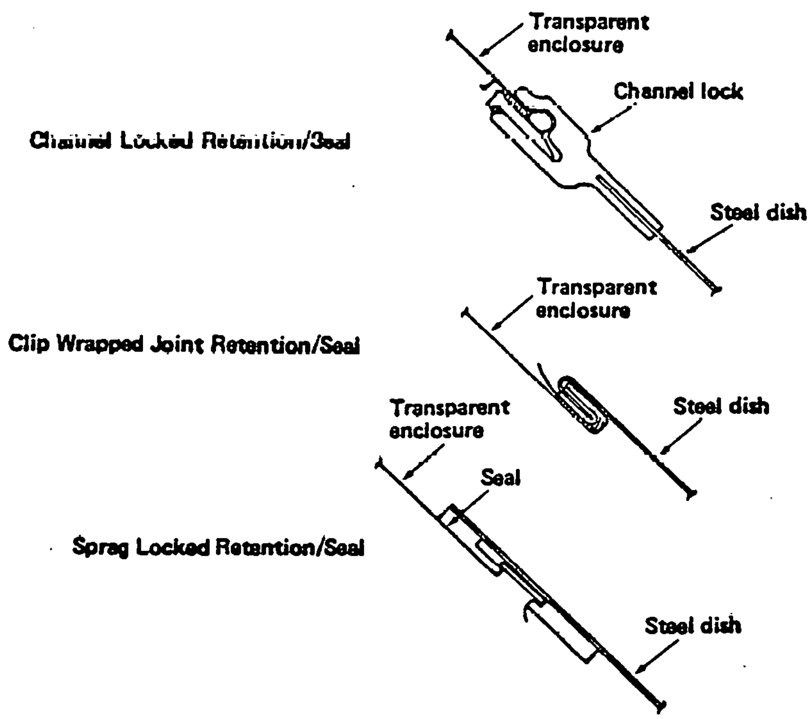

Figure 2.3.2.1-3. Interface Concepts (Self-energizing)

Description

The joint uses two FEP Teflon "U" shaped extrusions sized such that one fits inside the other with their open faces in the same direction. The inner extrusion is retained by the rolled lip of the base dish. The dome material is placed between the extrusions causing a self energizing retention force as shown in Figure 2.3.2.1-4.

Pre-assembly Status

The inner extrusion is part of the dish assembly; i.e., it is bonded or held in place by pressure sensitive tape. The bottom edge of the dome has been indexed during thermoforming to assure correct alignment. The exterior "U" extrusion is in the form of a continuous cord which is cut to length on assembly. A thin strip of adhesive is applied to the extrusion during its forming. The adhesive strip is protected by a plastic film which is peeled off during assembly, thus keeping the extrusion properly located.

Assembly Procedure

Step 1 - Place uninflated dome over reflector assembly.

Step 2 - Locate exterior "U" extrusion on dome index line, use exposed adhesive to hold in place.

Step 3 - Locally fold dome edge into extrusion and slide combination over prepared dish edge. A slight upward force is required to complete snapping action of mating extrusions. (See Figure 2.3.2.1-4)

Step 4 - Inflate dome, after entire circumference has been snapped in per Step 3.

Disassembly Procedure

Step 1 - Deflate dome.

Step 2 - Unsnap joint by pulling down.

Step 3 - Remove dome over reflector assembly.

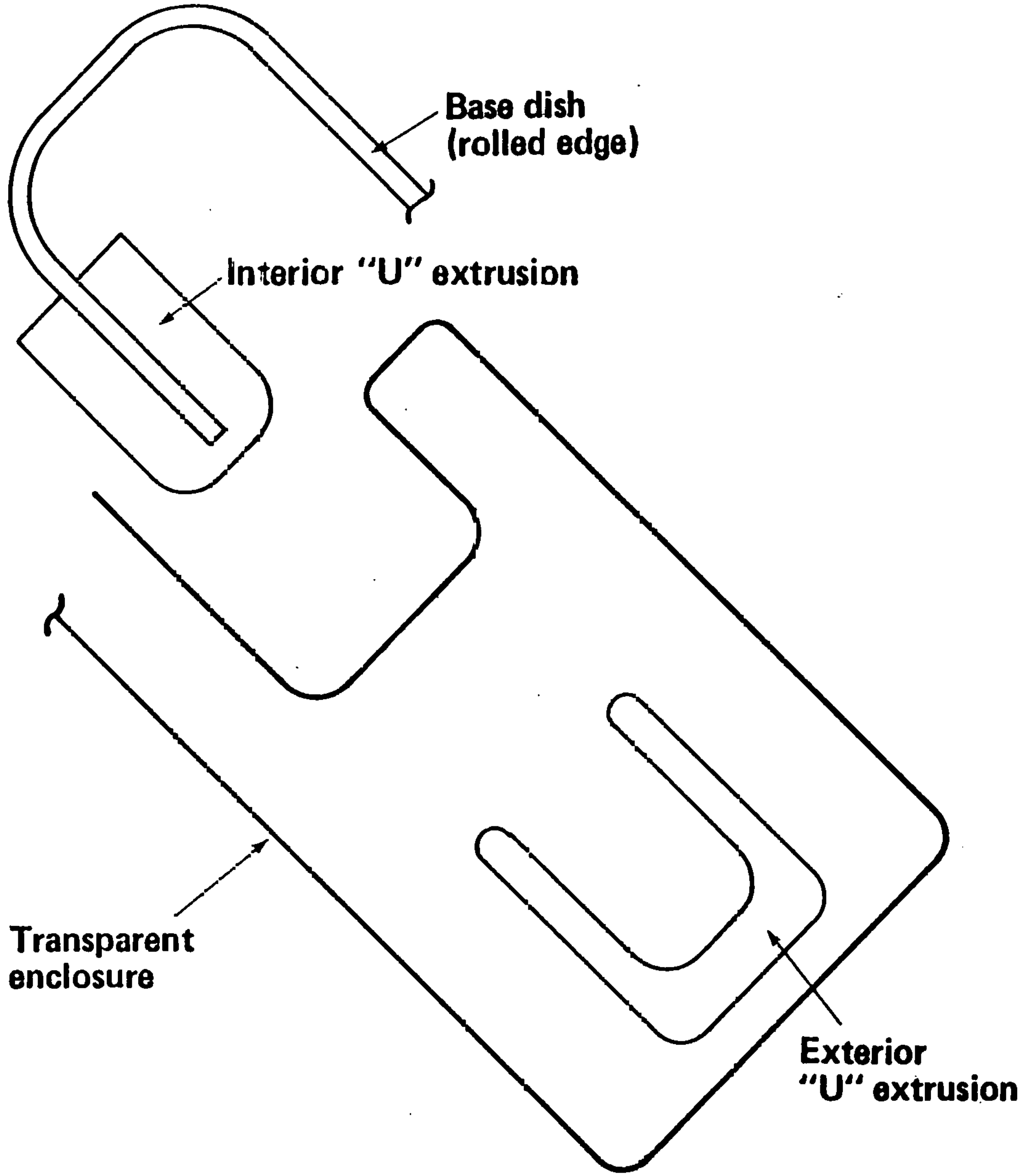

Figure 2.3.2.1-4. Clip Wrapped Joint Free Body Diagram

Manufacturing Considerations

The FEP extrusions can be rapidly produced, exhibit long storage life, and should cost less than five cents per foot.

The rolled lip on the dish requires a secondary metal forming process. Also the dome contour at the joint must provide adequate materils for folding, i.e., a short necked portion at constant diameter is required.

2.3.2.2 Protective Enclosure Materials Evaluation

Shortly after contract go-ahead a series of trips were taken to search the plastic film industry for candidate enclosure and reflector materials. A total of 14 companies were visited. In addition, many firms were contacted by telephone. Many were interested in participation in the development program. Some had a few candidates they could supply in the short term; however, the majority required additional time to make special process runs for this application. The result was a considerable delay in the start of materials screening tests and the realization that promising candidates would be supplied over a period of time rather than all at one time. Table 2.3.2.2-1 lists the suppliers that have participated to some extent, the materials that they manufacture or process and the status of testing of their films. The materials test plan prepared early in the program called for screening tests to be per formed on all promising candidates. This consisted of measuring the mechanical (yield strength, ultimate strength, percent elongation) and optical (specular transmittance) properties prior to, during and following exposure to accelerated ultraviolet exposure testing. The most promising materials, as determined by the U/V test, would then be tested for mechanical joint strength flammability, cleanability and creep i necessary. Real time and accelerated desert exposure of promising candidates was also planned and is now underway. The following paragraphs describe the testing completed to date.

Mechanical Properties

Table 2.3.2.2-2 shows the initial mechanical property data for materials. All materials exhibited adequate initial properties for further consideration as potential enclosure candidates.

Joint samples were prepared using Kynar-C and Melinex "O" to demonstrate the fabrication process for enclosures in Phase II. Table 2.3.2.2-3 shows results of tensile tests on joint samples. Melinex "O" was joined with a thermosetting polyester adhesive; and Kynar-C by heat sealing with application of pressure and a hot wire (similar to Tedlar sealing) Ref.2.3.2.2-1. The polyester joint was as strong as the parent material. In the case of the flourocarbon joint, sample failed adjacent to the joint, suggesting the material had thinned during the application of heat

TABLE 2.3.2.2-1

SUPPLIER	MATERIAL	STATUS
Allied Chemical	Petra, weatherable and non-weatherable polyester	Non-stabilized Petra screen tested desert test underway
Martin Processing	Weatherable Melinex "O" polyester with and without aluminization	Screen tested desert test underway
National Metalizing	Weatherable polyester with and without aluminization	Screen tested desert test planned
Dunmore	Metalized polyester	Screen tested
Pennwalt	KYNAR (flourocarbon)	Screen tested desert test underway
W.R. Grace (Cryovac)	Weatherable polycarbonate	Screen tested desert test underway
Amoco	Polyester-polycarbonate blend	Not received
Celanese	Polyester	Not received
Hercules	Weatherable polypropylene	Screen tested
Morton Chemical	Weatherable polyester and aluminized polyester with overcoating	In screen test
Optical Coating Lab	Metalized, coated polyester	Screen tested desert tests planned
American Enka	Weatherable Polypropylene	Not received
Dupont	Polyester, fluorocarbon	Screen tested
ICI Americas	Polyesters	Screen tested
Teijin America	Weatherable polyester	Not received

TABLE 2.3.2.2-2

INITIAL MECHANICAL AND OPTICAL PROPERTIES FOR CANDIDATE ENCLOSURE MATERIALS

MATERIAL	ULTIMATE STRESS MN/m^2 (PSI)	YIELD STRESS MN/m^2 (PSI)	ULTIMATE ELONGATION %	SPECULAR TRANSMITTANCE [1]
PETRA (UNSTABILIZED)	74.5 (10,000)	62.8 (9,100)	544	.89
MELINEX "O" (STABILIZED BY MARTIN PROCESS)	140 (20,300)	105 (15,200)	90	.84
MELINEX "O" (STABILIZED BY NATIONAL METALIZING)	185 (26,870)	132 (19,200)	132	.82
KYNAR A	162 (23,520)		80	.89
B	167 (24,170)		72	.88
C	153 (22,160)		82	.89
POLYCARBONATE (STABILIZED) 4 MIL	79.9 (11,590)	57.4 (8,320)	141	.88
8 MIL	70.1 (10,170)	56.4 (8,180)	129	.85
POLYPROPYLENE (UNSTABILIZED)	198 (28,740)	44.2 (6,410)	69	.80
(STABILIZED)	140 (20,270)	31.0 (4,490)	83	.76
TEDLAR (7826B)	78.2 (11,340)	34.5 (5,002)	180	.87

[1] 0.5° cone angle; normal incidence; AM2 spectrum

TABLE 2.3.2.2-3

JOINT TENSILE DATA FOR ENCLOSURE MATERIALS

MATERIAL	FAILURE STRESS MN/m^2 (PSI)	FAILURE MODE/REMARKS
POLYESTER JOINT (MARTIN PROCESS MELINEX "O") IMPULSE HEAT ADHESIVE BOND	210 (30,520)	MATERIAL SEPARATED - NOT AT JOINT
FLUOROCARBON JOINT (PENNWALT-KYNAR-C) FIRST ATTEMPT HEAT SEAL	70.3 (10,200)	MATERIAL SEPARATED ADJACENT TO JOINT

and pressure. Although adequate strength was demonstrated, it is believed that refinement of the technique would result in improvement in failure strength.

Specular Transmittance

Many material samples had specular transmittances that were within the acceptable range ($>$ .86). Some were submitted for purposes of determining initial mechanical properties and weatherability, with plans (by supplier) to modify or improve the transmittance at a later time if the material looked promising. The last data column of Table 2.3.2.2-2 shows the transmittances for materials received to date.

Accelerated Ultraviolet Tests

Survival in long-term exposure to U/V radiation is a major concern for candidate heliostat materials. Very little is known about accurately predicting life of materials exposed to solar radiation. Accelerated exposure testing is often undertaken to screen materials, but no attempts should be made to use the acceleration multiplier directly in the prediction of material life, unless real time testing of the same material has been performed previously and a correlation factor determined.

The purpose of the accelerated ultraviolet testing described here was primarily to provide a survivability ranking of candidates.

Figures 2.3.2.2-1 and 2.3.2.2-2 show the physical test setup, consisting of a solar simulator (Spectrolab X-200) and the target plane. The samples were held to a water-cooled panel and temperature controlled to approximately 80°F. The integrated acceleration rate for the region of 250-400 nanometers is 10 air mass 2 SUNS. Test results are shown in Figure 2.3.2.2-3 through 2.3.2.2-10.

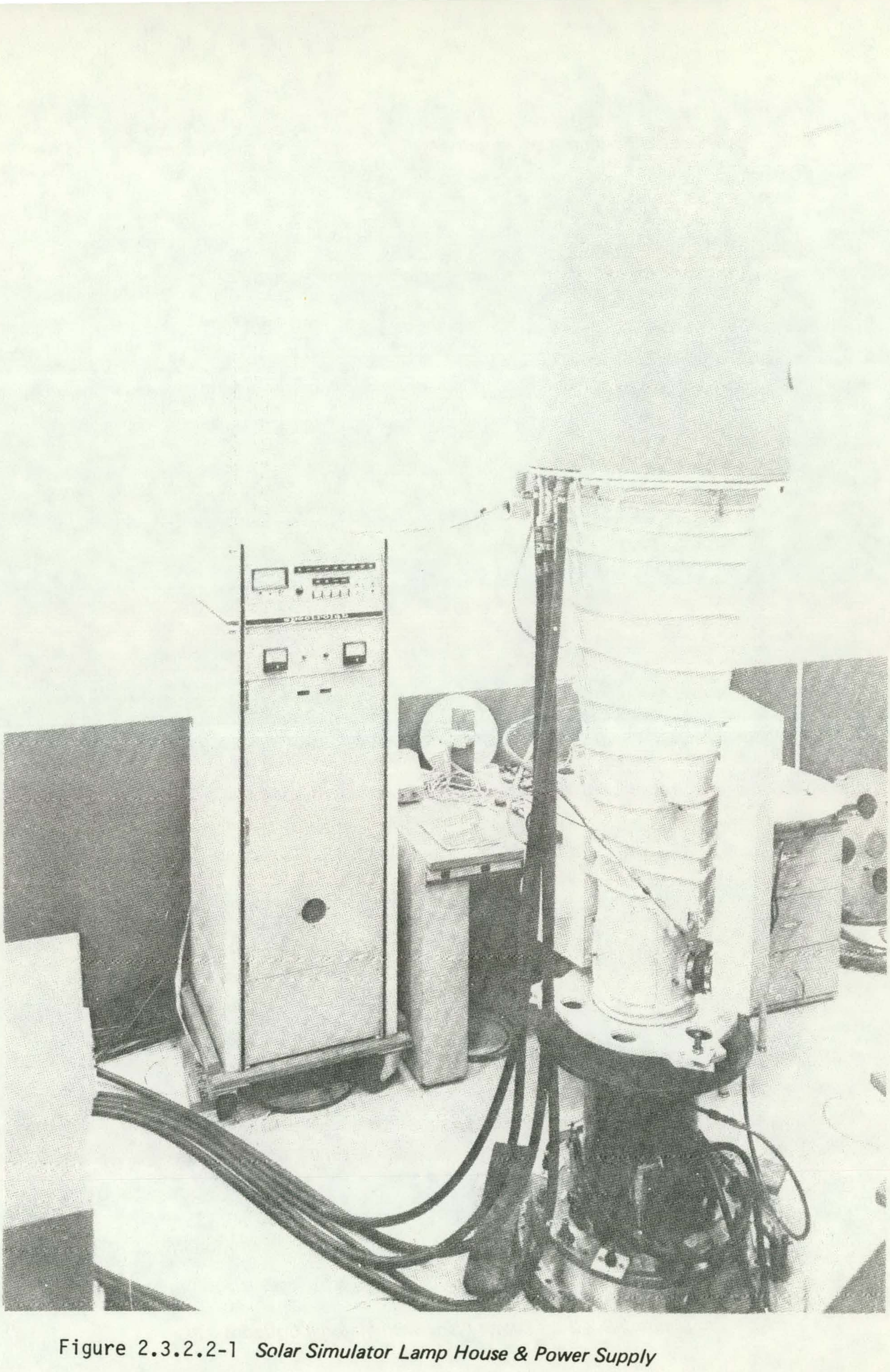

Figure 2.3.2.2-1 *Solar Simulator Lamp House & Power Supply*

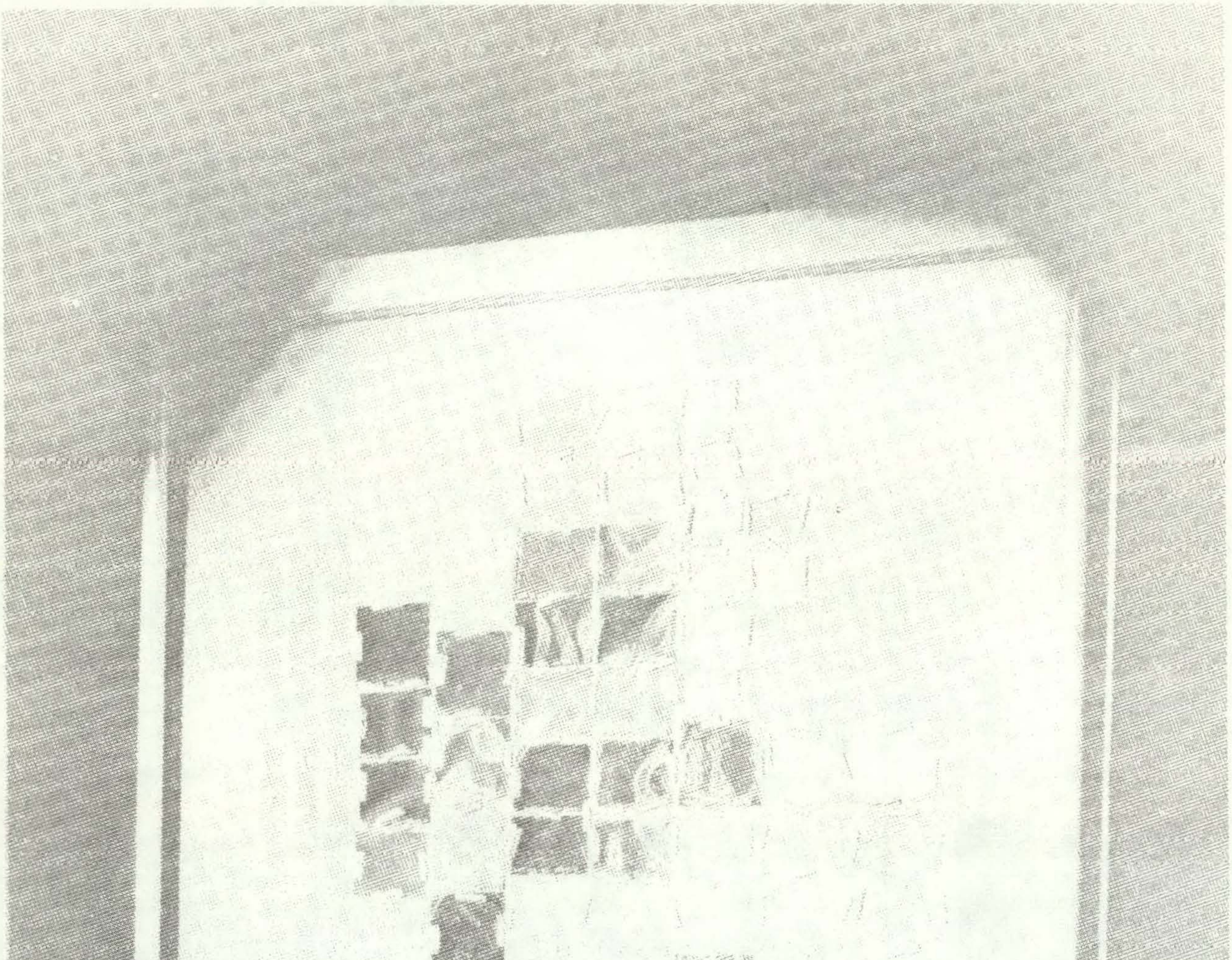

Figure 2.3.2.2-2 Target Plane with Material Coupons

Figure 2.3.2.2-3 *Kynar A U/V Exposure Data*

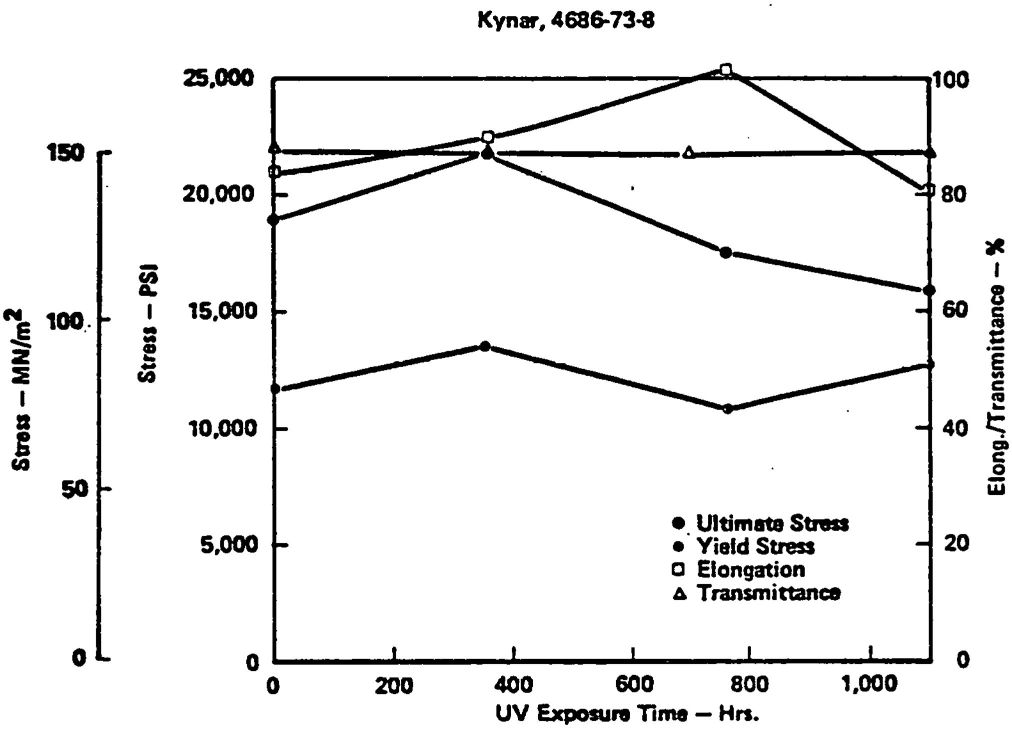

Figure 2.3.2.2-4 *Kynar B U/V Exposure Data*

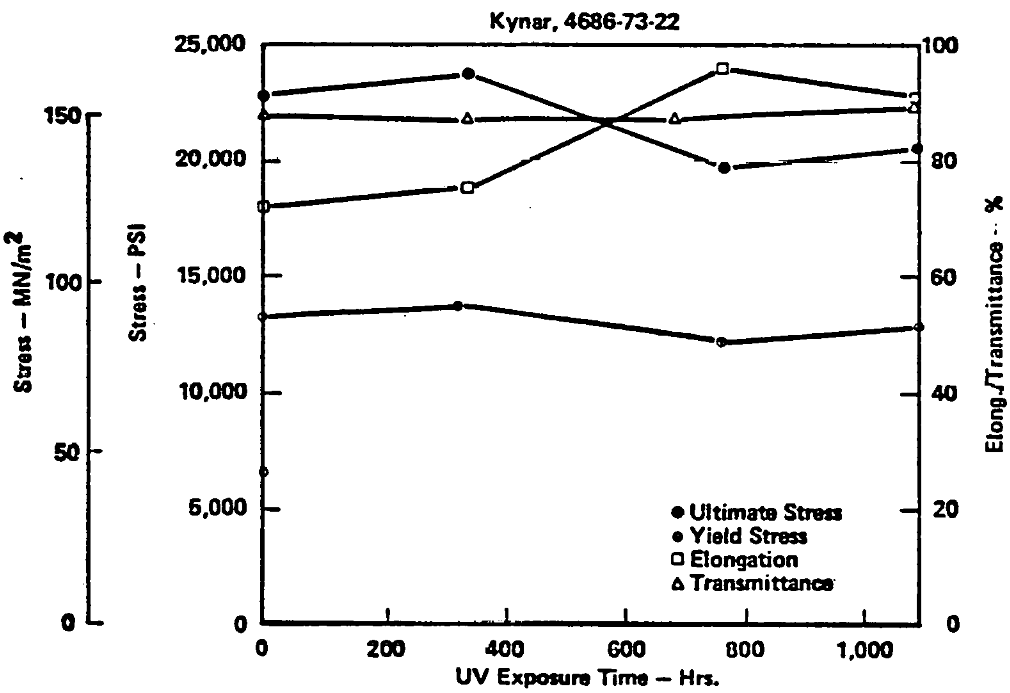

Figure 2.3.2.2-5 *Kynar C U/V Exposure Data*

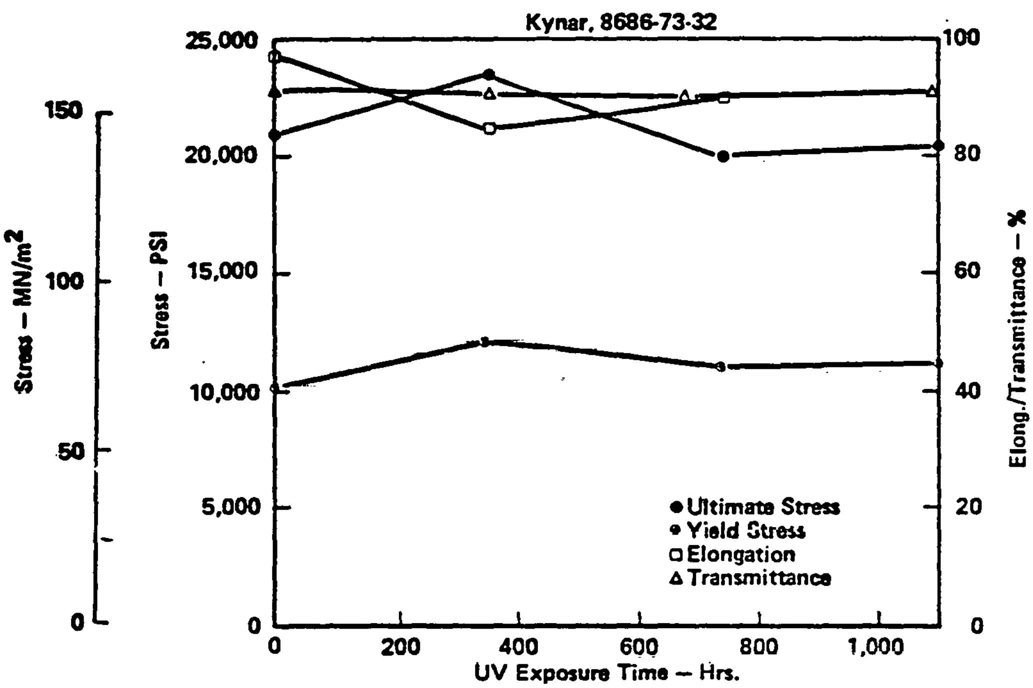

Figure 2.3.2.2-6 *Martin Weatherable Polyester U/V Exposure Data*

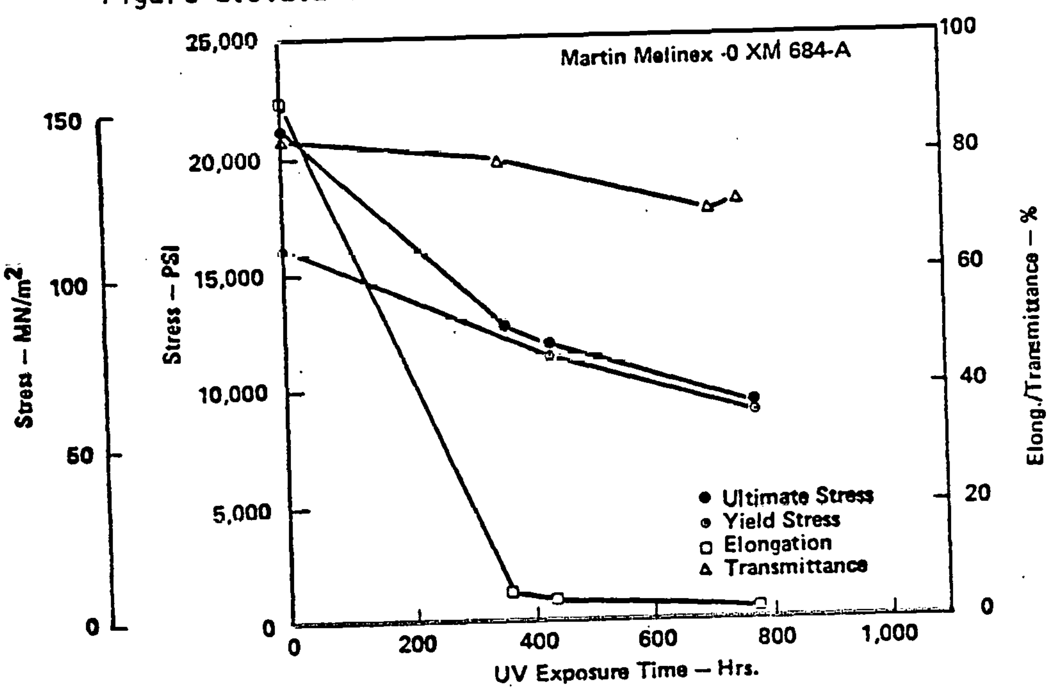

Figure 2.3.2.2-7 *National Metalizing Weatherized Polyester U/V Exposure Data*

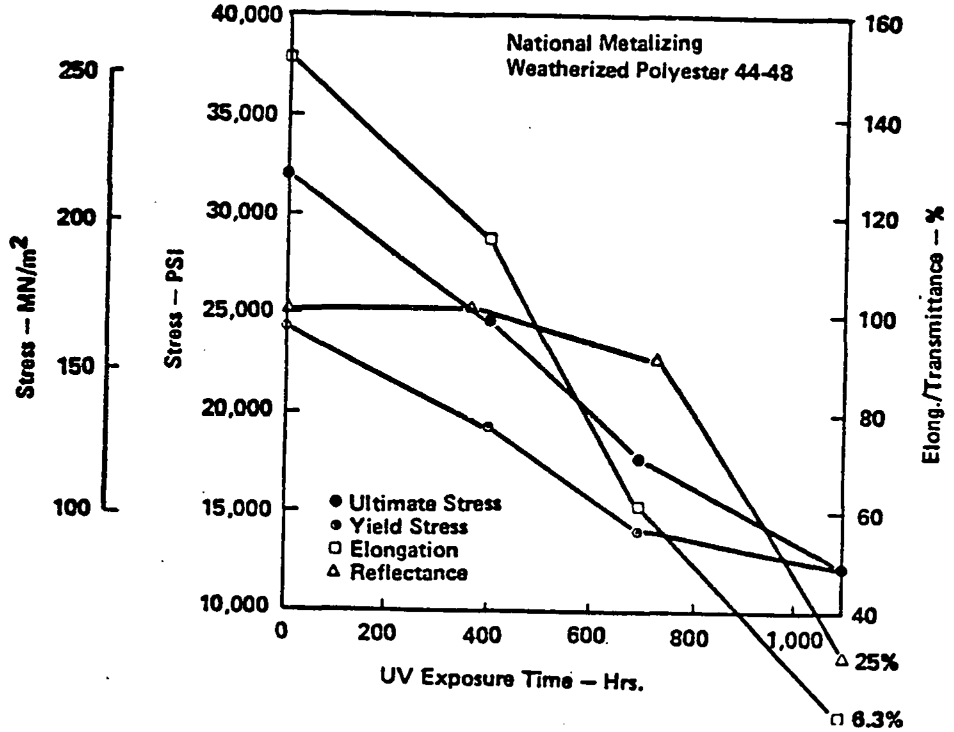

Figure 2.3.2.2-8 *Petra A U/V Exposure Data*

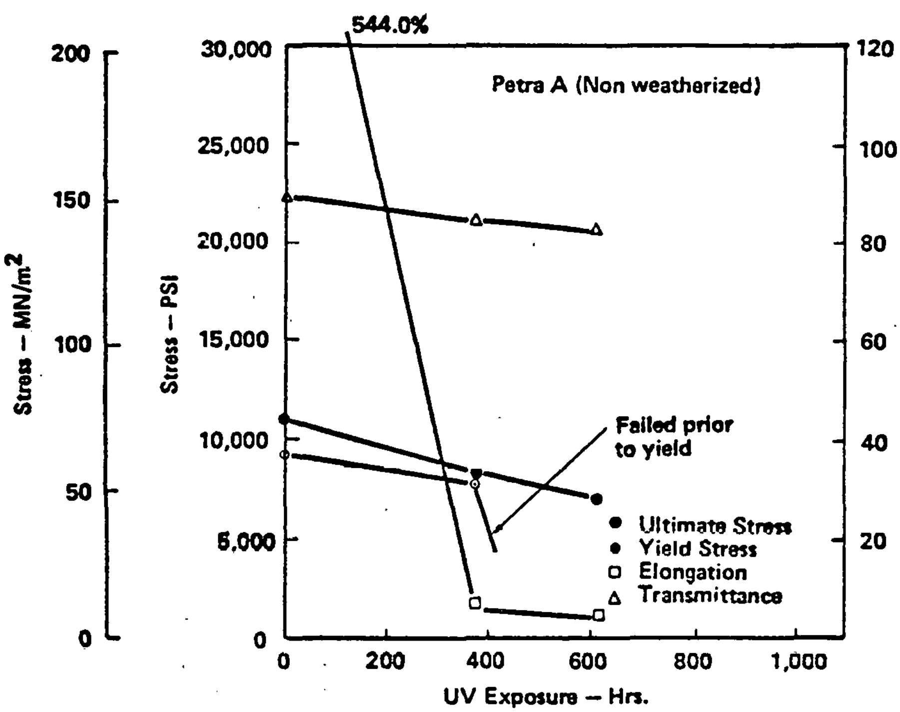

Figure 2.3.2.2-9 *8 Mil Weatherable Polycarbonate U/V Exposure Data*

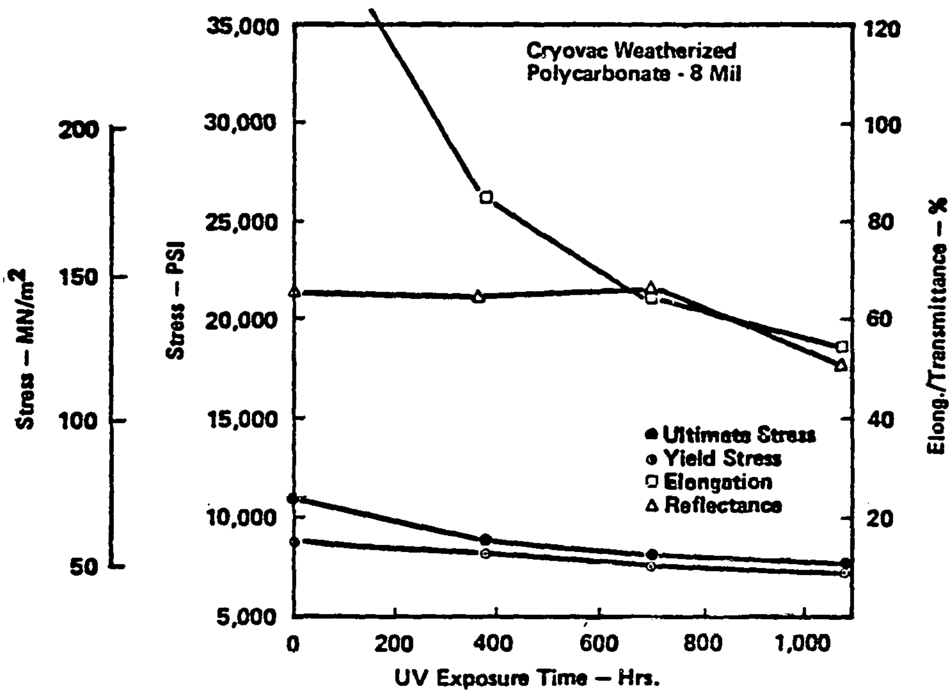

Figure 2.3.2.2-10 *4 Mil Weatherable Polycarbonate U/V Exposure Data*

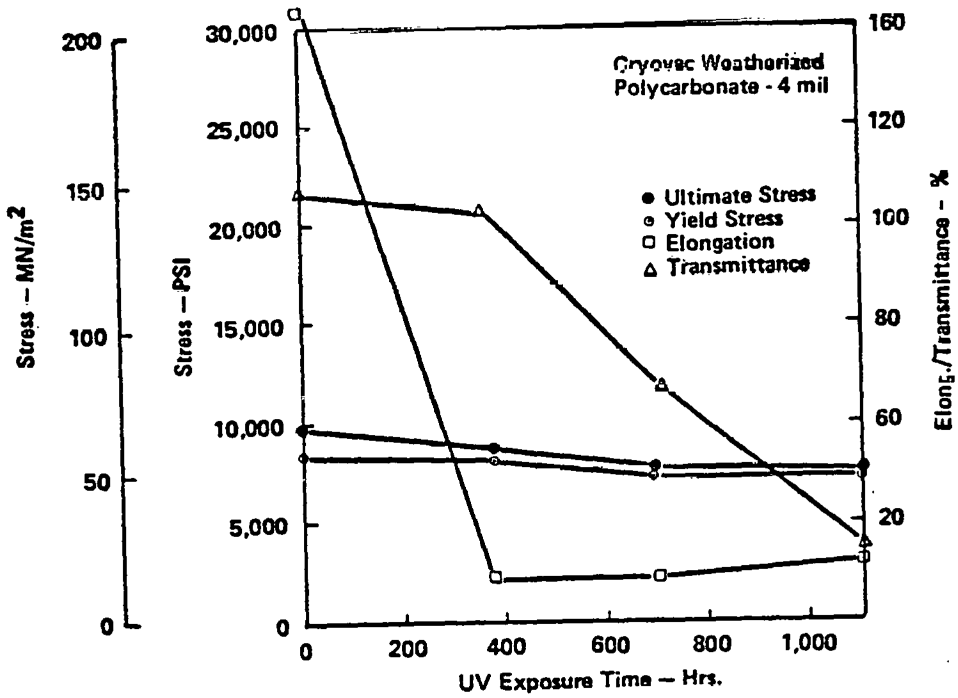

KYNAR showed the least degradation, both in optical and mechanical properties. The material is known to be inherently stable in the U/V. The degradation rates of the polyesters were similar, making ranking difficult. Polypropylene embrittled to the point where it could not be handled after 360 hours.

Examination of the above data would lead to the following ranking:

1) Kynar
2) Polyesters
3) Polycarbonate
4) Polypropylene

Predictions of film life can be best accomplished in actual desert exposure by simultaneously exposing samples in environments of one sun and multiple sun levels. This approach is being employed in this program by sending material coupons to the Desert Sunshine Exposure Test Facility (DSET) where they will be exposed to one and eight sun environments. Comparisons of damage rate data can then be made and the acceleration factor estimated. The accelerated data curves can be adjusted by this factor and material property versus real time predictions made. The only material for which applicable real time exposure data was found is an oriented polyester film which was U/V stabilized by Martin Processing Co. This material was removed from a greenhouse in Illinois, after a 15 year exposure (calculated to equal 10.5 years in Arizona). The surface of the sample was scratched from tree branches and leaves, washing, and handling, precluding valid specular transmittance measurements. The ultimate strength and percent elongation of the 15 year old material were reduced only 35 percent and 12 percent respectively, which is safely within design allowables. The material obviously has not reached the end of its life in the mechanical sense.

Examination of the accelerated ultraviolet test data (Figures 2.3.2.2-3 through 2.3.2.2-10) reveals a much greater rate of mechanical property degradation for the polyester than for the fluorocarbons. The Illinois greenhouse data, however, showed that weatherable polyester should retain mechanical properties well, with only moderate losses in strength and elongation after 15 years. Closer examination of the spectral content of the solar simulator and the spectral sensitivity of polyesters is of value in understanding severity of the U/V test.

The exposure for different materials subjected to an accelerated U/V test varies from material to material because of the spectral sensitivity variations among materials. For example, Table 2.3.2.2-4 below shows the most damaging wavelengths for several materials.

Table 2.3.2.2-4

SPECTRAL SENSITIVITIES OF SELECTED MATERIALS

POLYMER	WAVELENGTH OF GREATEST SENSITIVITY (Nanometers)
Polycarbonate	295
Polyethylene	300
Polypropylene	310
Polyvinyl Chloride	310
Thermoplastic polyester	290-320
Unsaturated polyester	325

Figure 2.3.2.2-11 compares the detailed spectral content of the solar simulator with that of the AM2 sun in the ultraviolet wavelength region. While the simulator did provide an integrated 10 AM2 U/V sun level, it can be seen that at specific bands higher or lower levels were present. With the exception of the 310-320 nm band, all wavelength U/V below 350 nm were greater than 10 suns. In the 300-310 nm band, which includes the wavelengths of greatest sensitivity for polypropylene and thermoplastic polyesters the level was 40 suns. Polycarbonate is most sensitive to 295 nm U/V, which for practical purposes does not exist in the AM-2 solar spectrum, but was present to some extent in the test.

Figure 2.3.2-11. Solar Simulator/AMZ Energy Distribution (Solar Sim at 10 UV Suns 250 to 400 nm)

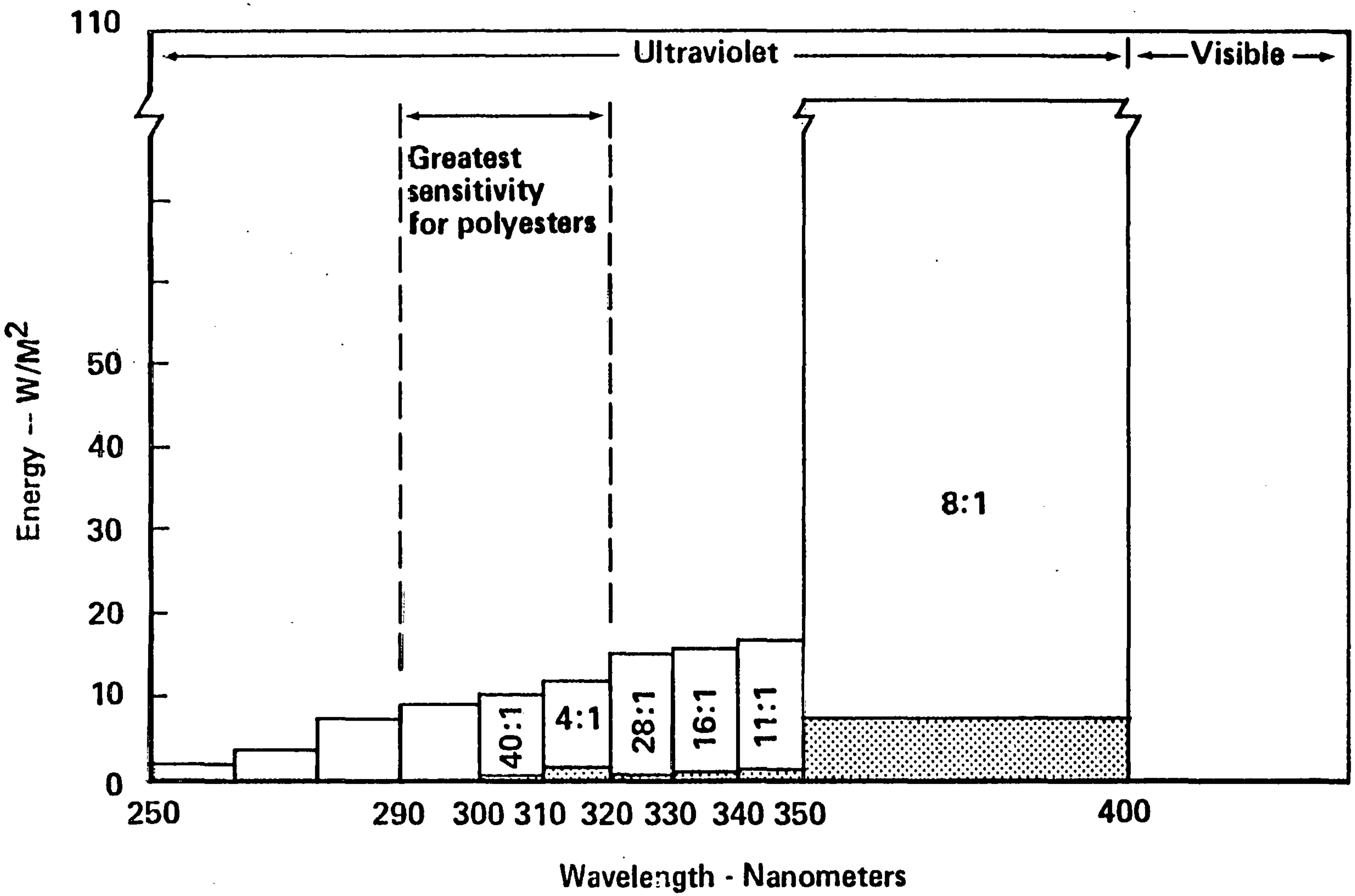

The principle message from the above is that the acceleration rates from the Kynar and polyester group were not the same. Furthermore, the actual acceleration rates are not known and must be determined through comparisons, material by material, under simultaneous real time and accelerated exposure with sunlight as discussed earlier.

Cost Analysis

Table 2.3.2.2-5 shows approximate projected costs for Tedlar, Kynar and polyesters, using preliminary cost per unit area data derived from discussion with suppliers. The last column gives cost per unit area per unit transmittance (squared).

Table 2.3.2.2-5

ENCLOSURE MATERIALS RELATIVE COSTS

MATERIAL	ANTICIPATED COST $/m^2$	SPECULAR TRANSMITTANCE	COST $/m^2 \tau^2$
Tedlar (8 mil)	11.76	.875	15.46
Kynar (4 mil)	2.07	.905	2.52
Polyester (3 mil)	0.54	.875	0.703

In conclusion, both Kynar and weatherized polyesters exhibit the ability to function satisfactorily as enclosure material. Kynar was shown to be U/V stable in the accelerated testing and as a polyvinylidene fluoride is well-known to be inherently stable. The 15 year greenhouse experience verified the ability of film processors to long-term weatherize polyesters that would otherwise be subject to embrittlement. Since polyester films have the lowest cost and stabilization appears feasible, a weatherized polyester is recommended for commercial plant protective enclosures.

2.3.2.3 Structural Analysis

The enclosure consists of a transparent spherical dome segment attached to a steel support ring which is supported by three steel stanchions. As shown in Figure 2.3-1, the enclosure sphere is truncated at 45^0 angles and a steel dish, welded to the steel support ring, forms the lower segment of the pressurized sphere.

Details of the structural analysis which support the design are described in the following sub-sections.

Design Loads - The principle loads acting on the enclosure are those caused by the environment (wind, snow, ice, and earthquake), and the internal static air pressure used to support the membrane enclosure.

Wind Loads - Undisturbed wind above smooth terrain is known to assume logarithmic velocity profile, according to atmospheric boundary layer theory. Design wind profiles are commonly specified by power laws which give results similar to a logarithmic description. These take the form:

$$V_z = V_{REF}\left(\frac{Z}{H_{REF}}\right)^{\alpha}$$

where V_Z = Wind velocity at height Z above ground.

V_{REF} = Wind velocity at reference height H_{REF}

α = Exponent affecting shape of profile.

Specification 001 requires that:

1) heliostats be designed for wind according to a power law with H_{REF} equal to ten meters, and α equal to 0.15, and
2) heliostats shall survive without damage a maximum wind velocity, including gusts, of 40 meters per second (90 mph) at ten meters above the ground.

Reference 2.3.2.3-1 gives the following equations for lift and drag respectively.

$$L = K_L \, q \, R^2$$

$$D = K_D \, q \, R^2$$

where K_L = Lift coefficient

K_D = Drag coefficient

q = Wind dynamic pressure

R = Dome radius

A wind tunnel test program (Reference 2.3.2.3-2) was carried out to determine the pressure distribution on enclosures and the affect on pressure distribution of "sheltering" due to the density of the array plus a peripheral fence. Testing was performed in the University of Washington Aeronautical Laboratory (UWAL) low-speed wind tunnel. Tests ranged from single units to 60 enclosure models in square and diagonal arrays, at varying spacing densities. Test runs were made with and without the peripheral fence and at different fence locations.

The aerodynamic lift and drag coefficients obtained from these tests are shown in Figures 2.3.2.3-1 and 2.3.2.3-2. These have been used to calculate lift and drag forces on the heliostat. Compared with the loads obtained from the previous equations, and used for earlier design, the loads obtained from wind tunnel test data show a reduction in drag force of 21 percent for a 9.69 m (31.8 ft.) diameter dome; but the lift force has not changed appreciably. Therefore, the loads obtained from wind tunnel test data have been used to determine the lowest cost design for the prototype heliostat. The lift and drag forces acting on the heliostat due to the peak survival wind of 40 meters per second (90 mph) are:

LIFT LOAD L = 32,399 Newtons (7,284 lb.)

DRAG LOAD D = 9,296 Newtons (2,090 lb.)

These maximum loads occur at the minimum array density of 0.22.

Figure 2.3.2.3-1 Wind Tunnel Test Data

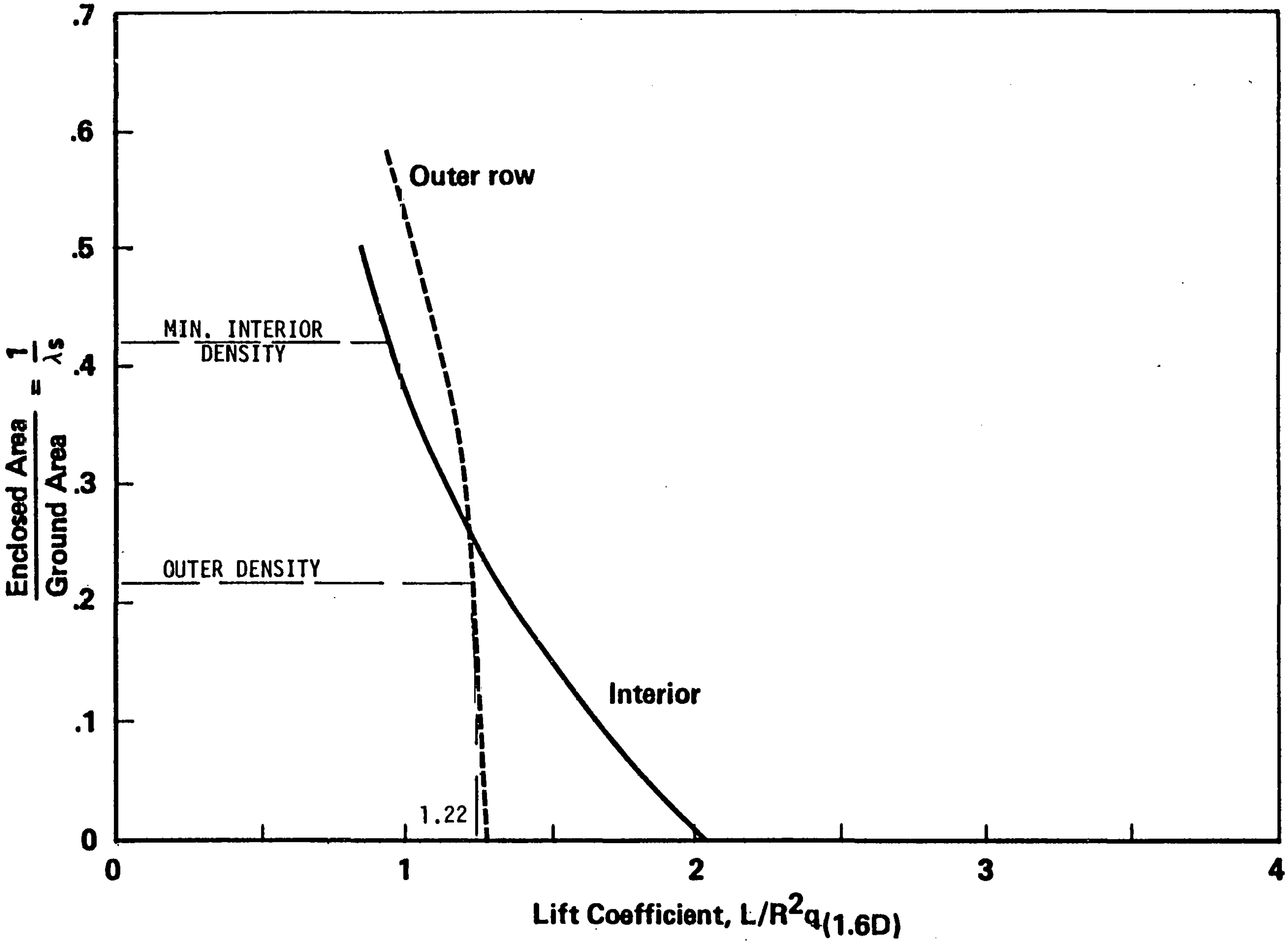

Figure 2.3.2.3-2 Wind Tunnel Test Data

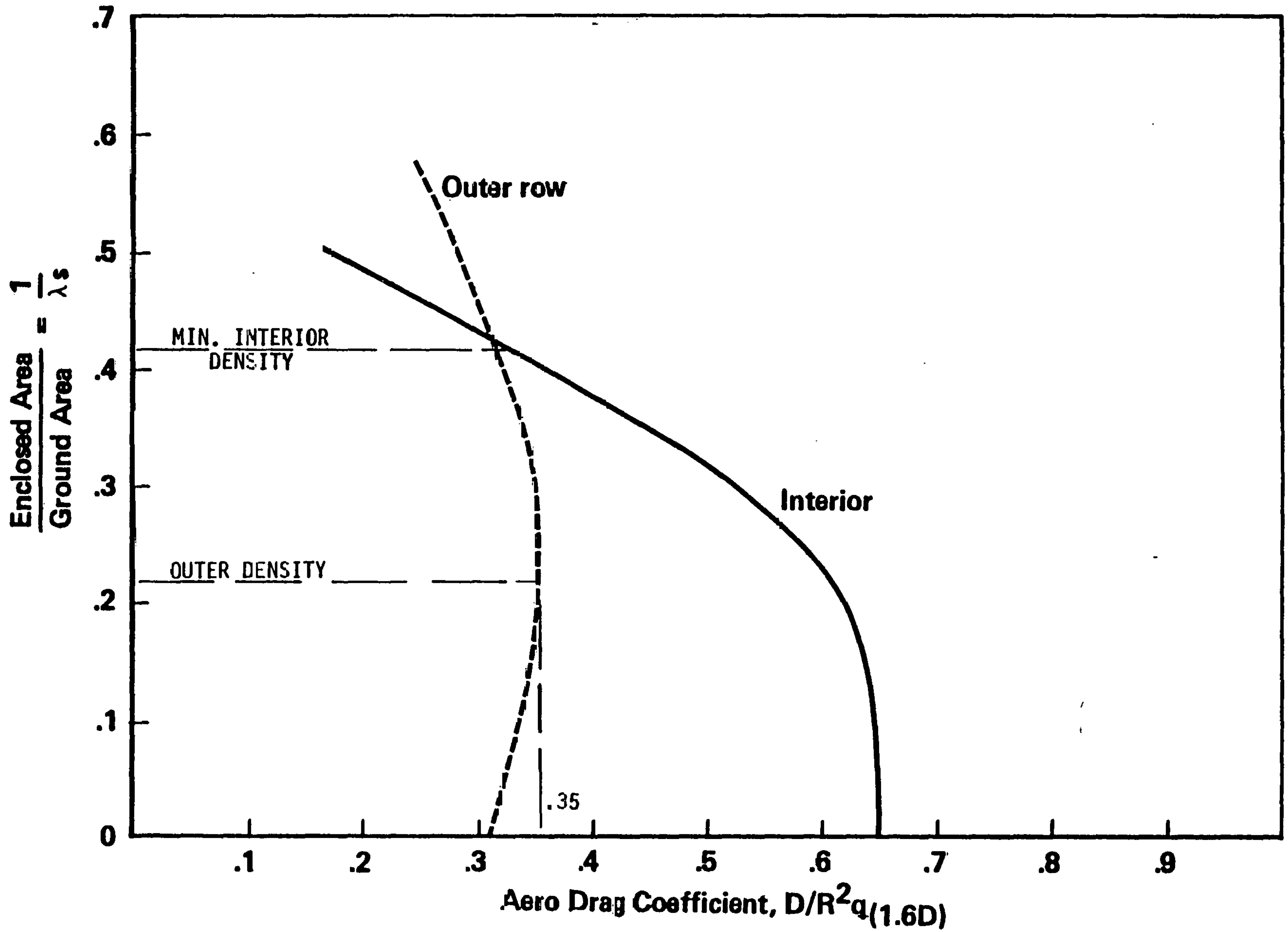

Enclosure Analysis

Transparent enclosure size is controlled by wind velocity and the allowable stress of the membrane material. The design nomograph obtained from the Heliostat Wind Tunnel Test Program, (Figure 2.3.2.3-3), permits determination of the allowable enclosure size based on array density, enclosure configuration, and enclosure material allowable strength.

Mechanical properties for weatherized oriented polyester supplied by the manufacturer gives a typical average value yield strength of 100 MN/m^2 (14,500 psi) with a reduction to 75.8 MN/m^2 (11,000 psi) at maximum design temperature (132^oF). Limited room temperature testing at Boeing has verified this data. Figure 2.3.2.3-4 shows a typical stress strain curve comparing Boeing test data with the manufacturer's test data. From Figure 2.3.2.3-3, at an array density of 0.22 and with an allowable membrane stress of 75.8 MN/m^2 (11,000 psi), the 9.69 m (31.8 ft.) diameter enclosure requires a membrane thickness of 0.003 inches.

Analysis of enclosure deflection was correlated to actual measured test deflection of the research heliostats at Boardman, Oregon. The data was then scaled linearly with dome diameter and as the square of the wind velocity. The analysis, as given by Reference 2.3.2.3-3, shows very little difference in deflected shape between truncated base angles of 50^o and 45^o. Accordingly, the base angle for the selected configuration has been reduced to 45^o which considerably reduces the size and cost of the base ring and dish structure. The deflected shape, with a maximum deflection of 5.31 cm (2.09 in.) is shown in Figure 2.3.2.3-5.

Internal Pressure Loads - The internal air pressure maintains the spherical integrity of the enclosure shape under maximum wind conditions. A pressure of 0.689 KN/m^2 (0.1 psi) exceeds the maximum 90 mph wind stagnation pressure.

Snow and Ice Loads - Specification 001 requires survival under a snow load of 250 Pascals (5 lb/sq ft.) and survival under a deposited ice layer 5.1 cm (2 in.) thick. It is assumed that snow and ice are deposited in a cosine distribution on the upper hemisphere. Pressure on the dome due to this coating of snow or ice is only 35 percent of the internal pressure.

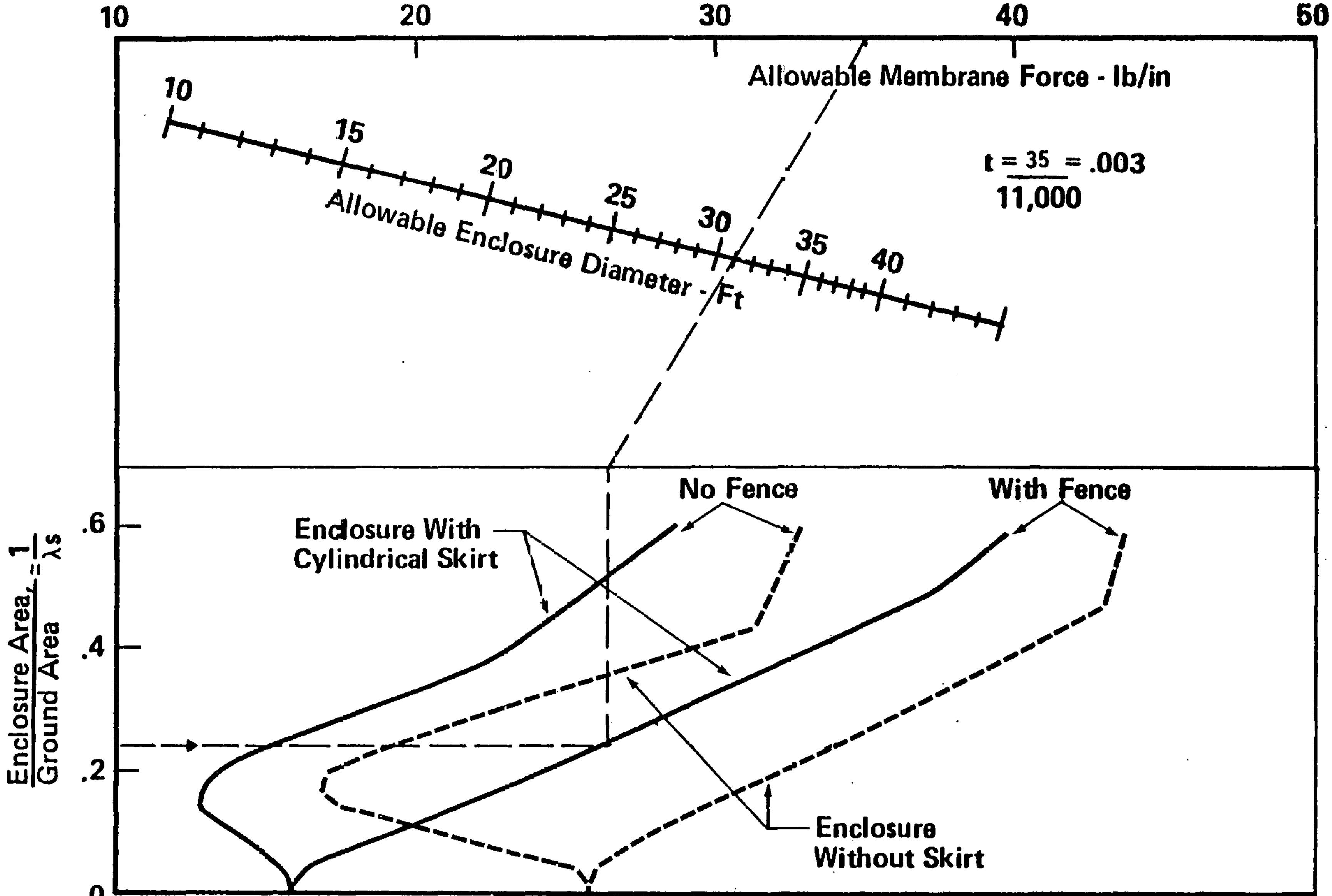

Figure 2.3.2.3-3 Allowable Enclosure Diameter From Wind Tunnel Test Results

Figure 2.3.2.3-4 Stress-Strain Curves for Weatherized Oriented Polyester

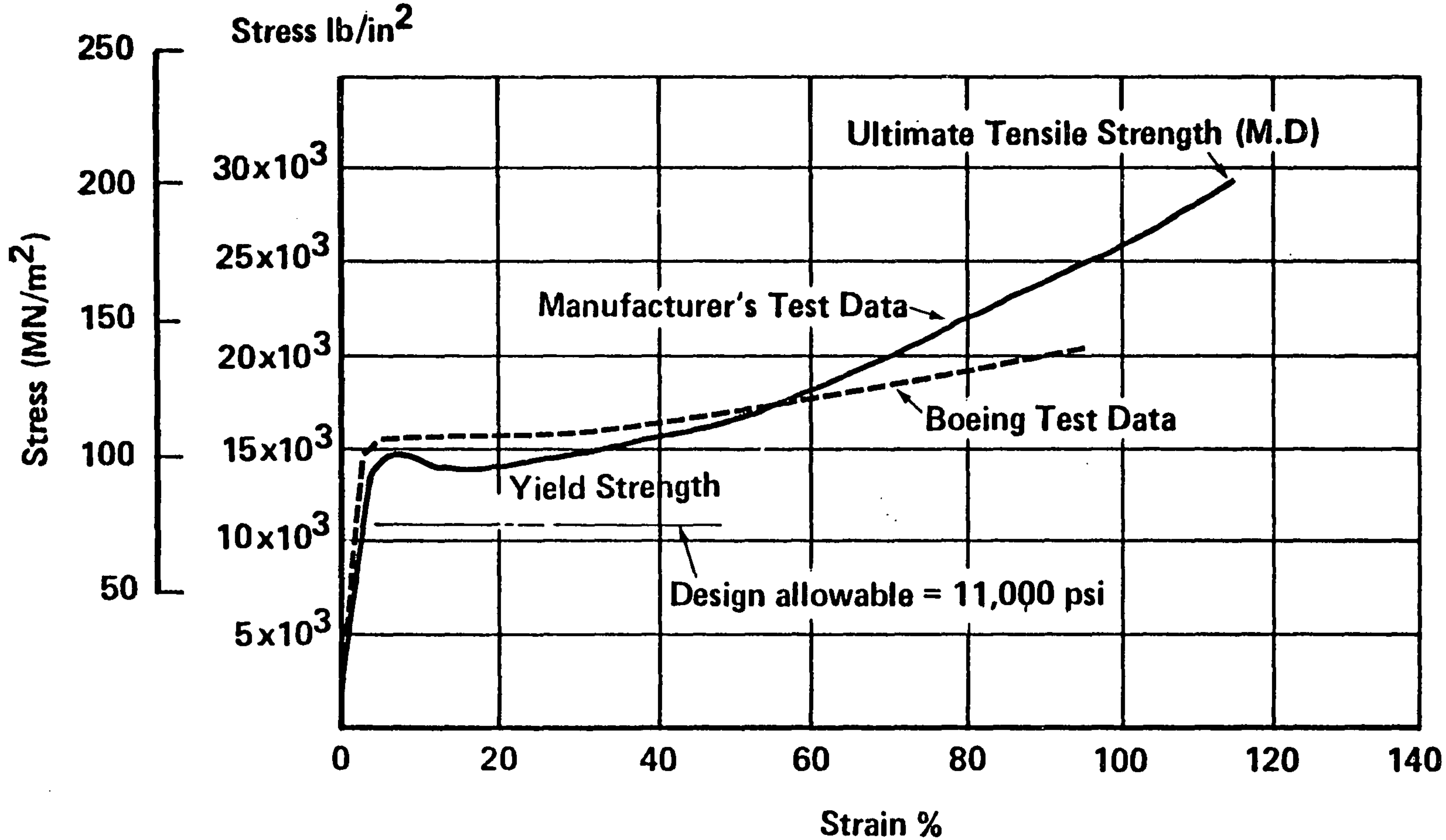

Figure 2.3.2.3-5 Dome Deflections at Peak Survival Wind Velocity

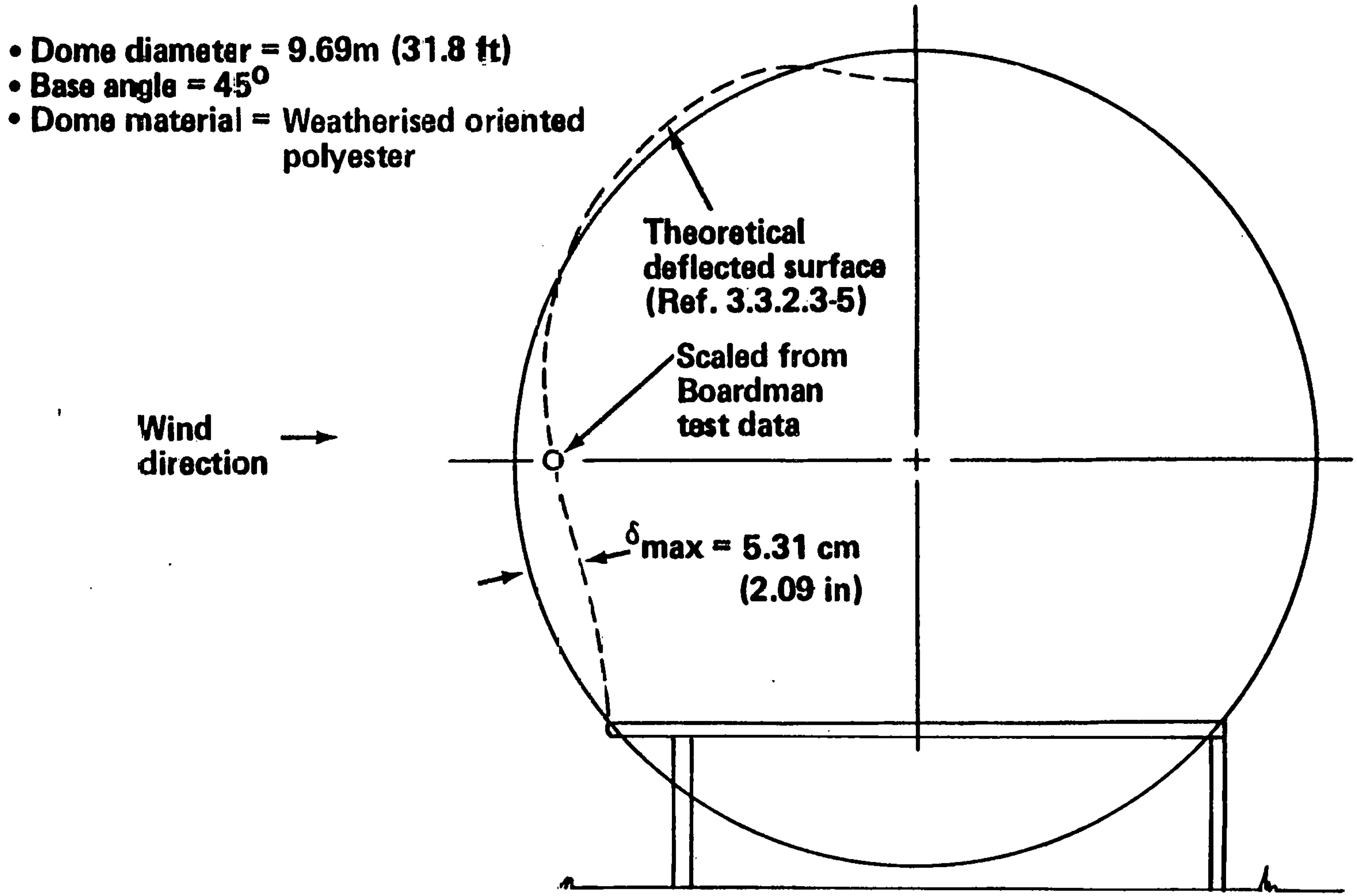

Earthquake Loads - An earthquake analysis of the enclosure using the uniform building code approach (Reference 2.3.2.3-4) has been made. Using the most conservative values for all coefficients gives an equivalent lateral force of 0.53 g's for Zone 4 Earthquake Design. Applying this acceleration to the mass of the enclosure, plus the mass of the enclosed air, results in a lateral force of 309 Kg (682 lb.) and a radial deflection 32 percent of that caused by the peak survival wind. Film stresses, due to earthquake loading, will be considerably less than that for the design maximum wind condition because the larger non-uniform aerodynamic pressure distribution will not be present.

Hail Loading - Specification 001 requires survival without damage of 25 mm (1 in.) hailstones at a velocity of 23 m/s (75 fps). Reference 2.3.2.3-6 documents the Boeing hailstone test program. The test results are shown in Table 2.3.2.3-1. These results show no penetrations at specification conditions for any of the materials tested. The minimum velocity required to cause penetration was 140 percent of the terminal velocity (75 fps). The larger hailstones did cause small indentations in the enclosure materials, as shown in Figure 2.3.2.3-6. Analysis of the environment and the effect of indentation show (see Figure 2.3.2.3-7) an optical transmittance loss after 15 years of 0.1 percent to 1.6 percent for the average and maximum areal density of hailstorms, respectively.

Table 2.3.2.3-1 Hailstone Test Results
(3/4 inch Diameter Hailstones)

					DAMAGE				
MATERIAL	Film Thickness (Mils)	Hailstone Weight Avg. (Grams)	Angle From Normal Incidence	Velocity (FPS)	Indentation Diam. (Inches)	Specular Transmittance (%)	Loss In Yield Strength (%)	Loss In Ultimate Strength (%)	Velocity at Failure (FPS)
TEDLAR (Polyvinyl Flouride)	4	7.9	0°	76.3	.40	56	0.7	0.9	122
• In Laboratory		8.8	45	74.8	[1]	--	---	---	---
		8.6	60	74.8	NONE	--	---	---	---
• On Heliostat In Field	4	8.0	0°	76.2	.39	--	---	---	106
		8.1	45	77.3	[1]	--	---	---	---
		7.9	60	77.3	NONE	--	---	---	---
MELINEX O (Polyester)	2	8.4	0°	74.8	.37	77	2.9	0	113
		7.3	45	74.8	NONE	--	---	---	---
		9.1	60	73.4	NONE	--	---	---	---
PETRA A (Polyester)	5	7.5	0°	74.3	.23	71	0	0	104
		9.0	45	74.3	NONE	--	---	---	---
		---	60	----	----	--	---	---	---
POLY CARBONATE	3.5	7.8	0°	73.4	.46	24	0	9.5	>117
		7.0	45	73.4	NONE	--	---	---	---
		---	60	----	----	--	---	---	---

[1] Fine Scratch Lines, ½ inch long

Figure 2.3.2.3-6 Hailstone Test Results

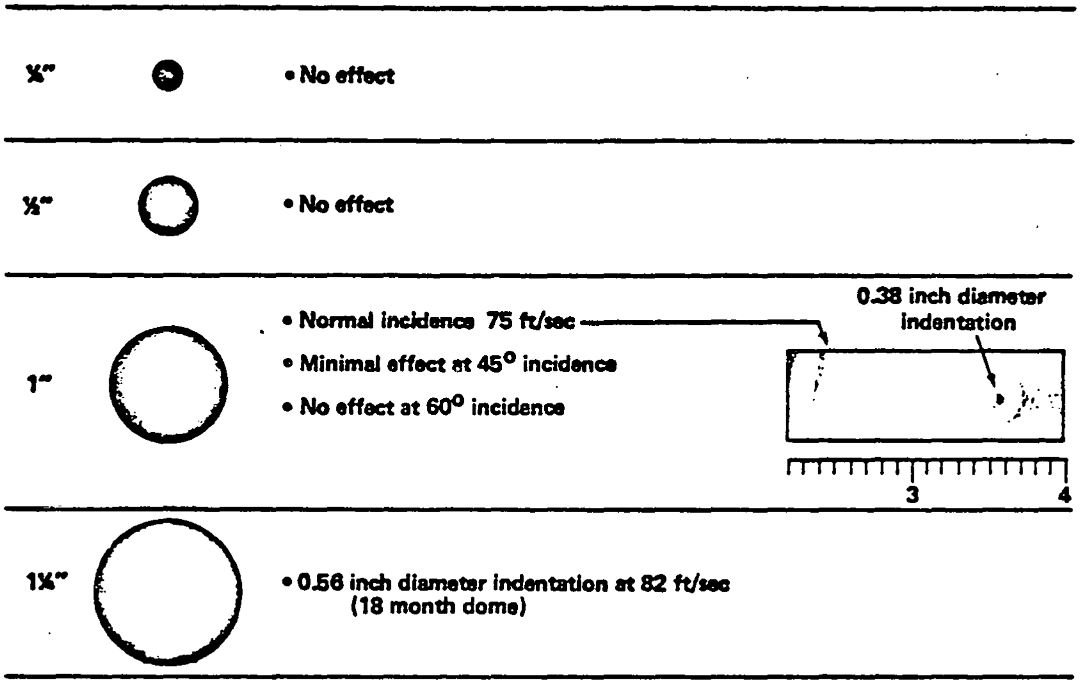

Figure 2.3.2.3-7 Effect of Hailstone Environment on Optical Performance

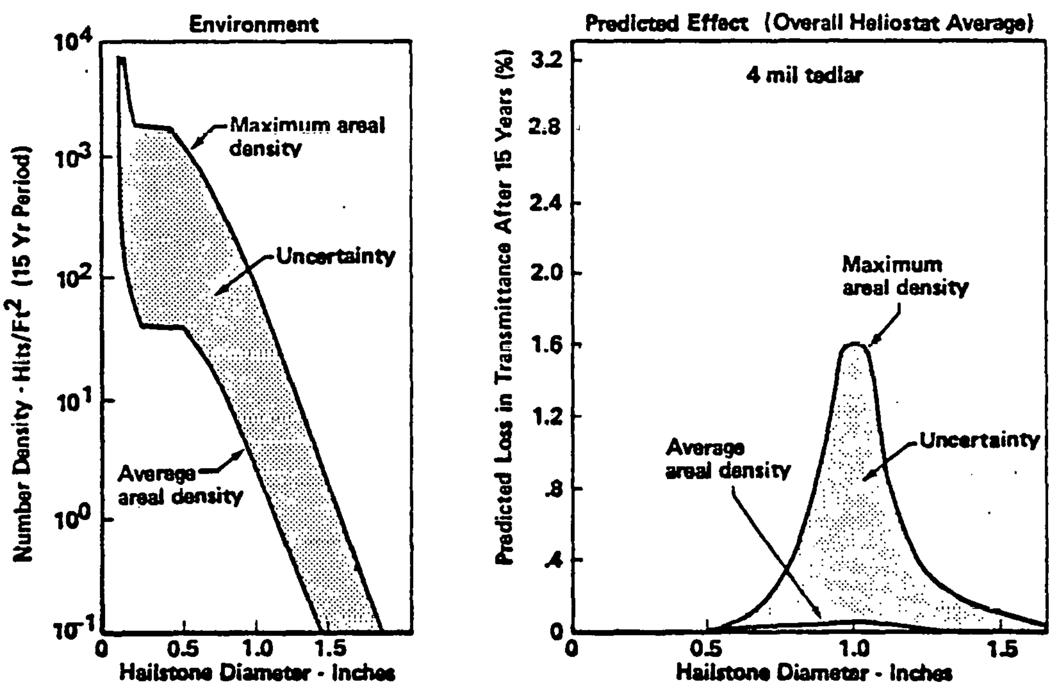

2.3.3 Base/Foundation

2.3.3.1 Configuration

The base/foundation (see Figure 2.3.3.1-1) consists of a base dish welded to a ring and support stanchions which transmit the loads to concrete foundation piles in the ground. The base dish provides for attachment of the dome and completes the spherical pressure enclosure. Air loads on the enclosure are transmitted to the piling through the ring and stanchions.

This recommended configuration was evolved from trade studies which evaluated variations of several basic concepts such as shown in Figure 2.3.3.1-2. Designs were screened on the basis of relative manufacturing, installation and operation and operating costs. Figure 2.3.3.1-3 shows a cost comparison of two basic concepts. Concept No. 1 has the features of the recommended configuration while Concept No. 2 represents the configuration of the Boeing research heliostats. At the high production/installation rates, Concept No. 1 can be highly automated and results in a considerable cost reduction. Further considerations in the comparison are listed in Table 2.3.3.1-1. The most significant (other than cost) advantages of Concept No. 1 are:

1) It provides a nearly airtight enclosure resulting in low pressurization airflow and a minimum of dust contamination of the mirror.
2) The total heliostat can be efficiently assembled in the factory eliminating field assembly.
3) Factory assembly will minimize initial internal contamination.
4) Augered, grouted piling is adaptable to automated high-rate installation.

The following is a description of the recommended configuration. The major components are:

- Three embedded concrete stanchion piles used for mounting protective enclosure support structure.

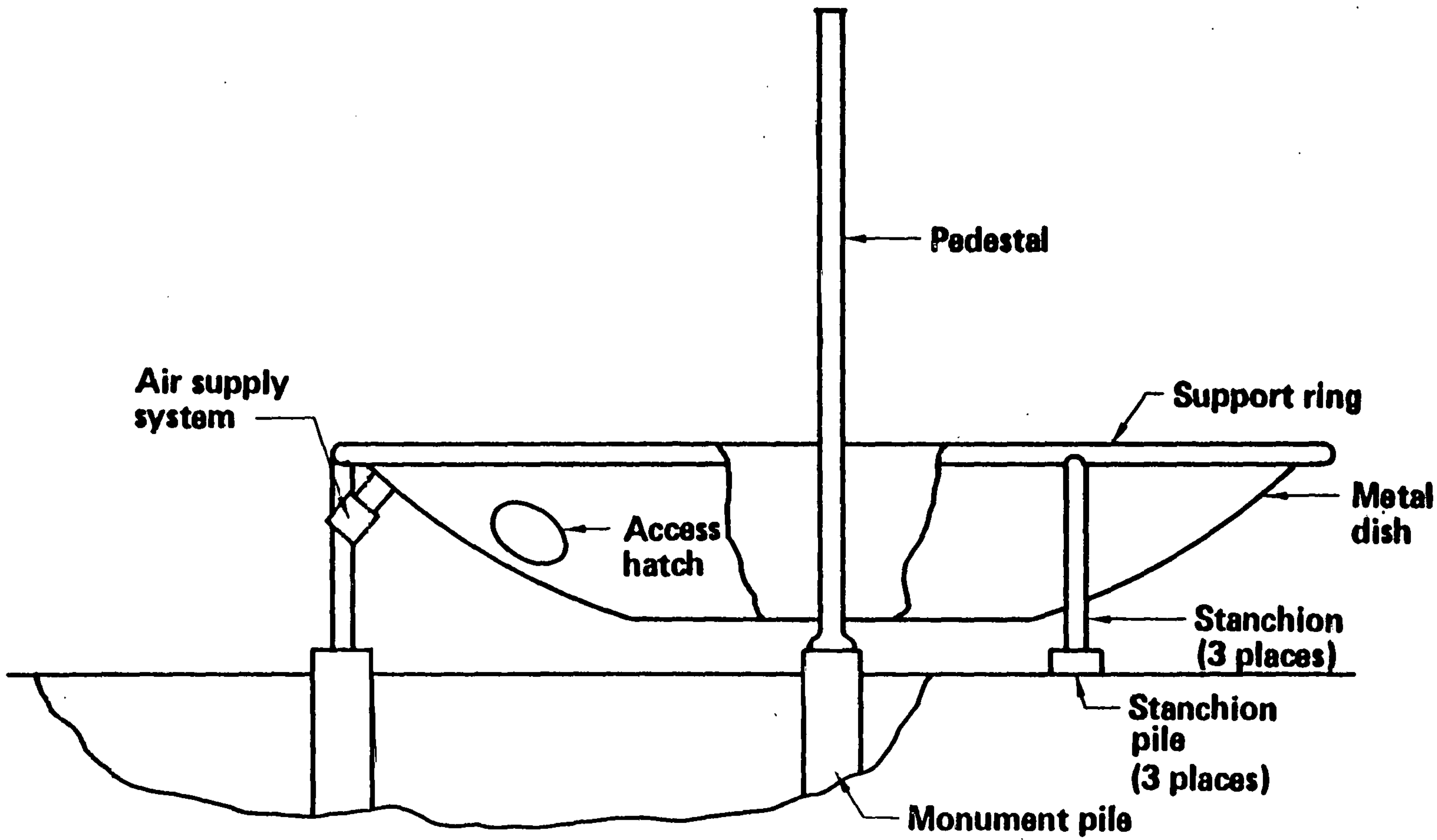

Figure 2.3.3.1-1 Base Foundation

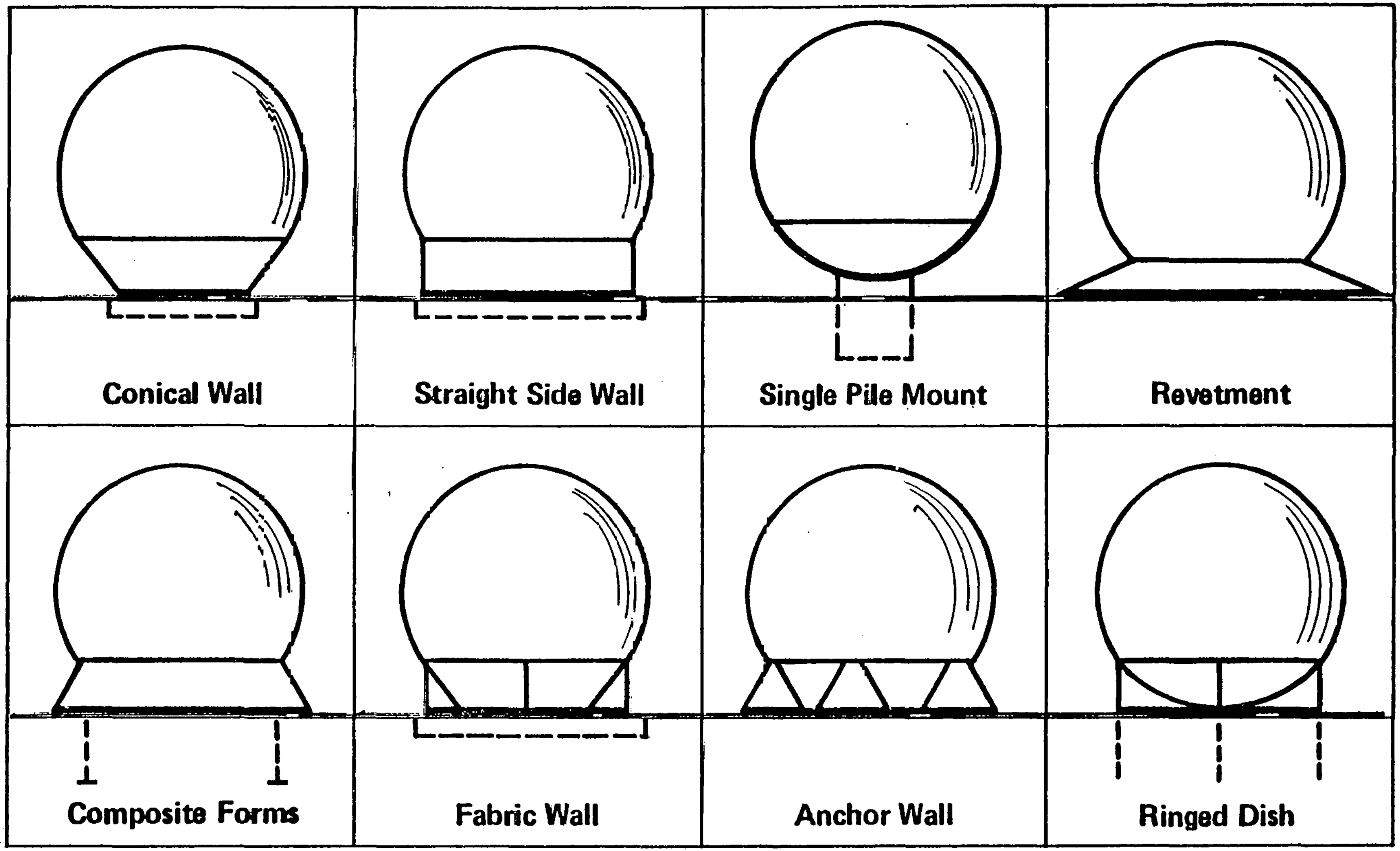

Figure 2.3.3.1-2. Concept Classifications

Concept No. 1

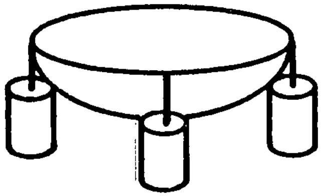

(Metal dish, pile support)

Concept No. 2

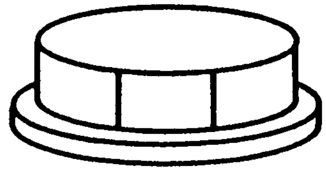

(Steel sidewall, concrete slab)

Costs
(@ 250,000 units)

Concept No. 1	Concept No. 2
Manufacturing (1.00)	Manufacturing (1.28)
Installation (1.00)	Installation (1.56)
Operating (1.00)	Operating (1.50)

Figure 2.3.3.1-3. Concept Analysis Relative Cost Comparison

Items	Concept 1	Concept 2
Pedestal isolation	Low mechanical coupling	Moderate mechanical coupling
Site preparation	Minimum	Moderate
Contamination	Low (minimum air flow)	Medium (high air flow)
Maintenance	Minimum internal cleaning (low contamination)	Scheduled internal cleaning (medium contamination)
	Filter replacement minimum	Filter replacement scheduled
Erosion	Minimal effect on foundation	Potential for continual settlement of foundation
Corrosion	Minimum - zero ground contact	Susceptible - ground level contact
Parasitic power	Low consumption (designed in air flow)	High potential consumption (difficult to seal)
Design versatility	Adaptable to various subground structures	Limited to slab type subground structure
	Potential for total factory assembly of heliostat	Limited to on-site assembly

Table 1.3.3.1-1 Further Considerations

- One embedded concrete monument pile used for mounting the reflector assembly support structure.
- A spherical segment preformed metal dish.
- A metal pipe support ring and stanchions which transmit enclosure leads to the stanchion piling.
- A steel pipe pedestal which supports the reflector assembly.
- An air supply system which maintains the internal pressure and filters the supply air.

Approximately 3975 Kg (1,800 lbs.) of steel and 0.84 m^3 (1.1 $yds.^3$) of concrete are used in the fabrication of these components, which are described in the following paragraphs and shown in Figure 2.3.3.1-1.

Pile Design and Installation

All four concrete piles have a 35.6 cm (14.0 in.) diameter. The three stanchion piles are embedded 2.4 m (8.0 ft.) below ground level. The monument pile is embedded to a depth of 1.8 m (6.0 ft.). The above dimensions assure that adequate soil adhesion is developed to resist the forces generated at the pile surfaces by the gravity forces and maximum wind loads. Each pile is capped with a steel plate. The method of anchoring the steel cap plates by stud welding to the rebar cage is presently under review. An optional method of anchoring consists of using three or four 1.58 cm (5/8 in.) diameter, headed studs, which are 19.05 cm (7.5 in.) long. These studs would be stud welded to the caps. This approach should provide a cost savings in both installation and materials.

An automated procedure having a 40 heliostat foundations/per day/per machine capability has been developed for the installation of the augered piles (see Section 3.0). This procedure will maintain the placement tolerances depicted in Figure 2.3.3.1-4, and does not require extensive site preparation.

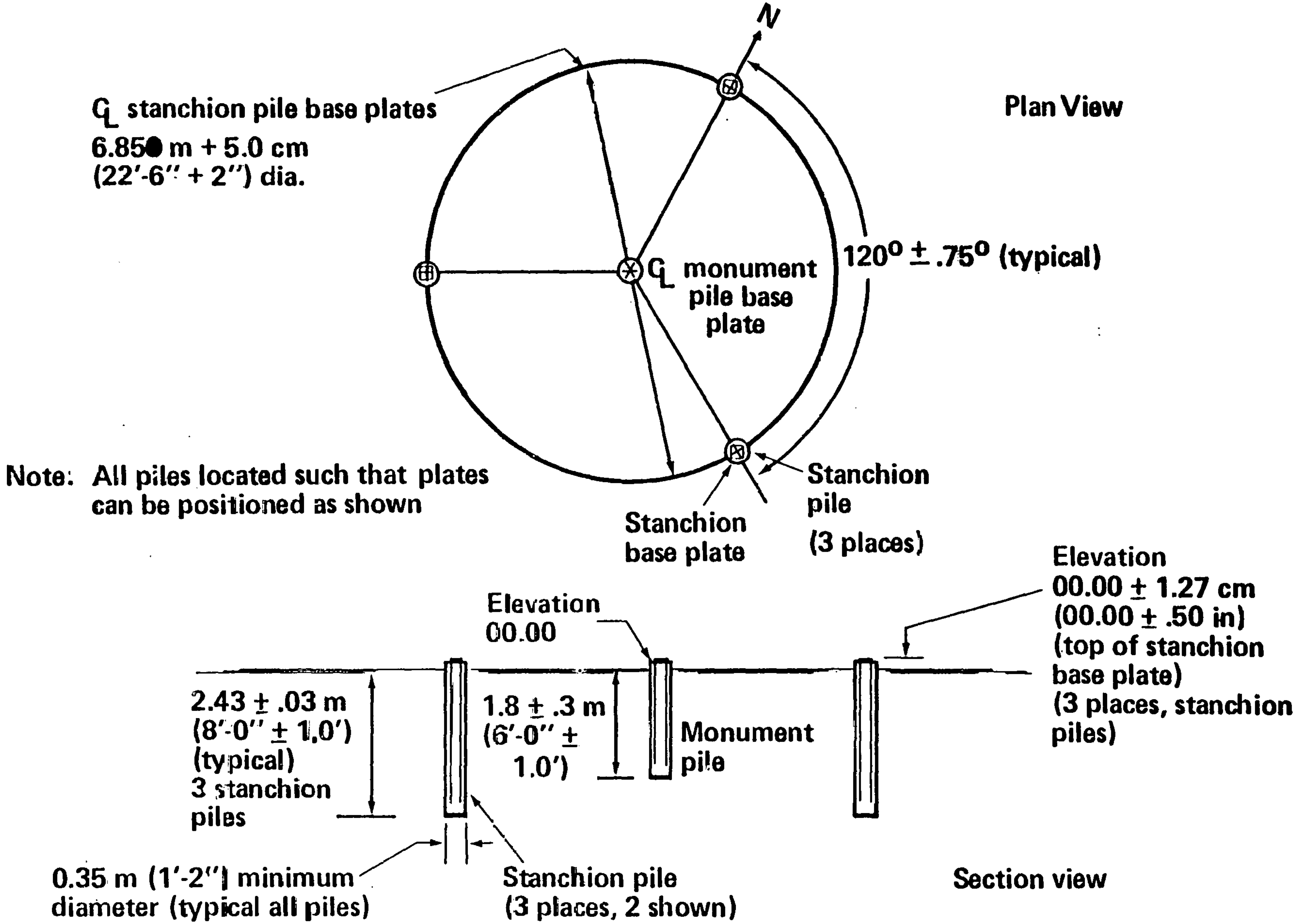

Figure 2.3.3.1-4. Pile Plot Plan

Support Ring and Stanchions

The support ring and stanchions transmit enclosure loads to the stanchion piles (see Figure 2.3.3.1-5). The choice of pipe material and size was determined by a stress/deflection analysis versus cost. This optimization resulted in a standard 10.16 cm (4.0 in.) pipe for both the ring and stanchions.

Preformed Metal Dish

To capitalize on the inherent advantages of factory assembly line rates and low costs, the dish is designed for press forming. Using present metal technology, it is estimated that a dish can be formed with a resultant average thickness of 0.066 cm (0.026 in.). This results in a dish weight of 226.5 kg (500 lb.). At present, a study investigating the possible substitution of a fabric dish is underway but it is premature to provide comparisons between metal and fabric at this time.

The access hatch located on the dish is eliptical in shape. This has the dual advantage of an inside pressure augmented sealing force, yet allows complete removal of the hatch by rotating and tipping. This removal aspect provides rapid maintenance of the electronics package which is mounted on the inside surface of the hatch.

Pedestal

The standard five inch pipe pedestal provides a positive reference point for the gimble drive assembly. The importance of this reference point and its stability are reflected in the 14.12 cm (5.56 in.) outside diameter of the steel pedestal which allows only a 0.048 cm (0.019 in.) deflection during maximum dynamic loading conditions.

A grommet type seal is placed between the pedestal and dish. This seal minimizes the mechanical load coupling and also accommodates sliding movement between the above members during installation.

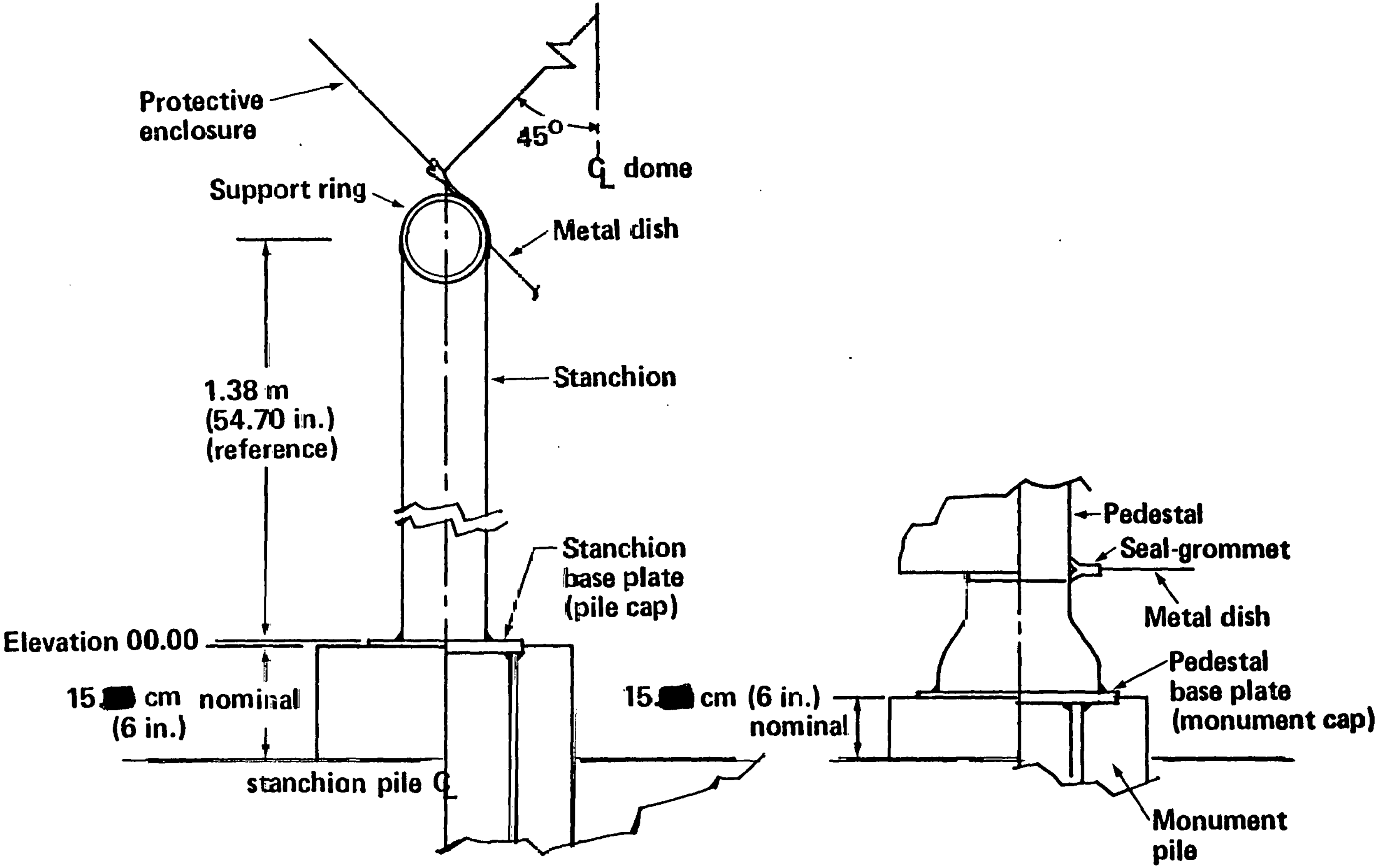

Stanchion Mount Detail

Pedestal Mount Detail

Figure 2.3.3.1-5 Base/Foundation Details

Air Supply System

The air supply system is designed to complement initial cleanliness of the factory assembled heliostats. This cleanliness is an inherent advantage of a controlled factory environment.

A survey of available filter system schemes led to the conclusion that the most cost effective way to reduce contamination and maintain reflector performance at minimized maintenance costs, was to drastically reduce air flow into the dome. Therefore, a design target leak rate of 0.006 m^3 per min (0.2 CFM) at a positive pressure differential of 0.5 cm Hg (0.2 in. Hg) has been set. However, imposed on this steady state leak rate is a possible intermittant flow requirement, due to changes in barometric pressure and ambient temperature. A psychrometric study has been initiated based on climatological data. The intent of this study is to establish the impact of climatological changes on air supply design requirements.

The system filter design is based on a light-scattering model of dust accumulation on the reflector. The model utilized long-term airborne particulate data from two locations in Arizona, and an average air flow of 0.014 m^3 per min. (0.5 CFM). The model assumed an allowable decrease of reflectivity of five percent in 15 years.

The study recommended a Gelman Type E prefilter, and a Gelman Acropor membrane filter of 0.45 micron pore size, or equivalent filters. For the high airborne particulate environment of the Phoenix area, the prefilter would be changed yearly and the membrane filter would be changed at the end of 15 years. For the low airborne particulate environment of the Grand Canyon area, the prefilter and the membrane filter would need replacement only after 15 years. The loss of reflectance with time is directly proportional to the airflow rate. At 0.2 CFM the loss in reflectance would be two percent. The detailed analyses using this model are included in Appendix C.

The remaining effort for Phase I will be directed at refining the air supply design and minimizing costs. With respect to this effort, a central air system is also being studied as an option.

Protective Enclosure Retention

The interface between the protective enclosure and the base/foundation is discussed in Section 2.3.2 "Protective Enclosure."

Finishes

The above ground base structure will be primed and painted with synthetic white enamel. This includes the interior of the dish.

Installation Welds

Anchoring of the heliostat assembly is accomplished by field welding the three stanchions and pedestal to the pile caps. The welding procedure and welder qualification will conform with those established by the "American Welding Society" for structural welds.

2.3.3.2 Structural Analysis

The lift and drag forces on the dome due to the maximum survival wind conditions are reacted at ground level by horizontal and vertical loads plus an overturning moment as shown in Figure 2.3.3.2-1. The overturning moment results in an up load on the windward side of the dome and a down load on the opposite side. These loads are reacted with adequate margin of safety by three concrete piles 35.56 cm diameter (14 in.) which are buried 2.44 meters (8 ft.) in the ground. The loads are transferred from the pile by side friction between pile and soil and by bearing pressure at ground level. Soil bearing pressure due to foundation weight is only 21.5 KN/m^2 (450 psi) and no soil stabilization is required.

The lift and drag forces on the dome are transferred to ground level by a circular support ring mounted on three vertical stanchions. The support ring is made from steel pipe and is designed by limiting bending between vertical supports. Figure 2.3.3.2-2 shows the stress levels and deflections for pipe sections between 8.89 cm O.D. (3.5 in.) and 13.97 cm O.D. (5.5 in.) due to 90 mph wind loads. Support ring deflection was limited to 13.2 cm (5.2 in.) in order to ensure adequate clearance between the dome and the reflector, with the reflector in the most adverse position. Four inch A.P.I. 5LX x 52 steel pipe (4.5 in. O.D.) was selected for the support ring material, to limit the ring deflection under load and also to achieve the lowest cost design for the heliostat support structure. Figure 2.3.3.2-2 shows that with this pipe section, the stress levels are below the yield stress of the material and that adequate clearance is ensured at maximum survival wind condition.

The support ring is welded to the top of the stanchions which are also made from the same 4" diameter pipe material. The bottom of each stanchion is welded to a 1.27 cm (1/2" thick) A.537 steel base plate mounted on top of the concrete pile (see Figure 2.3.3.2-1). The base plate is welded to four 1.59 cm diameter (5/8 in.) A615 steel rebars embedded full depth in the concrete pile.

The stanchions transfer horizontal shear, and vertical loads, from the support ring to ground level. The loads cause bending, direct tension, and shear

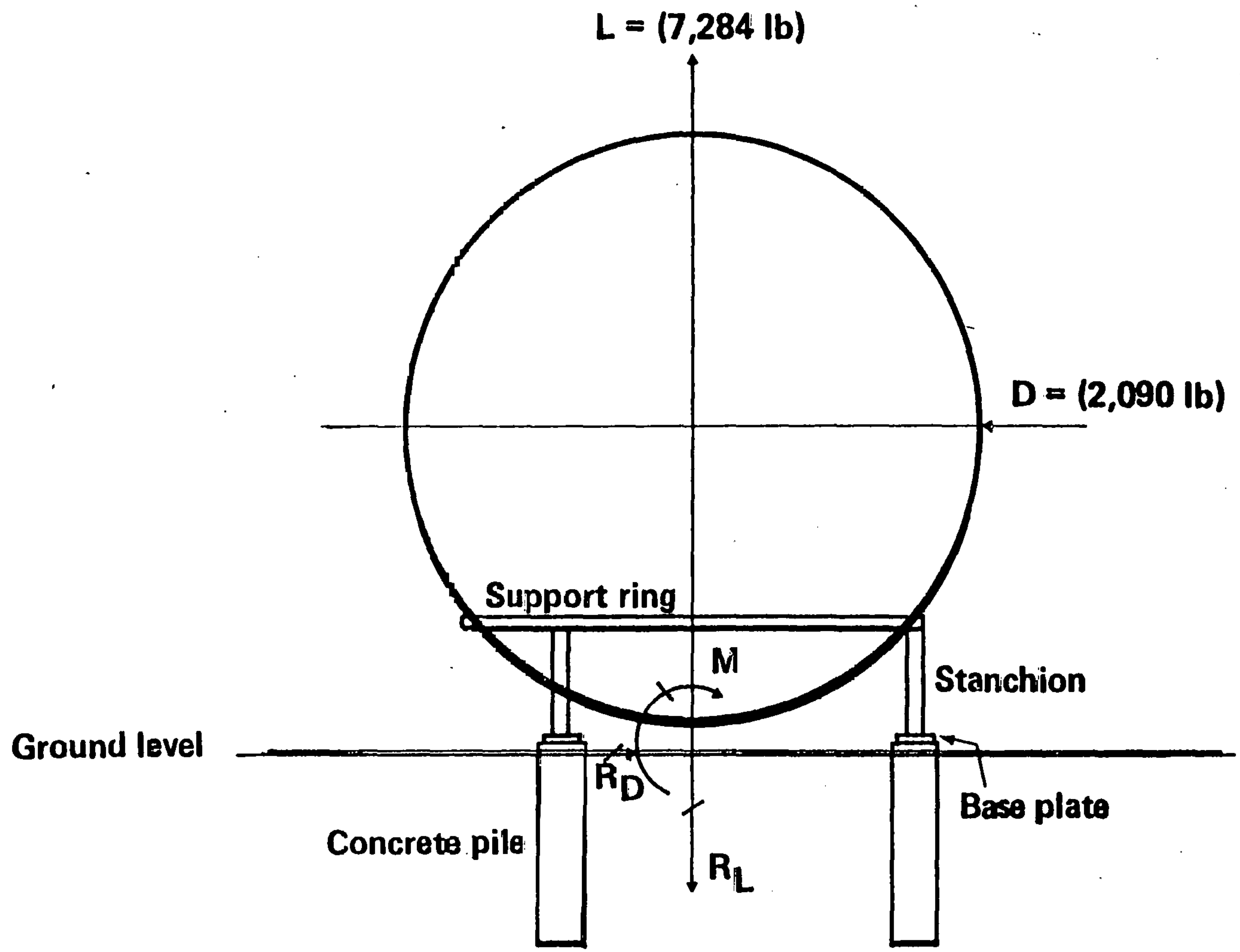

Figure 2.3.3.2-1 Heliostat Base Support Loads

Figure 2.3.3.2-2 Stress and Deflection
Heliostat Support Ring Mounted on 3 Piles

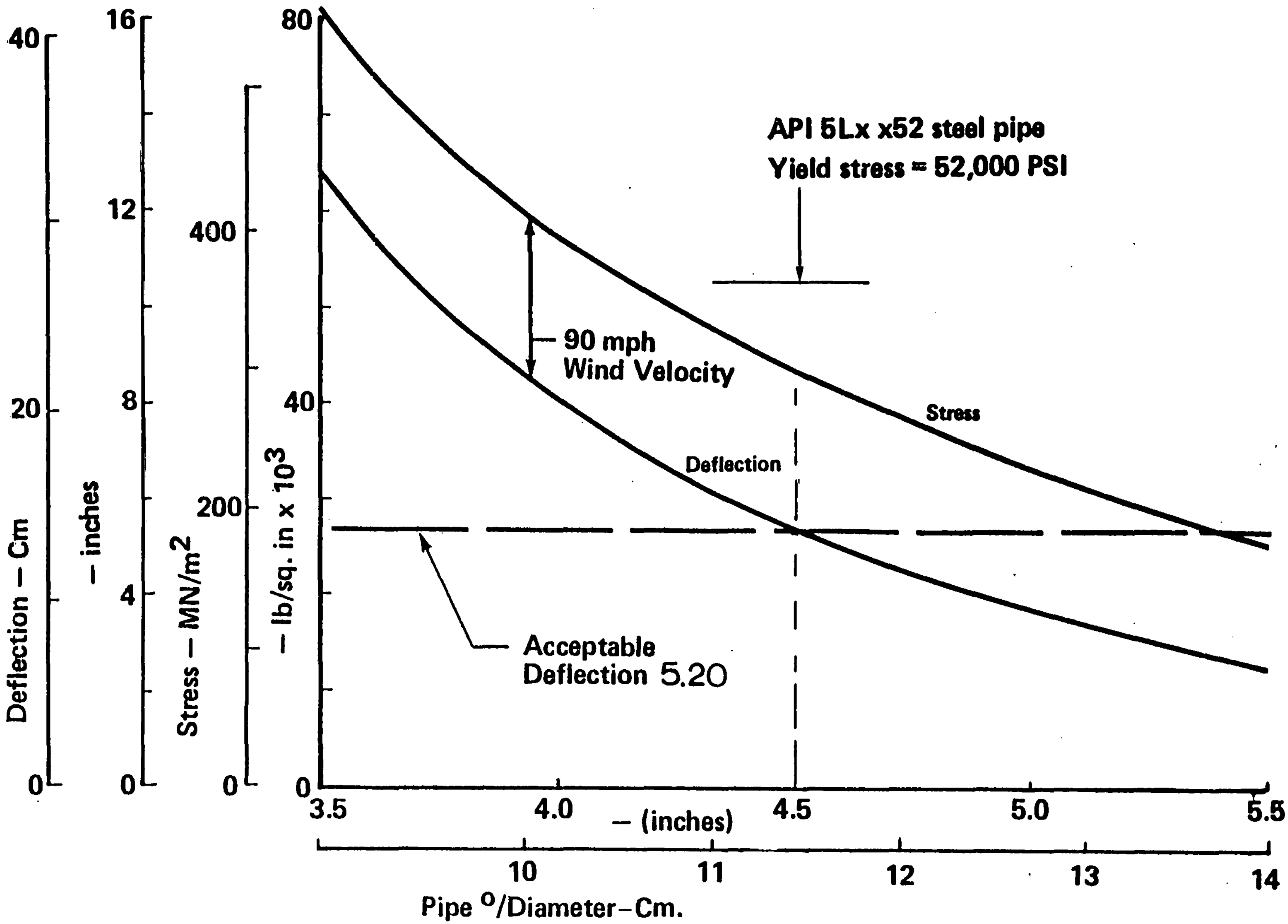

stresses in the stanchion. Stress level in the 4 in. pipe section is 91.63 MN/m^2 (13,290 psi), well below the 358.5 MN/m^2 (52,000 psi) yield strength of the material.

The stress level at the weld between stanchion and base plate is 154.4 MN/m^2 (22,391 psi) due to the maximum survival wind condition. This is safely within the allowable value of 165.5 MN/m^2 (24,000 psi) for fillet welds proposed in Table 1.5.3 of the Manual of Steel Construction.

2.3.4 Reflector Assembly

2.3.4.1 Configuration

The reflector assembly consists of a bi-axially stretched reflective aluminized polyester membrane bonded to a light-weight circular aluminum frame. (See Figure 2.3.4.1-1.

The overall diameter of the reflector assembly is 9.3 m (30.5 ft.) This size was selected on the basis of the cost/performance optimization as discussed in Section 2.3.1.3.

The design is further optimized by gravity focusing the reflective membrane. Gravity focusing is accomplished by pretensioning the reflective membrane during assembly. This procedure results in a controlled sag due to gravity. The controlled sag produces a parabolic reflector, with a predictable focal length. A 4.14 MN/m^2 (600 psi) pretension stress level is selected to produce a correct focal length for far field heliostat A. This focal length (pretension) provides best field performance when used for all heliostats in the array.

Reflector Frame

The reflector frame consists of three circular rim segments, three T-fittings, three spokes, and a center hub. The circular rim segments are produced by ram forming thin-walled, 12.7 cm (5.0 in.) diameter aluminum-alloy tubing. The spokes also use the same type of tubing. The T-fittings and center hub are aluminum alloy castings. The T-fittings couple the rim segments to the spokes. The spokes are located below the rim to provide reflector membrane clearance. The center hub is designed to attach with the spokes and also accomodate the Gimbal Drive System such that the Gimbal elevation axis closely coincides with the reflector frame center of gravity, thereby eliminating a counter-weight. The joints in the reflector frame are made by electromagnetic swaging. This method of joining has been utilized in a previous reflector assembly and represents a substantial savings in cost versus welded or conventional mechanical type joints.

Reflective Membrane

The reflective membrane is made by thermo/adhesive joining wide panels of aluminized polyester film. The film thickness if 0.005 cm (0.002 in.). Laboratory measurements have established a reflectance value of R = 0.91 and a joint ultimate stress of 105 MN/m^2 (15,190 psi).

Dispersion Errors

The frame is designed for stiffness to minimize the overall dispersion characteristics of the reflector surface. Analysis of the design indicates that the maximum dispersion angle is 0.0006 radians due to out of plane static sag of the frame (see Figure 2.3.4.1-2). The maximum frame sag occurs when the reflector is in the horizontal position. The sag diminishes as the reflector is rotated out of the horizontal plane, thereby reducing the dispersion angle.

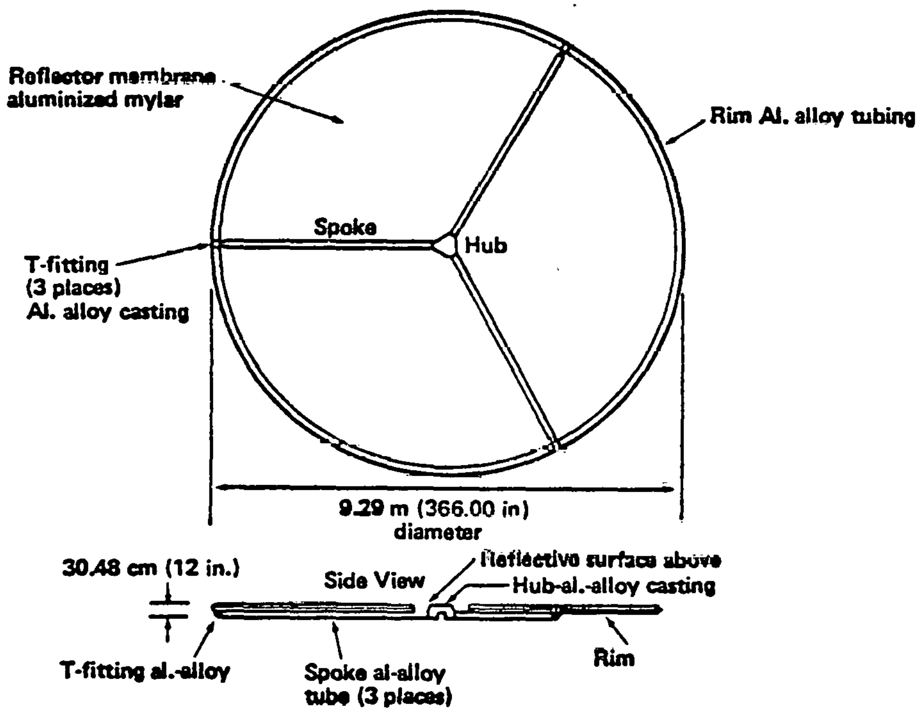

Figure 2.3.4.1-1. Reflector Assembly

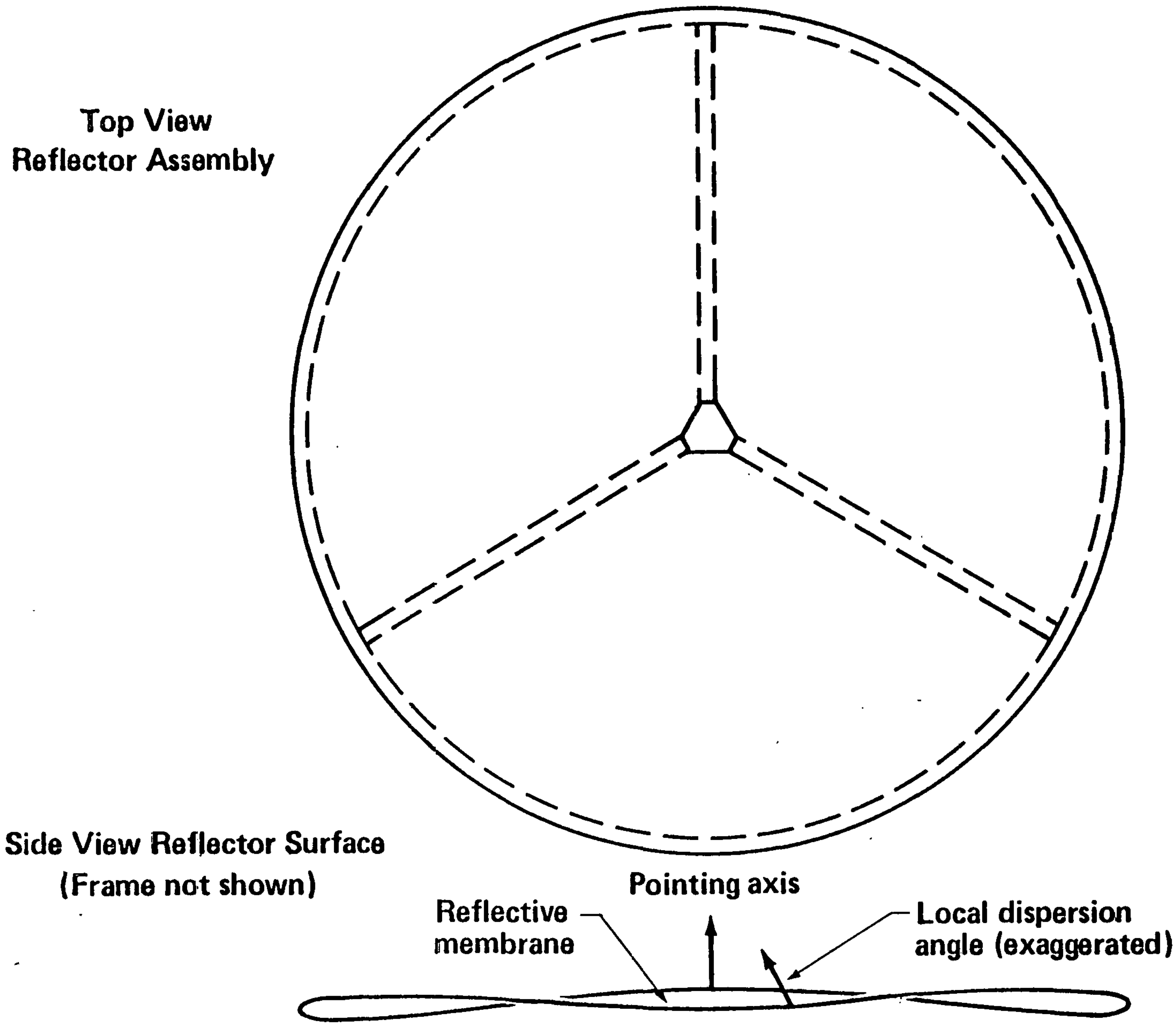

Figure 2.3.4.1-2 Dispersion Angle

2.3.4.2 Reflector Materials Evaluation

A weatherized polyester substrate (weatherized Mylar D, with Melinex "O" or Celanar 4000 as options) with an unprotected aluminum coating has been specified for the commercial plant reflector design. A weatherized substrate is specified because data obtained from previous research experiments (Ref. 2.3.4.2-1) revealed some mechanical property degradation of the reflective membrane substrate. Early studies showed that unprotected aluminized films do not degrade optically over long term (9 years) in a laboratory environment. Experimental data from Reference 2.3.4.2-1 revealed a slight amount of specular reflectance loss ($\sim$1% in 16 months). On this basis, development of a protective coating for aluminum was initiated in this effort, and will proceed as a continuing program to assure availability if required.

Testing has been performed and is continuing on metalized polyester films with protective coatings and weatherized substrates. Candidate films prepared cooperatively by industry suppliers were first screened for specular reflectivity and if promising were exposed to accelerated simulated sunlight testing. Those candidates showing most promise are tested for mechanical properties and subjected to real-time and accelerated outdoor desert exposure testing.

As discussed in Section 2.3.2.2, the start of material screening testing was delayed due to late delivery of candidate materials. New materials are still coming in for evaluation at the time of this report.

Table 2.3.4.2-1 lists the materials and respective suppliers for candidates received for test to date. To the right, in the appropriate columns, are shown the specular reflectances taken on the Boeing bi-directional reflectometer at 0.15^{o} cone angle with a 628 nanometer wavelength source. As can be seen, a variety of film processors are represented. The reflectance is, of course, generally higher as the cone angle is increased from 0.15^{o} upward. Figures 2.3.4.2-1 through 2.3.4.2-4 are plots of specular reflectance as a function of cone angle for the various candidates.

The overcoated material supplied by National Metalizing was provided with the explanation that the substrate material was a poorer quality than that which they had given us when attempting to optimize absolute

Table 2.3.4.2-1

SPECULAR REFLECTANCE FOR VARIOUS SUBSTRATE/COATING COMBINATIONS

MATERIAL	SPECULAR REFLECTANCE @ .15° CONE ANGLE; 633 NANOMETER SOURCE			
	UNSTABILIZED SUBSTRATE NO OVERCOAT	UNKNOWN SUBSTRATE OVERCOATED	STABILIZED SUBSTRATE NO OVERCOAT	UNSTABILIZED SUBSTRATE OVERCOATED
MYLAR (UNKNOWN DESIGNATION)-ALUMINIZED (NATIONAL METALIZING)				.68
MYLAR D - ALUMINIZED (NATIONAL METALIZING)	.88			
MYLAR D - ALUMINIZED (DUNMORE)	.86			
MELINEX 442 - ALUMINIZED (DUNMORE)	.83			.76
MELINEX O - ALUMINIZED (MARTIN PROCESSING)			.78	
MELINEX O - ALUMINIZED (MORTON CHEMICAL)	IN TEST			IN TEST
UNKNOWN POLYESTER SUBSTRATE (OPTICAL COATING LABORATORY)				
SILVERIZED	.88	.84		
ALUMINIZED		.65		

NOTE: ALL DATA SHOWN ARE SINGLE WAVE LENGTH DATA (633 NM). INTEGRATED AIR MASS 2 REFLECTANCE DATA ARE EXPECTED TO BE 3% HIGHER.

Figure 2.3.4.2-1. Specular Reflectance vs. Cone Angle

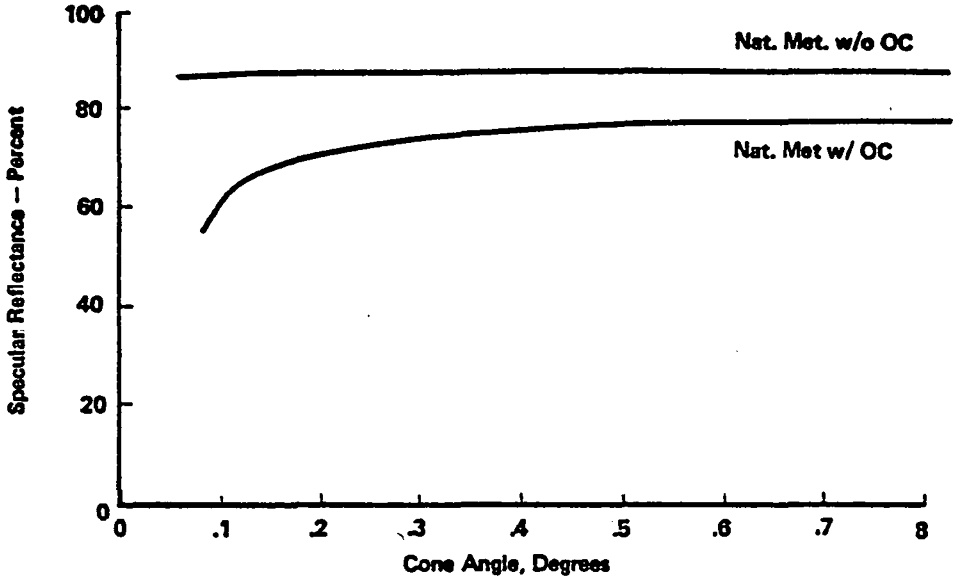

Figure 2.3.4.2-2. Specular Reflectance vs. Cone Angle

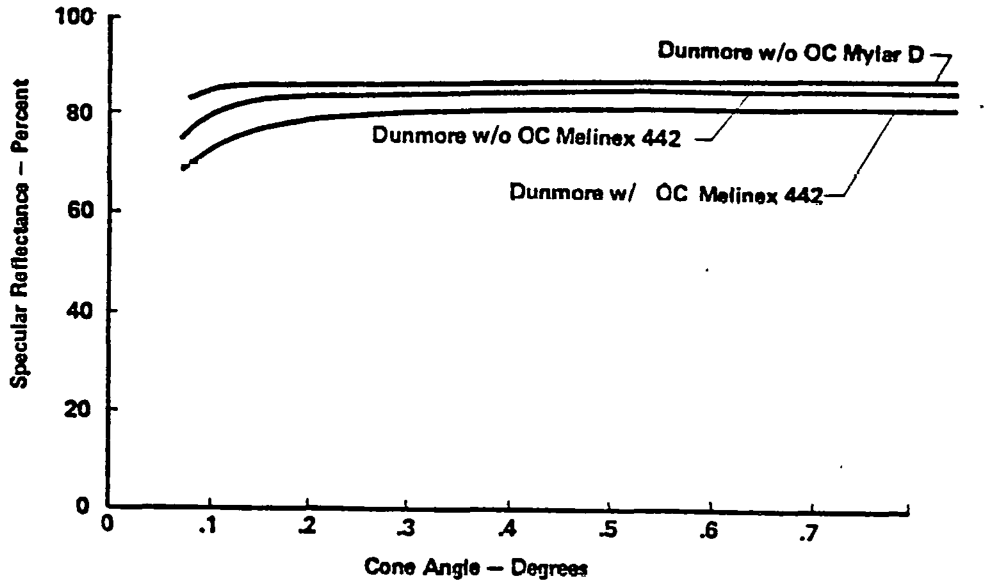

Figure 2.2.4.2-3. Specular Reflectance vs. Cone Angle

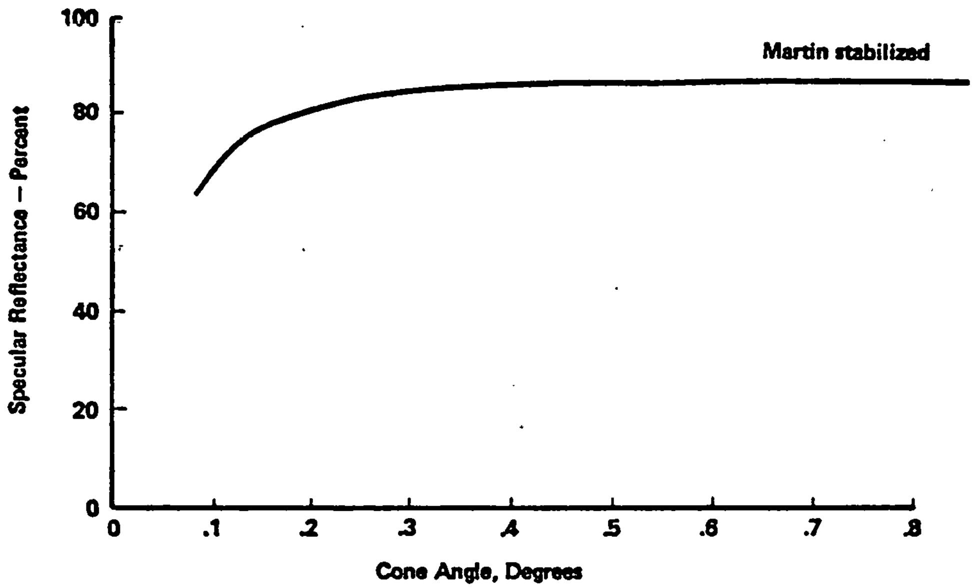

Figure 2.2.4.2-4. Specular Reflectance vs. Cone Angle

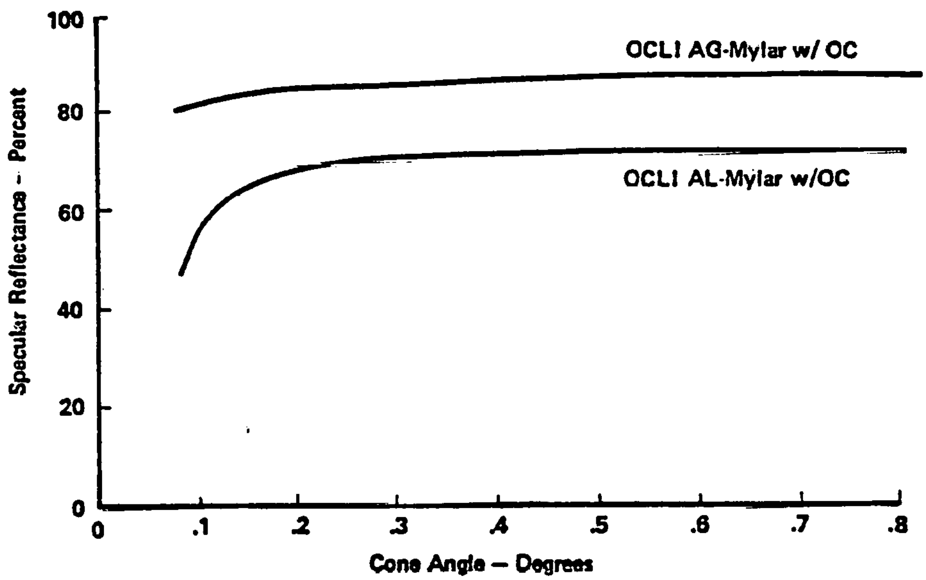

reflectance. The purpose of the candidate was for overcoating weatherability evaluation.

Dunmore provided Mylar D in earlier research and it was seen to have a reflectance of 0.86. For this effort, they provided candidates of overcoated and uncoated aluminized Melinex 442. As seen in the table, the loss in specular reflectance due to the coating was .07. This loss would probably be too great a penalty to pay regardless of protection provided.

The Martin Processing Melinex "0" with aluminum and no overcoating data shown in Figure 2.2.4.2-3 indicates that, while the reflectance is an acceptable .86 at cone angles of 0.4 and greater, the reflectance decreases below 0.4 and is only .76 at a cone angle of 0.15. This is possibly due to the stabilization process and its effect on the surface quality of the substrate.

Morton Chemical has recently provided aluminized polyester with and without overcoating for evaluation. Test results were not yet available at reporting time.

Aluminized polyester with overcoating and silverized polyester with and without coatings were provided by Optical Coating Laboratory. The aluminized material had low reflectivity at all cone angles and would not be a viable candidate as received. The silverized material is the most impressive of all the combinations evaluated thus far. As noted at the bottom of Table 2.3.4.2-1, the values of the table should be upward adjusted by about 3% because, from experience, integrated reflectance values are known to be higher than single wavelength values (628 nm) by about that amount. This then results in a specular reflectance of approximately .87 for overcoated silverized polyester.

From the initial reflectance data discussed above, the following preliminary conclusions may be drawn:

1) The highest reflectivity materials before coating were aluminized Mylar D (National Metalizing) and silverized polyester, both having approximately 91% reflectance. High uncoated (metalized) substrate values will be required to allow some loss due to subsequent coating and still retain adequate coated reflectance.

2) The Dunmore and National Metalizing overcoated samples were excessive in specularity loss from the coating process. Exposure testing will be performed to evaluate weatherability of coatings.

3) The Martin process appears to "roughen" the Melinex surface and reduce reflectance. Further development would be required to warrant continued evaluation of this material as a reflector candidate.

4) The coated material with the highest reflectance is coated silverized polyester supplied by Optical Coating Laboratory.

Accelerated simulated sunlight exposure tests have been performed. The results are only partially available at report time. The purpose of this testing is to attempt to obtain early indication of weatherability improvement by coating. Results will be provided in the final report. Samples have been prepared and will soon be sent to a facility for accelerated and real-time desert exposure to assist in predicting useful life. As they are received and screened, additional samples will be sent for desert exposure tests.

2.3.4.3 Structural Analysis

The reflector support structure consists of a circular ring 9.29 m (30.5 ft.) in diameter, and three radial support arms all made from aluminum tube 12.7 cm (5.0 in.) diameter with 0.198 cm (.078 in.) wall thickness. The radial arms are joined together at a central hub casting which is attached to the gimbal mounted on the vertical reflector pedestal. The hub casting accomodates the gimbal drive motors such as to eliminate the reflector imbalance about the gimbal elevation axis.

2.3.4.3.1 Design Loads

The reflective assembly is protected from the severe elements of the environment (wind, snow and ice) by the protective enclosure. Design loads are due to membrane tension, gravity, temperature, reflector drive, and earthquake. These loading conditions are discussed below.

2.3.4.3.1.1 Membrane Tension

The reflective membrane is tensioned by pre-stretching to a uniform biaxial tension of 4.14 MN/m^2 (600 psi) and bonding to the circular support ring. Polyester material of 0.05 mm (.002 in.) thickness is used for the reflective membrane. Prestress in the membrane is low compared to the material yield stress of 100 MN/m^2 (14,500 psi). Therefore, long term creep effects will not cause significant loss of membrane tension.

Variations in temperature and humidity will cause changes in membrane stress. Differential expansion of the polyester and aluminum support structure over an extreme temperature range of 60°C (140°F) to -30°C (-20°F) will result in a change of plus or minus 30 percent from the nominal membrane stress of 4.14 MN/m^2 (600 psi). The effect of humidity on membrane stress is less pronounced than that of temperature. It tends to reduce the effect of temperature because relative humidity tends to decrease as temperature increases.

2.3.4.3.1.2 Gravity Loadings

A convenient way of expressing reflector membrane deflection in relation to performance is given by the reflector focal length corresponding to the parabolic deflection mode that the membrane assumes. Figure 2.3.4.3-1 shows focal lengths for a uniformly stretched circular membrane as a function of membrane stress and angle of tilt of the reflector plane from vertical. Focal length is independent of membrane thickness and diameter. Focal lengths as indicated in the figure were included in performance optimization studies which resulted in selection of the 4.14 MN/m^2 (600 psi) membrane prestress. The axis of the deflected parabolic surface remains essentially normal to the plane of the reflector support ring, regardless of the angle of tilt. Therefore, gravity deflections will not significantly affect beam pointing accuracy.

The reflector structure was analysed using a Nastran Computer Program for loads due to gravity, temperature, and membrane tension. Figure 2.3.4.3-2 shows the "Math Model" for this analysis. Stress levels were found to be very low and the structure is designed by stiffness. With the reflector horizontal, the maximum out-of-plane deflection of the circular ring between support arms, due to the combined loading condition, is 0.19 cm (0.075 in.) (see Figure 2.3.4.3-3). This is the displacement of grid point 101 relative to grid point 105. This deflection causes a maximum angular deviation of a small portion of the reflector surface from the normal reflector plane of 0.012° which will have negligible effect on performance. The vertical deflection at the ends of the support arms causes a rigid body downward translation of the ring of 3.4 cm (1.34 in.). Adequate clearance (0.85 cm) between the reflector plane and the central mounting hub is provided to accommodate, without interference, the vertical deflection of the ring plus sag of the membrane.

Stress levels in the central mounting hub are also low, but in order to limit the reflector ring deflection the minimum bending section through the hub is designed to maintain the stiffness of the basic support arm.

The reflector pedestal is made from a five inch diameter A.P.I. 5LX x 52 steel pipe. The base of the pedestal is bell shaped to a 8.625 inch diameter.

Figure 2.3.4.3-1 Reflector Focal Length

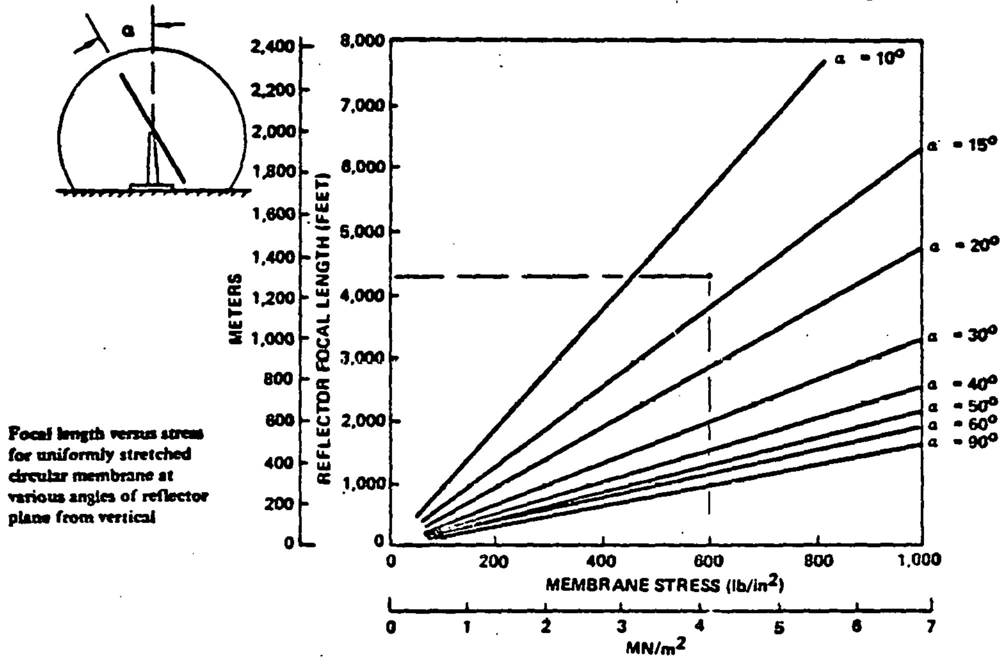

Figure 2.3.4.3-2 Reflector Structure Math Model

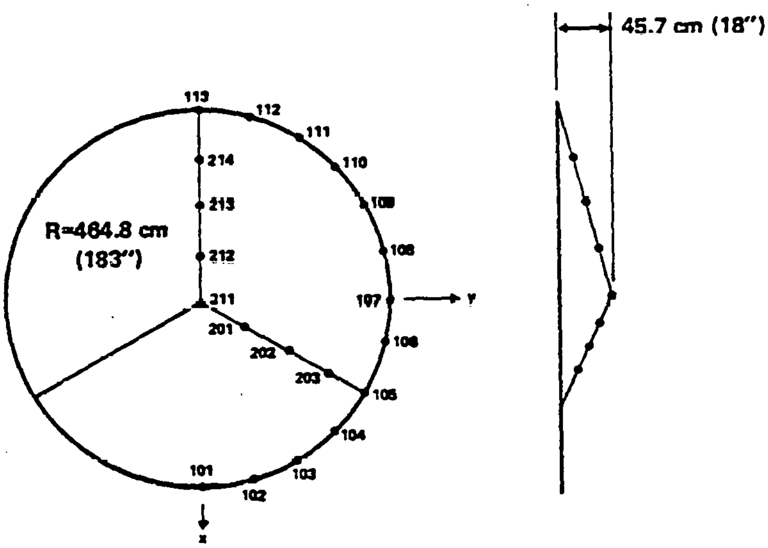

Ring radius = 464.8 cm (183")

Ring section = 12.7 cm (5 in.) O/diameter x 0.198 cm (.078 in.) wall thickness

Support arm section = 12.7 cm (5 in.) O/diameter x 0.198 cm (.078 in) wall thickness

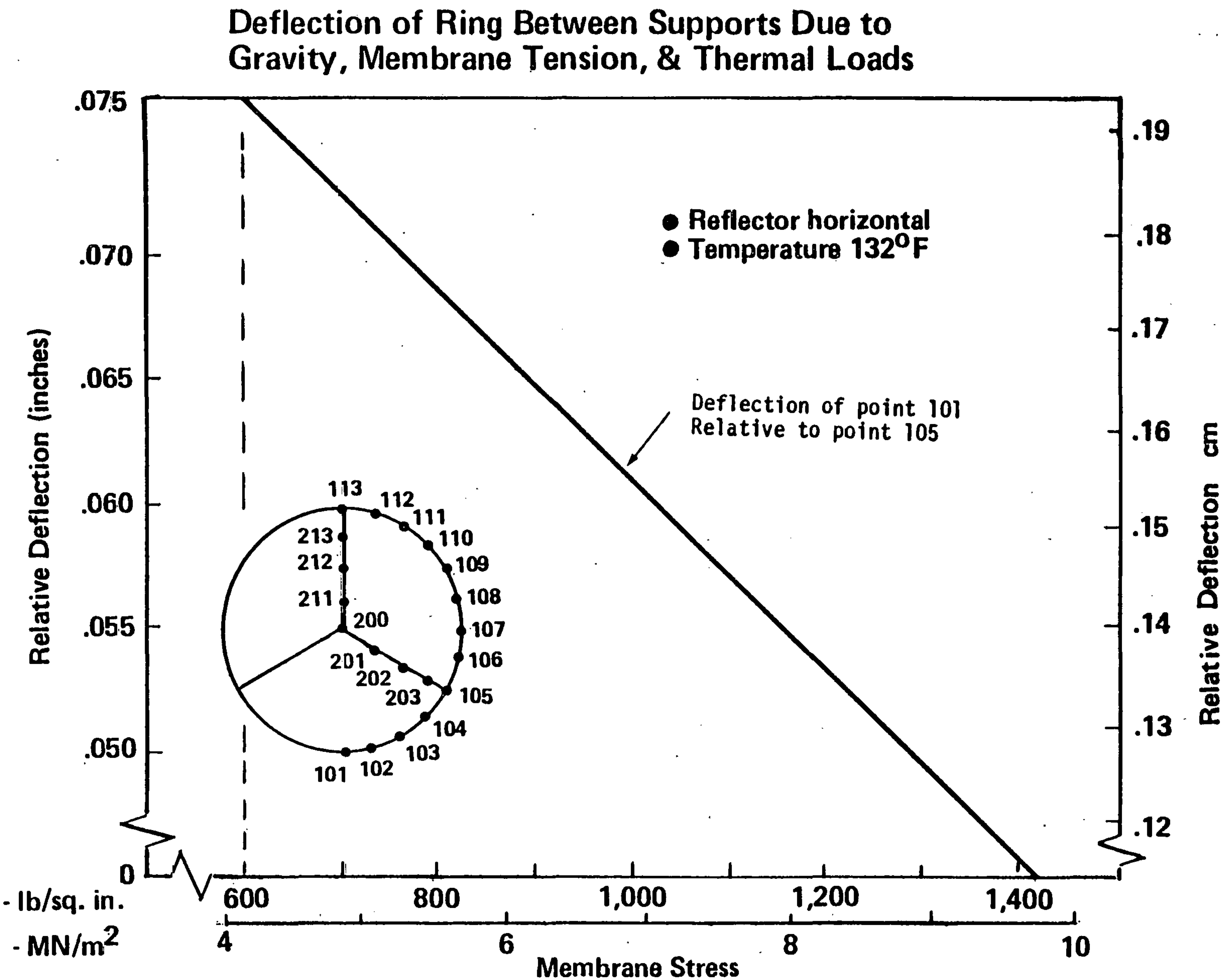

Figure 2.3.4.3-3 Reflector Structural Deflections

This is welded on installation to a base plate on the pedestal foundation pile. The 1.8 m (6 ft.) augured pedestal foundation pile is embeded with four 1.59 cm (5/8 in.) diameter A.615 steel full-depth rebar welded to the 1.27 cm (1/2 in.) thick steel base plate. The pedestal carries gravity loads plus torque loads due to the motor driven reflector as shown in Figure 2.3.4.3-4. The pedestal has been analyzed as a beam column. The stress levels are minimal and the deflection at the top of the pedestal is only about 0.01 degrees. The allowable deflection will ultimately be based on beam pointing error optimization.

2.3.4.3.1.3 Earthquake Analysis

A seismic analysis of the reflector assembly has been conducted using the design earthquake response spectra shown in Figure 2.3.4.3-5, as taken from Reference 2.3.4.3-1. A peak ground acceleration of 0.35g's was assumed equal to that measured in the 1940 El Centro Earthquake, as reported in Reference 2.3.4.3-2. This approach meets the requirements of Seismic Zone 3 (Uniform Building Code) which is the design requirement defined in Specification 001. The fundamental frequency of the reflector assembly supported by a 12.7 cm (5 in.) diameter steel pipe was calculated to be 2.094 Hz. The peak response of this dynamic system to the above seismic environment, assuming 2 percent of critical damping, is then 7.44 cm (2.93 in.) and 1.31g's. Adding this displacement to the maximum seismic deflection of the enclosure (0.68 inches) gives a total deflection of 9.17 cm (3.61 in.). The design provides a clearance of 19.8 cm (7.8 in.) between the reflector and the dome. Peak bending stress in the reflector pedestal support due to earthquake loading is 54 MN/m^2 (7,836 psi) which is well below the design allowable.

Figure 2.3.4.3-4 Pedestal Loads

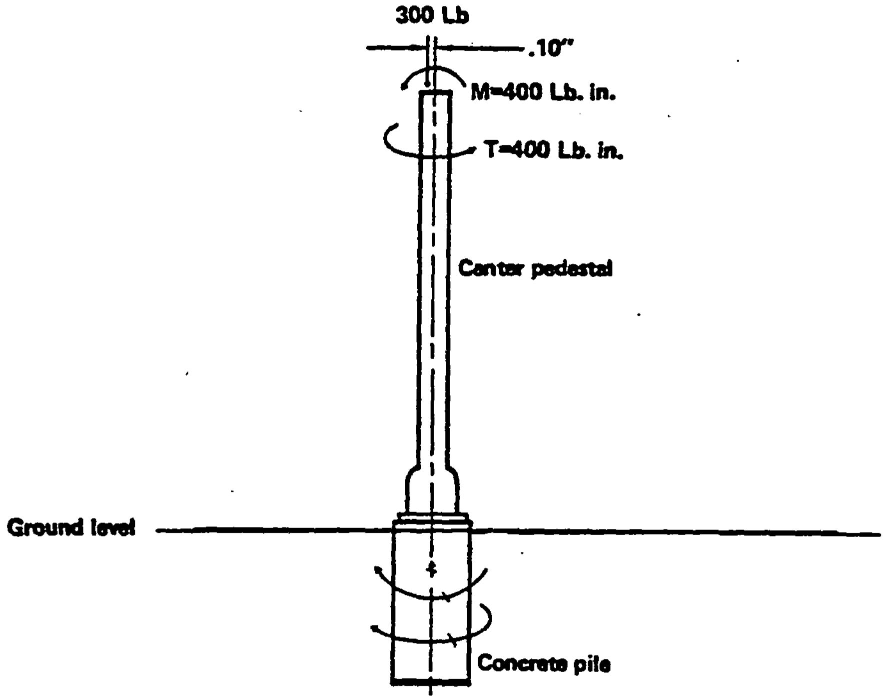

Figure 2.3.4.3-5

Horizontal Design Response Spectrum for 2% Critical Damping

Scaled to 1g Horizontal Ground Acceleration

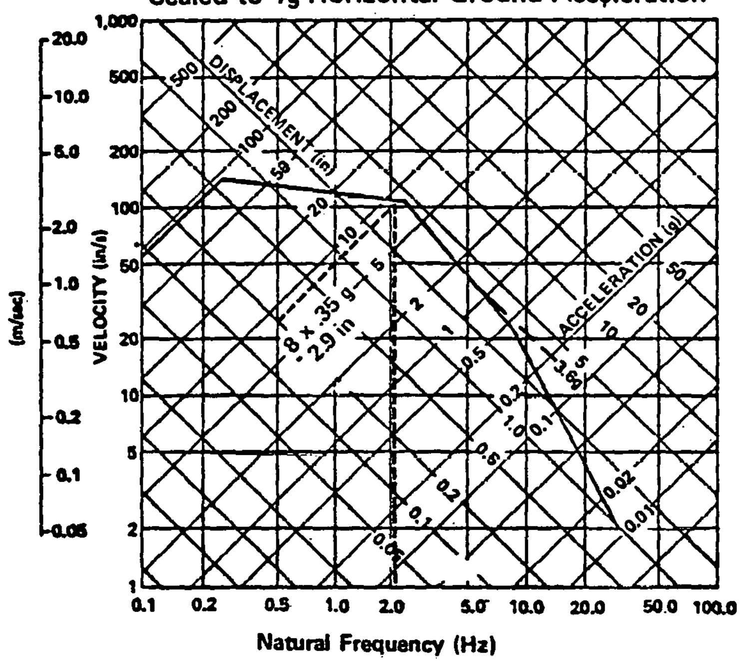

2.3.5 Gimbal/Actuator Assembly

Two subcontractors are presently developing competitive preliminary designs for the gimbal/actuator assembly. They are Clifton Precision, Clifton Heights, PA 19018, a division of Litton Industries; and Berger Lahr Corporation, Peterborough Road, Jaffrey, NH 03452.

A new specification control drawing (SCD) was prepared to delineate gimbal/actuator requirements. The SCD was written to permit as much design flexibility as possible, and the subcontractors were encouraged to innovate. Only certain parameters were tightly controlled; i. e., those which affect total system performance such as pointing accuracy. A copy of the SCD has been included as Appendix A.

2.3.5.1 Subcontractor Progress

Clifton Precision - To date, the subcontractor has not formulated a final design and cost estimate. Telephone discussions and a meeting at Boeing have been held for coordination. One item discussed was the use of a synchro/analog-to-digital converter to measure gimbal shaft position instead of a digital shaft encoder. Cost of the synchro/analog-to-digital converter was forecast to be lower than the cost of a digital shaft encoder.

Berger Lahr - Berger Lahr is working with BEI Electronics Inc. (encoders) and Decoto (gimbal assembly). A firm design and cost forecast has been received.

Details on the designs proposed by each subcontractor along with projected cost figures will be published in the final report.

2.3.6 Controls

The design of the heliostat controller has been refined and simplified to enhance high volume, low cost production. Functionally, there have been no changes.

The refined design, shown in Figure 2.3.6-1, incorporates improvements which eliminate all hand soldering and most hand assembly, reduces parts count by combining parts with a common function, and improves reliability by reducing parts count.

A single power transformer with three secondaries will be designed to replace the three transformers previously used in the three "off the shelf" power supplies. Rectifiers, filters and regulators will be added to the single PC board. Push-on terminals will be used for the power cable with a push in strain relief. An edge card connector will be incorporated for connecting transformer secondaries to the circuit board. Unregulated unfiltered DC will be used for the stepper motors, filtered DC will be used for the modem transmitter, and regulated filtered power will be used for the remainder of the electronics including the micro-processors.

The printed circuit board will provide for an edge connection to the transformer secondaries. All other active and passive components are located on the printed circuit board. Parts will be selected to permit 100 percent automatic insertion and flow soldering. There will be no hand wiring.

The data bus coupling transformer has been redesigned to provide simplified field installation of the data bus cable (see Figure 2.3.6-2). The data bus "J" box with terminal strips is no longer required (see Figure 2.3.6-3). Installation time and hardware costs have been greatly reduced.

All inputs and outputs to and from the PC card are made via low-cost, machine installed connectors so that replacement of any part of the control electronics will be quick and easy. This is especially important for field maintenance.

The amount of cost reduction resulting from this redesign will be defined in the final report.

Figure 2.3.6-1 Heliostat Controller

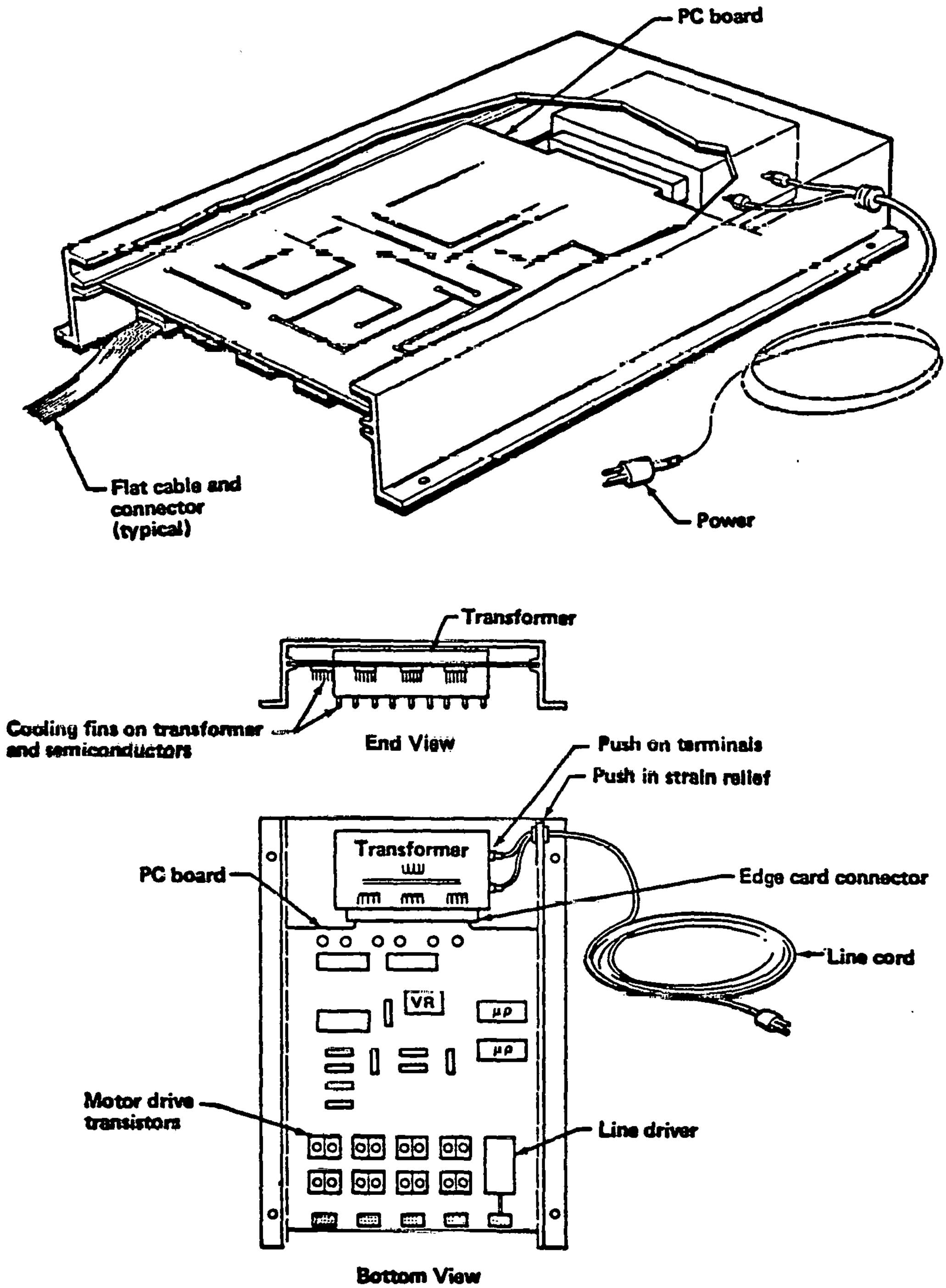

Figure 2.3.6-2   Data Bus Transformer

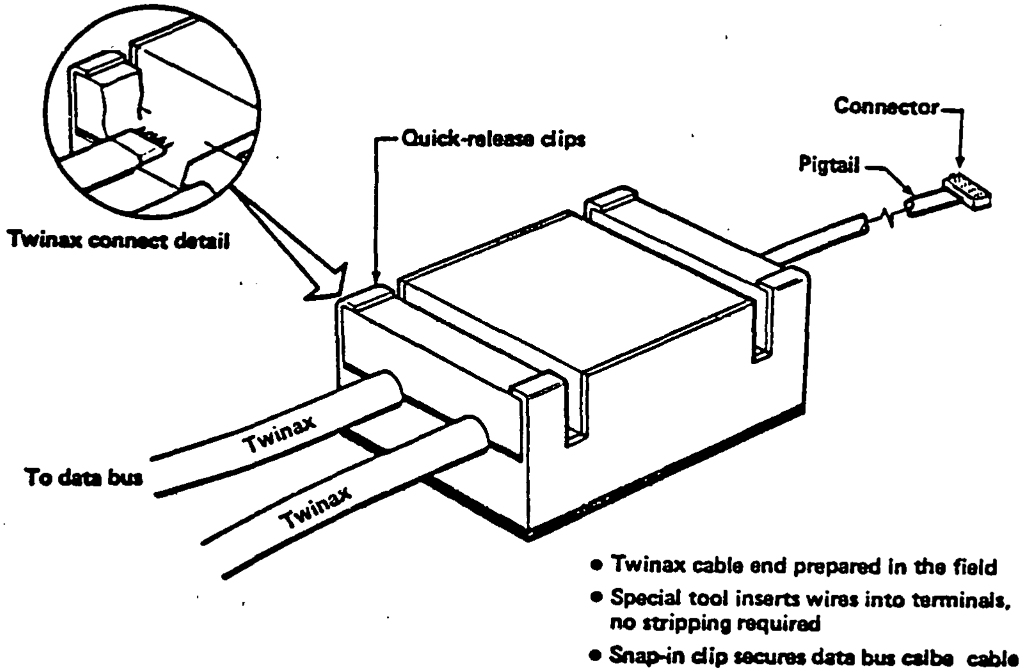

Figure 2.3.6-3   Heliostat Controller Installation

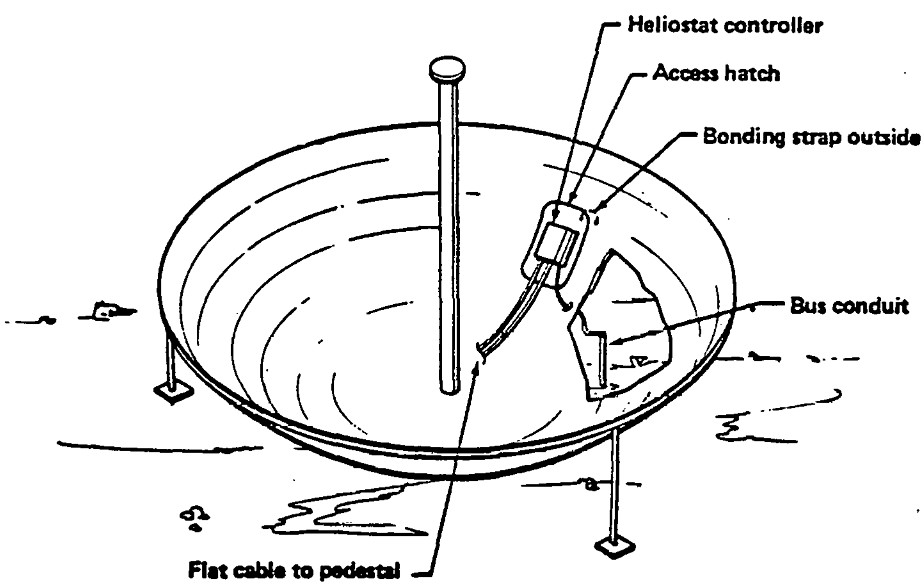

3.0 MANUFACTURING/INSTALLATION CONCEPTUAL DESIGN

The conceptual design of manufacturing/installation processes has three major objectives:

1) To influence heliostat component design trade-offs to:

- be compatible with maximum utilization of automated tooling
- simplify design to minimize manufacturing/assembly functions
- minimize the logistics of handling and transportation from raw materials to the completed heliostat on site
- simplify the site preparation and installation procedures.

All of these functions contribute to cost optimization.

2) To develop the fabrication/assembly/installation plans which:

- can accommodate the specified production rates
- provide conceptual designs of the automated tooling
- evaluate production rates of the tooling to define total tooling required
- define the total facility for manufacture, assembly and installation.

3) To develop manhours and manpower requirements for functions in the manufacturing/installation process, including the logistics of transporting heliostat assemblies from the manufacturing facility to each heliostat site.

The first objective above supported the optimization of cost whereas, the second and third objectives provided a firm basis for cost definition of the capital investment in facilities plus the manufacturing/installation labor cost.

To accomplish the above objectives, it was necessary to establish a scenario of plant sizes and plant locations to provide a basis for the manufacturing and installation planning which subsequently is used to define costs. The following defines the scenario (ground rules) for each of the three specified production rates:

1) A solar central receiver power plant has 25,000 heliostats.

2) Relatively small land areas will be dedicated to high density installation of solar power "parks." A solar power "park" is some multiple of individual solar plants, as defined in Item 6.

3) Solar parks are located in the reasonable vicinity of population centers to assure local availability of manufacturing, assembly and site installation labor. The number of solar power "parks" is a function of the specified production rates as defined in Item 6.

4) For the purpose of costing the delivery of materials, assume Phoenix, Arizona as an average location for sites.

5) Transport over dedicated roads will be utilized within the boundaries of the solar park. Solar parks are widely separated in the eight southwestern states, precluding dedicated roads between solar parks.

6) A separate scenario is assumed for each of the three specified production rates as discussed in the following and summarized in Table 3.0-1

<u>25,000 Heliostats Per Year</u>

A solar park will contain ten power plants (250,000 heliostats).

The park will be completed in ten years. Each plant within the park will be installed sequentially such that one plant installation is complete each year. Three parks are completed in 30 years.

<u>250,000 Heliostats Per Year</u>

A solar park will contain 30 power plants (750,000 heliostats).

Each power park is completed in ten years. An average of 3 - 1/3 parks are in simultaneous construction. Ten parks are completed in 30 years.

Plants will be installed sequentially such that three plants per park are complete each year (ten plants total per year).

TABLE 3.0-1

SOLAR PLANT INSTALLATION SITE ASSUMPTIONS

	Annual Production Rate		
	25,000	250,000	1,000,000
Heliostats Per Plant	25,000	25,000	25,000
Total Plants in 30 Years	30	300	1,200
Number of Solar Parks	3	10	12
Plants Per Park	10	30	100
Years to Complete a Park	10	10	10
Plants Complete Per Year Per Park	1	3	10
Number of Parks in Simultaneous Construction	1	3 1/3	4
Plants Complete Per Year	1	10	40

1,000,000 Heliostats Per Year

A solar park will contain 100 power plants (2,500,000 heliostats).

Each power park will be completed in ten years. Four parks are in simultaneous construction. Twelve parks are completed in 30 years.

Plants will be installed sequentially such that ten plants per park are complete each year (40 plants total per year).

In utilizing the above scenario, the manufacturing/installation plan was further developed using the groundrules established in Table 3.0-2.

As seen in Table 3.0-2, the manufacturing plan provides for an on-site assembly facility at each solar park location. This facility completes all the fabrication and installation of heliostats for the 10 year construction period of the solar park. At the high production rates as many as four parks are in simultaneous production. The following describes one such facility and the manufacturing concept which will achieve the high installation rates.

3.1 HELIOSTAT MANUFACTURING CONCEPT

The smaller components and detail parts which are readily shipped by truck or rail will be procured from off-site sources. The large components such as the base dish and the enclosure will be manufactured on-site. Table 3.1-1 is a Make/Buy list for heliostat components. Figures 3.1-1 through Figure 3.1-9 illustrate the approach to the manufacturing plan. The incoming procured components and the raw material stock for the "make" components flow through receiving/inspection stores adjacent to the production assembly lines. The parts handling equipment and the manufacturing assembly tooling will be highly automated to achieve the production rates. Three basic branches of the assembly line are:

1) Base/foundation structure,
2) Reflector assembly, and
3) Enclosure fabrication.

TABLE 3.0-2

MANUFACTURING/INSTALLATION GROUNDRULES

	ANNUAL PRODUCTION RATE		
	25,000	250,000	1,000,000
Manufacturing/Assembly Facilities per park	1	1	1
Heliostats per year per Facility (park)	25,000	75,000	250,000
Working days per year	250	250	250
Heliostat production per day	100	300	1,000
Number of shifts per day	1	2	3
Effective hours per day	8	15	22
Heliostats production per hour	12.5	20	45.5
Dimensions of Plant (miles on a side)	1.5	1.5	1.5
Dimensions of Park (miles on a side)	5	8.5	15.0
Average distance from Mfg. Fac. to site (miles)	2.5	4.0	7.5

Table - 3.1-1

MAKE/BUY PLAN

Support ring - segments	B	277-10048-41
Stanchions	B	277-10048-5
Pedestal	B	277-10048-6
Enclosure attach ring	B	277-10048-X
Reflector ring comps & spokes	B B B	277-10051-7 Tube ring 277-10051-8 Tube Supt 277-10051-9 Tube supt
Hatch assy	B	277-10048-10
Flanges - hatch	B	277-10048-13 & -14
Gimbal assy	B	
Air Supply assy	B	277-10052-1
Relief Valve assy	B	277-10052=2
Electronics equipt. & Harness wire	B	
Piling installation	B	277-10050-1
Hub	B	277-10054-1
Tee's	B	277-10053-1, -2
Base dish	M	277-10048-3
Enclosure	M	277-10049-1
Heliostat Assy & instl	M	277-10048-1
Reflector assy	M	277-10051-1 & -2

These three basic lines feed to the final assembly area. The final assembly position installs and pressurizes the enclosure. The completed heliostat is then attached to the heliostat transporter and delivered to the heliostat site. The heliostat assembly fixture is the transportation fixture which is designed to also facilitate the installation at the site. The conceptual designs of the manufacturing processes and automated tooling are described in the following paragraphs.

Base Assembly

The support ring is fabricated from six component parts; three ring segments, and three stanchions. These are loaded into the assembly jig and welded as shown in Figure 3.1-1.

The dish is fabricated from five steel sheets (roll stock), butt welded together to form a single roll. This roll is passed through the forming press to shape the dish and then through the circle shear, where the dish is trimmed to net size. The sequence of operations is shown in Figure 3.1-2. The dish is now routed to the sub-assembly area where the prefabricated hatch and enclosure attachment ring are installed.

The support ring and dish assembly are routed through the cleaning-priming and painting facility before routing to the welding station. For welding, the dish is positioned on the support ring and welded in place (see Figure 3.1-3). The support ring/dish assembly and the pre-fabricated reflector pedestal are loaded into the base assembly fixture (see Figure 3.1-4) which will precisely locate the pedestal with respect to the base assembly. The fixture provides a rigid structure to support the heliostat through assembly and will remain with the heliostat until installation in the field. This fixture and its interfaces with the transporter and the foundation at the site will be further described in the installation conceptual design, Section 3.2.

Reflector Assembly

The three ram-formed reflector ring components, three spokes, attachment tees and the cast center hub fitting are purchased components. These

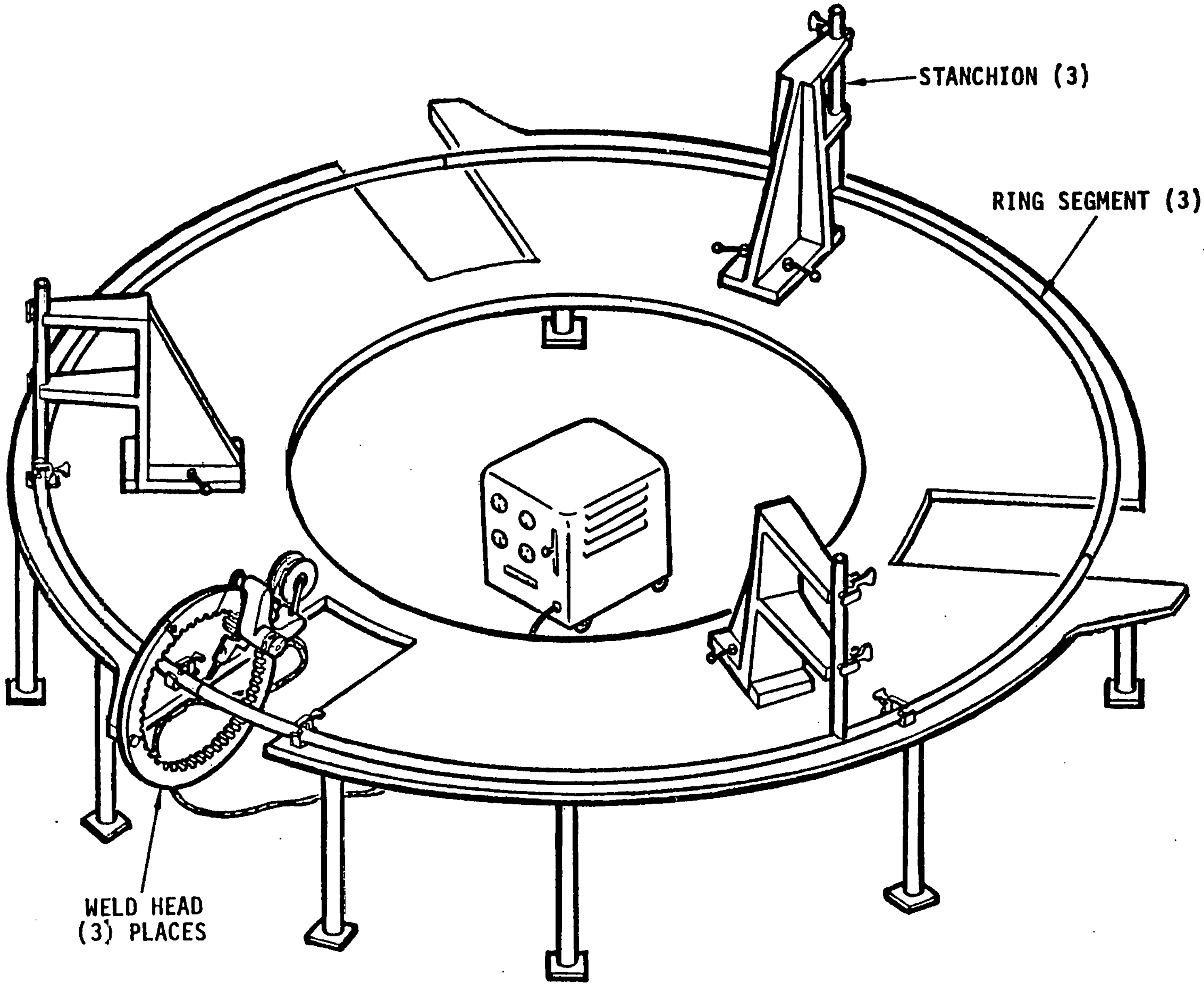

Figure 3.1-1 Support Ring Welding Fixture

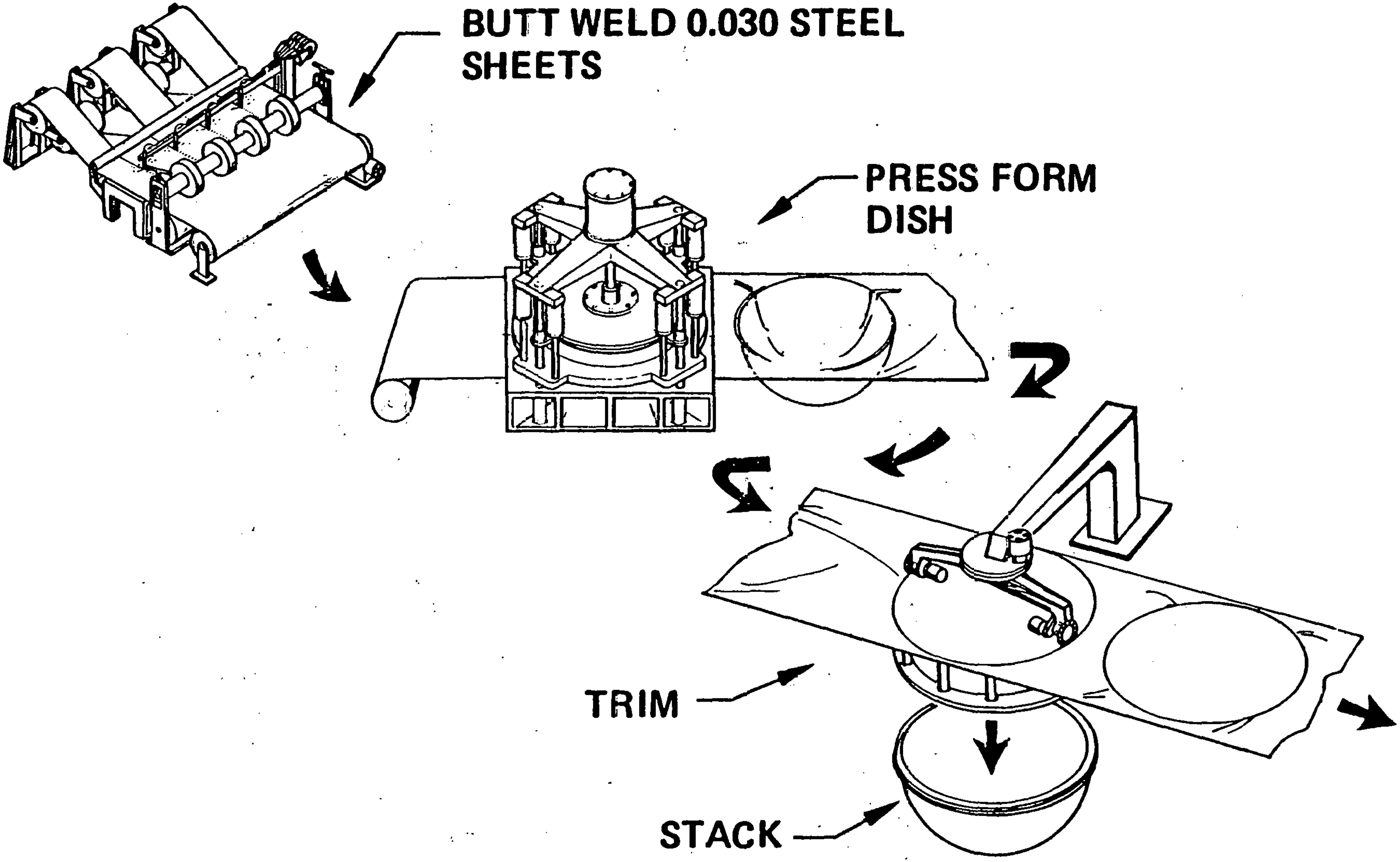

Figure 3.1-2   Dish Fabrication

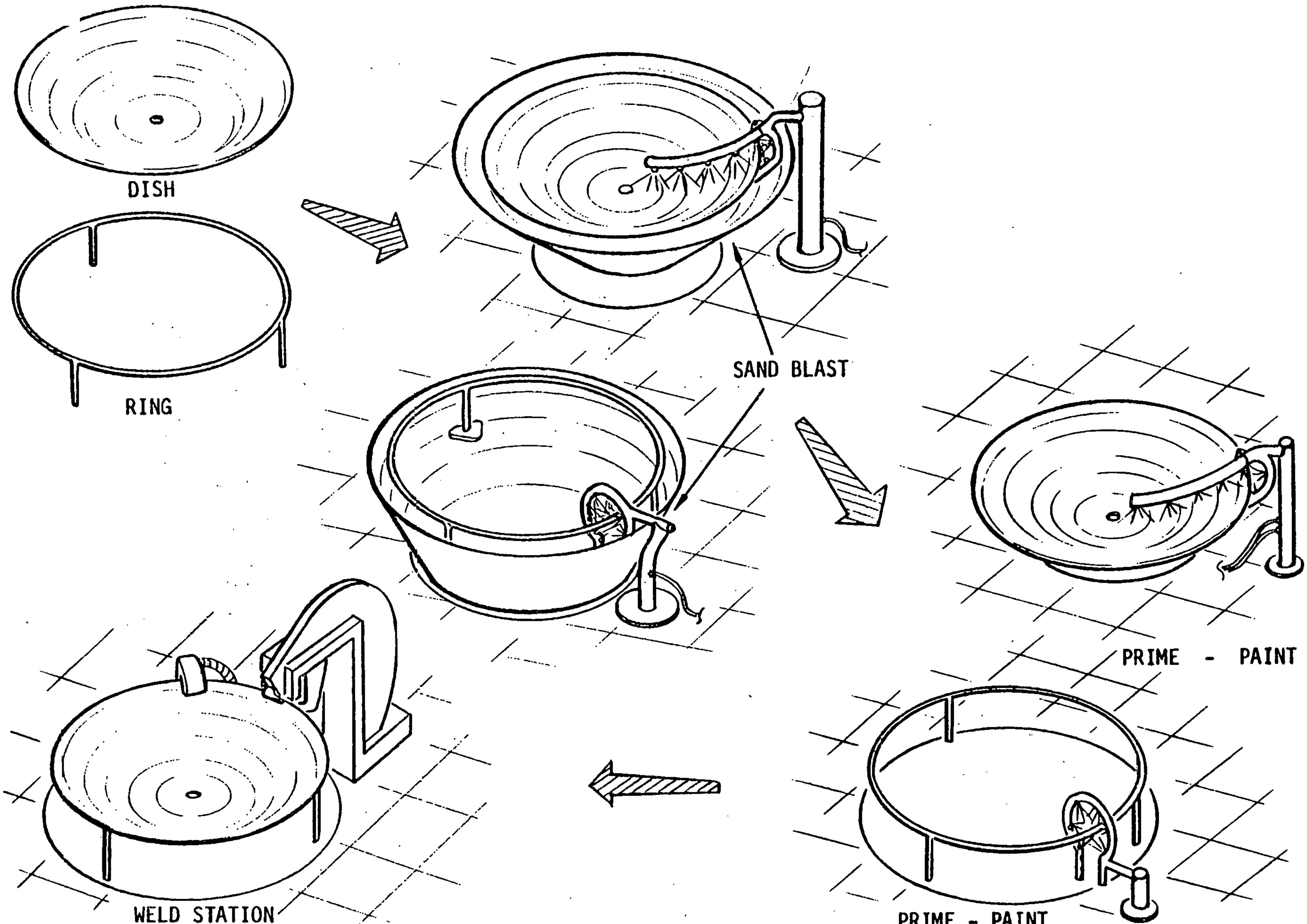

Figure 3.1-3 Clean, Paint and Weld Station

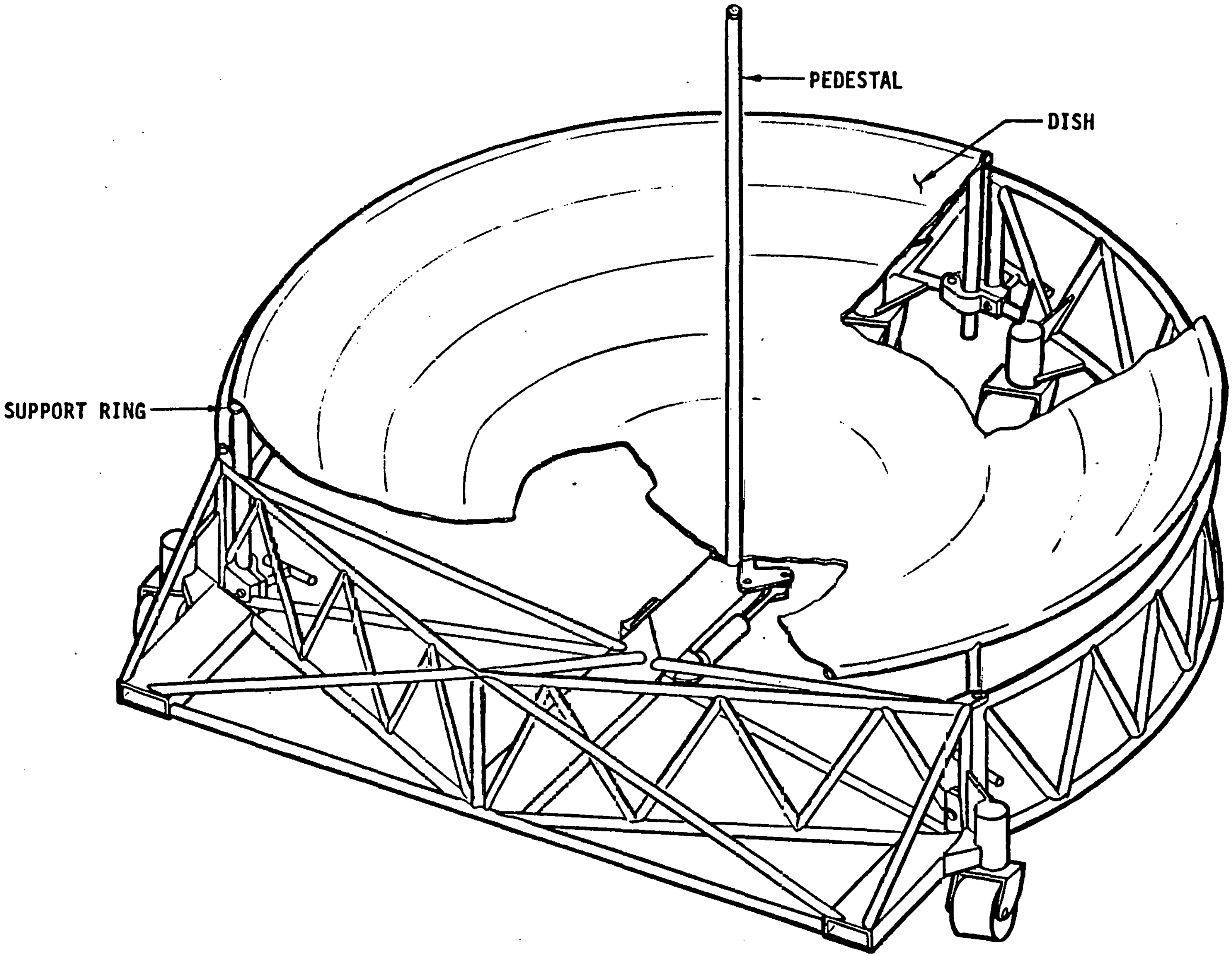

Figure 3.1-4 Base Assembly and Transportation Fixture

items flow from reflector assembly stores to the fixture as shown by Figure 3.1-5 where the components are properly positioned and held to a planar surface during the electromagnetic swaging of each joint. The finished ring structure assembly is then moved to the final reflector assembly jig.

The aluminized Mylar reflector membrane will be procured in approximately 139.7 cm (55 in.) width rolls. Each reflector membrane will require seven widths of the Mylar. The strips will be bonded together on a continuous flow tool designed to handle, support and protect the delicate film. The bonded seams (six) will utilize a sandwich type lap joint with a solid form polyester thermosetting adhesive. The adhesive will be activated and cured in place by an electrical impulse heater.

The reflector ring is prepared for the membrane bonding operation by cleaning the bond surface of the ring with solvent. Heat activated adhesive tape is then positioned on the ring and heat-tacked at ten inch intervals. The Mylar film used as the reflective surface is handled on two rolls in a scroll arrangement as illustrated in Figure 3.1-6. A length of the film is rolled off the dispenser-roll across the area where the bonding is done. The scrap film is rolled up on a take-up roll. The reflector ring is then positioned under the length of film. Clamp rings from above and below the film sheet clamp the film and stretch it over the reflector ring. Simultaneously, a cutter on the upper ring shears off the circular section of film held by the clamps. Next, a heater ring drops down on the assembly to bond the reflective film to the reflector ring. After bonding, the clamp rings are released and the reflector moves on to have the film trimmed to the outside edge of the bond line. The completed reflector is then moved to position for assembly to gimbal mounting plate.

<u>Enclosure</u>

The enclosure is thermoformed from a weatherized polyester flat sheet blank. This thermoforming technique has been demonstrated by small models but requires further development for forming of full scale enclosures.

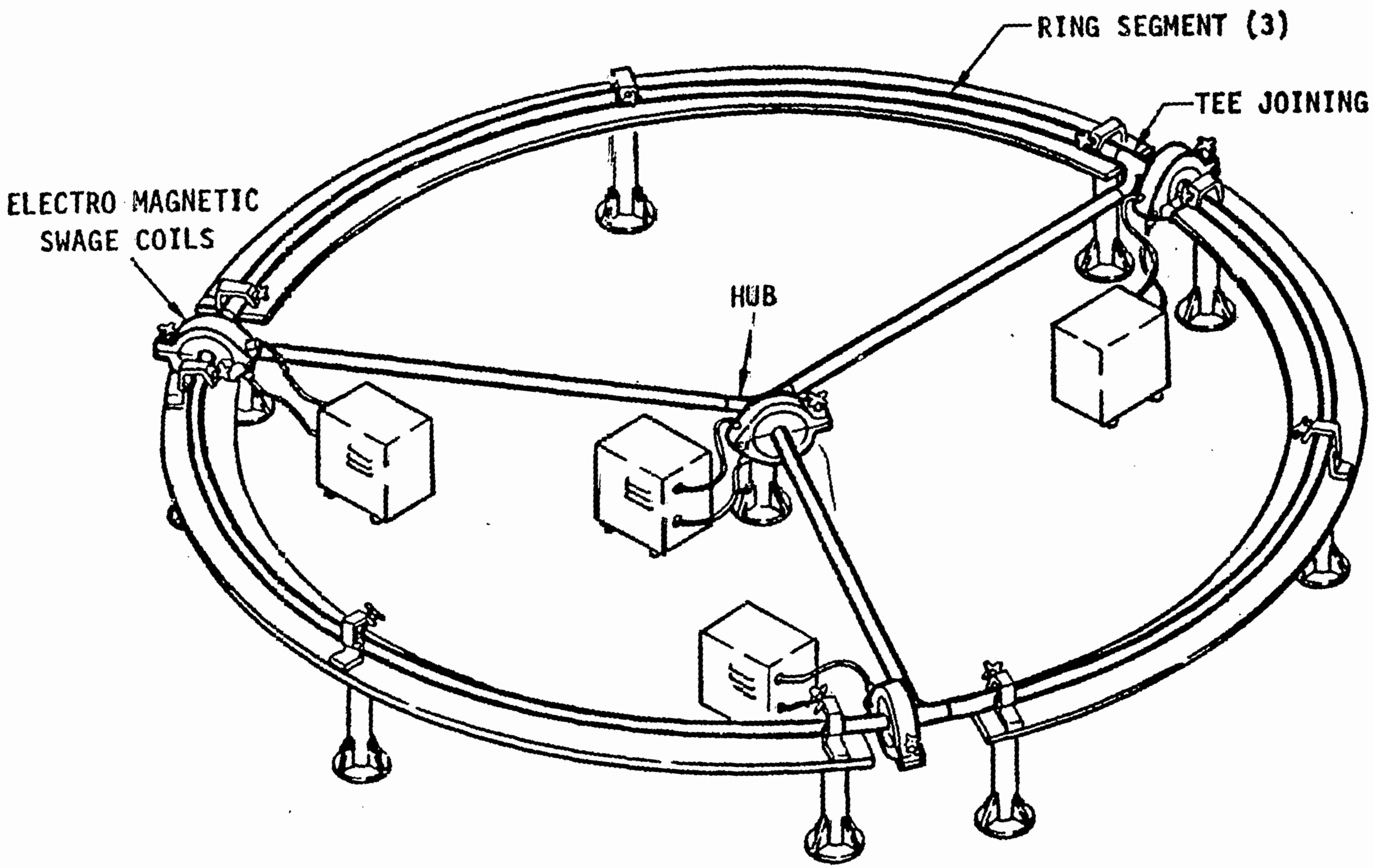

Figure 3.1-5   Reflector Ring Assembly Fixture

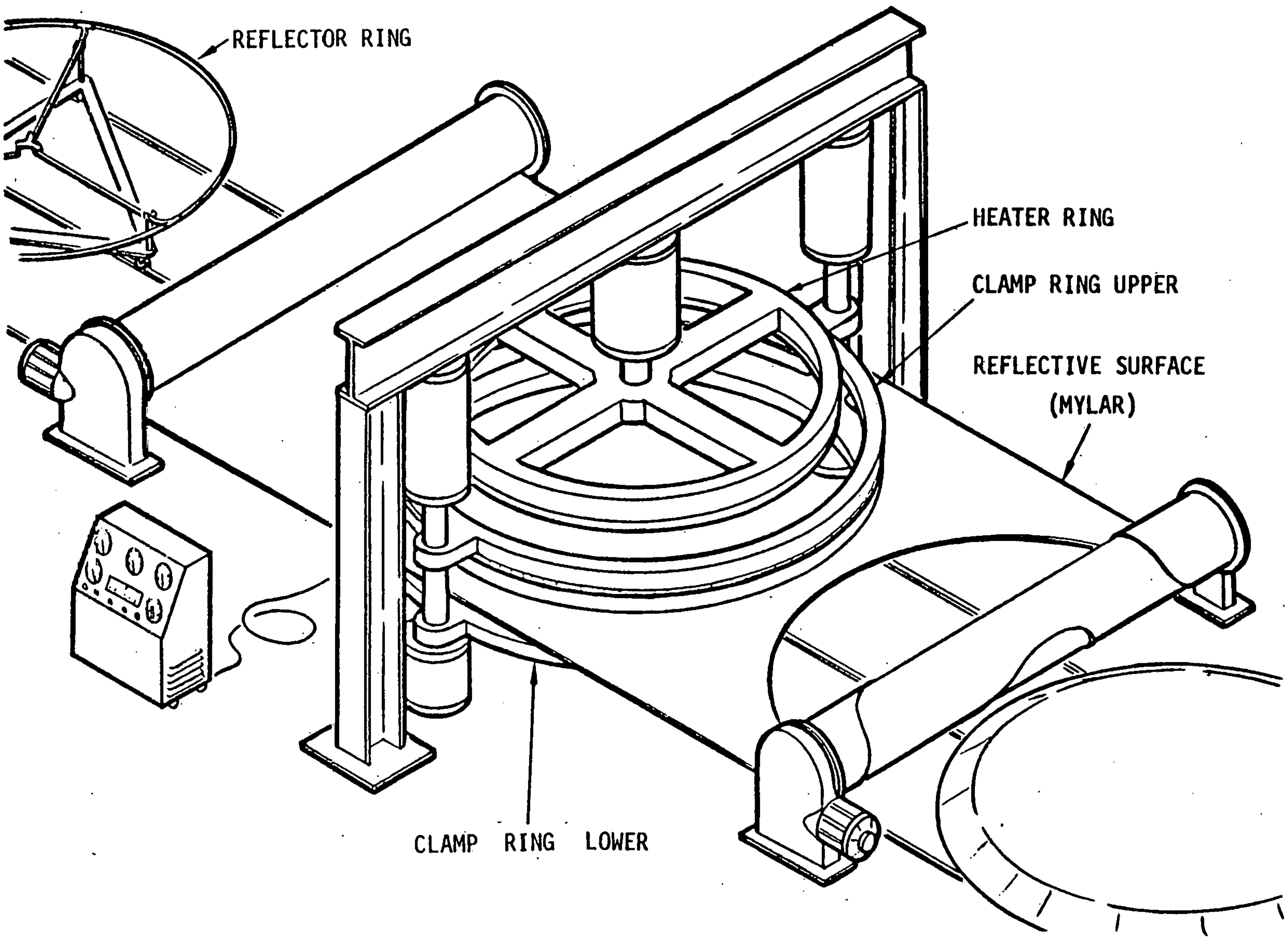

Figure 3.1-6 Bonding Reflective Surface to Ring Assembly

The development work to date has been with polyester film "Petra A". Radiant heat lamps have been used as the heat source in the facility diagrammed in Figure 3.1-7. A picture of a dome being formed is shown in Figure 3.1-8. Developmental tests have varied the heat rate and domes have been blown to various expansion ratios. The maximum expansion ratio achieved to date was approximately 30. This expansion ratio was limited by the heating capacity of the facility. Every increase in heat input to the film, during both heat-up and blowing has resulted in increased expansion ratios. A 31.8 ft. diameter enclosure will require expansion ratios of 40 and 110, if blown from blanks of 10 ft. and 6 ft. respectively.

The higher expansion ratios are expected to be feasible. However, since the available width of the polyester blanks may be limited, experimental domes have been successfully blown from blanks that have been joined. Hot bar sealed joints and fused laminates have been blown to expansion ratios of six. If a seamed blank of width equal to the base diameter (22.5 ft.) were used, the required expansion ratio would be approximately 6.8.

Both the optical properties and the strength properties of the thermoformed enclosure material can be expected to be as good as or better than the initial properties of the film.

A conceptual design of the thermoforming facility is shown in Figure 3.1-9. This equipment will be located in a high bay, semi-clean room area of the manufacturing assembly facility. The blown enclosure is removed from the heat facility and moves directly to the final assembly area.

Final Assembly

The heliostat final assembly area will be a high-bay completely enclosed area in which a semi-clean room environment can be maintained. Before entering this area the painted base assembly will be vacuum cleaned to remove dust and other contaminants accumulated in the welding and paint shops. The base assembly is now moved into the final assembly area to

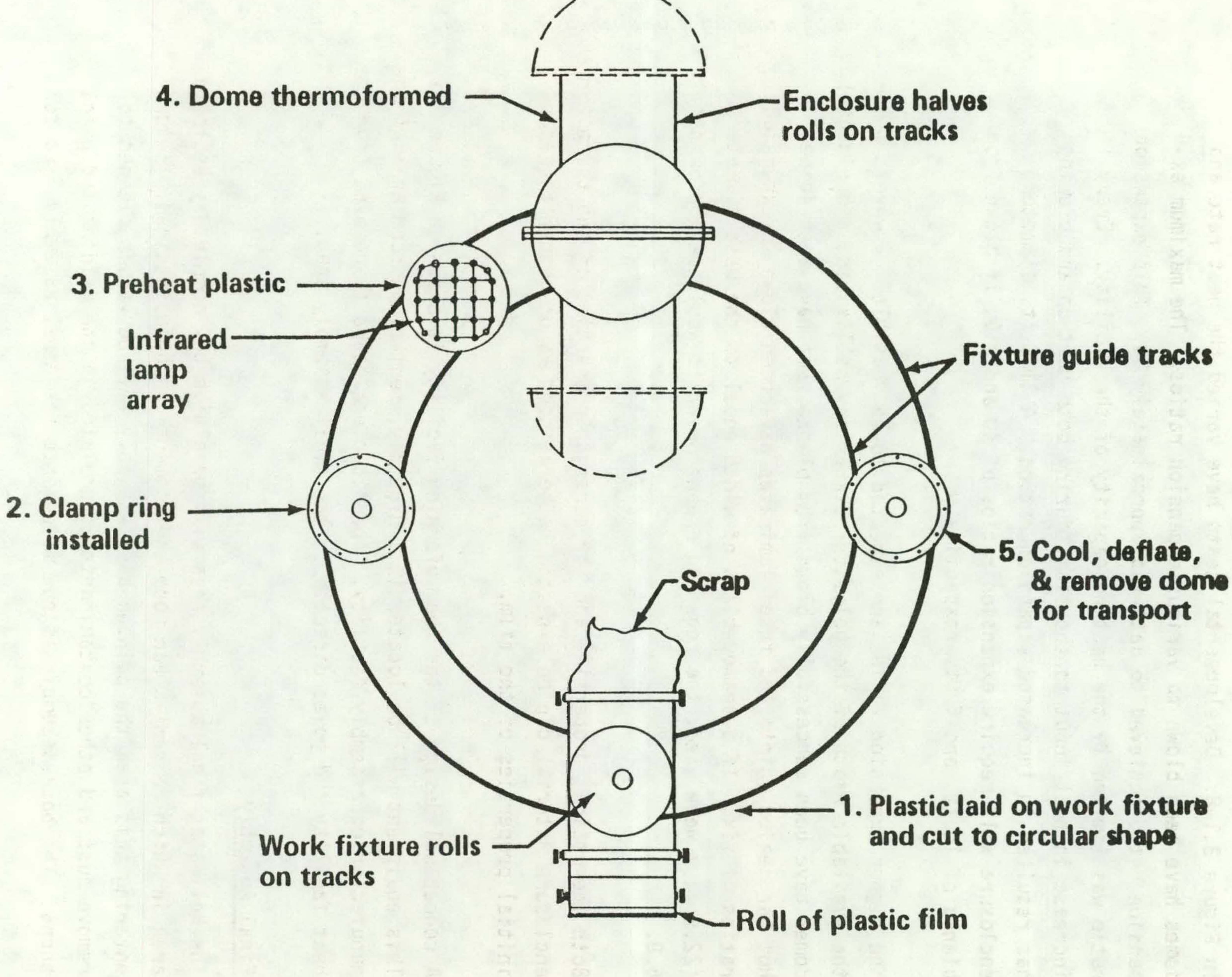

Figure 3.1-7 Enclosure Thermoforming Facility

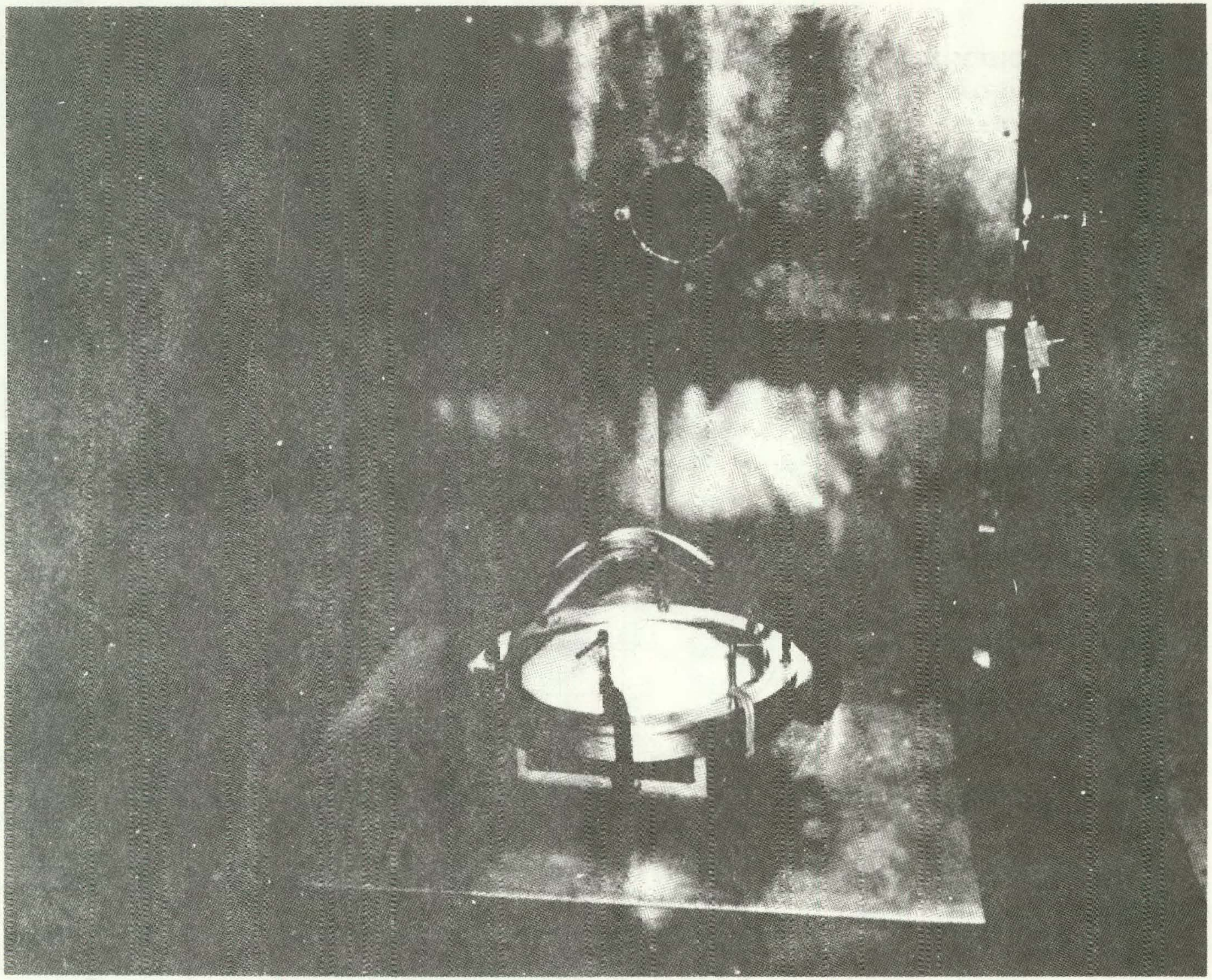

Figure 3.1-8. Experimental Enclosure Forming

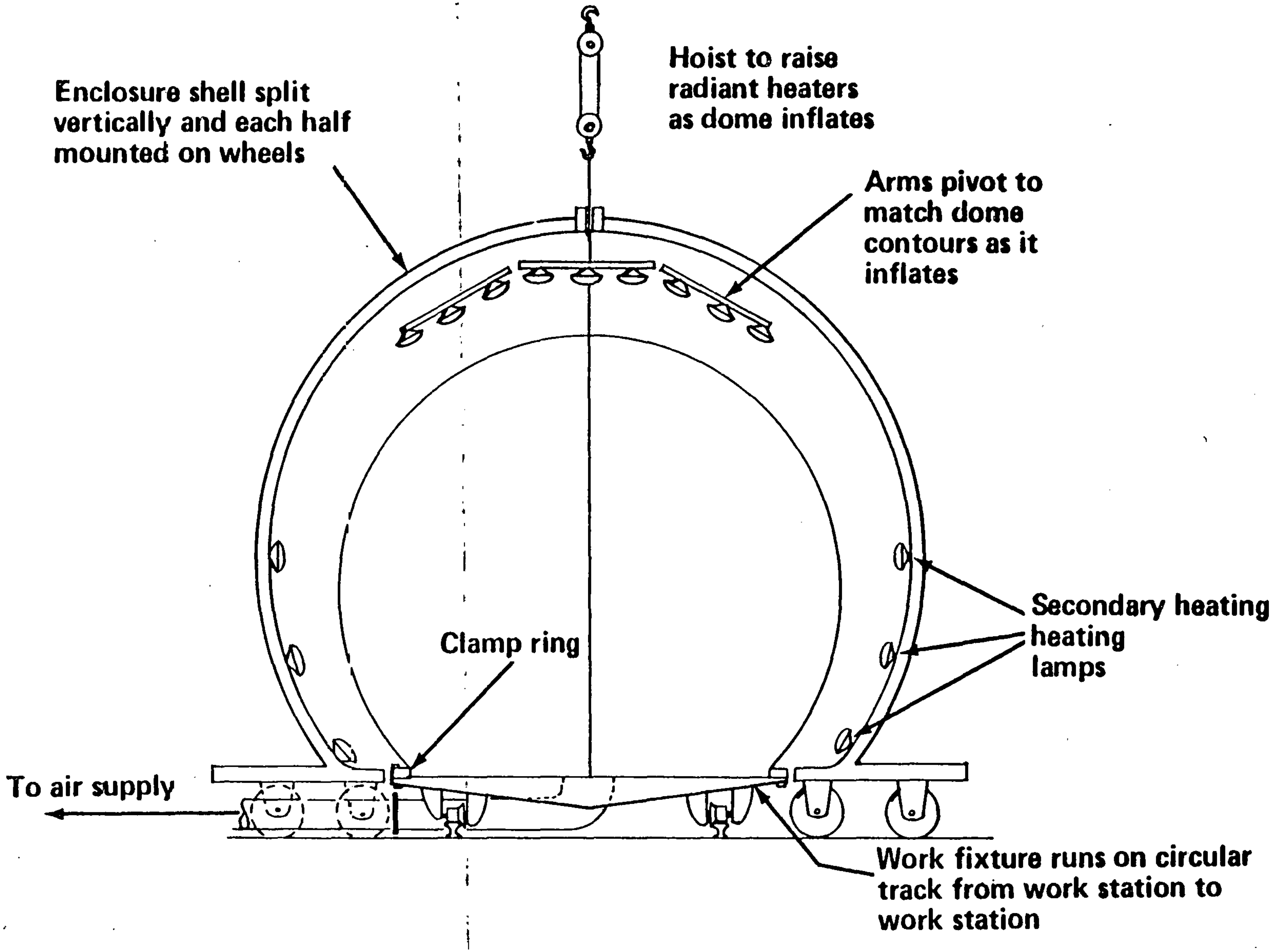

Figure 3.1-9 Section Through Thermoforming Facility

the first of three positions. Position 1 will install the heliostat controller, power and signal "J" boxes, drive and gimbal assemblies and blower unit. The interconnecting harness will then be hooked up and a functional test run to assure proper operation.

Position 2 will install the reflector assembly and rotate it to a 60° angle to facilitate the enclosure installation (see Figure 3.1-10).

Position 3 will install the enclosure using overhead hoist and tag lines. The enclosure is secured to the base, sealed and inflated (see Figure 3.1-11).

The completed heliostat with its transportation fixture is then attached to the transportation tractor and leaves for the heliostat installation site.

3.2 HELIOSTAT INSTALLATION CONCEPT

Heliostat foundations are installed at the surveyed locations in the field. The foundations consist of reinforced augercast concrete piling. Three pilings interface with the base stanchions and a center piling interfaces with the pedestal. The Lee Turzillo Contracting Company has provided an analysis and design of the automated equipment for installing the piles. The equipment consists of a drill platform mounted on a motorized tractor vehicle and a companion vehicle which carries the grout mixture and provides the pumping capability. This equipment is illustrated in Figure 3.2-1. One set of this equipment drilling and grouting four piles simultaneously is capable of installing 40 heliostat sets of piling in an eight hour shift. A follow up vehicle will install and level the reinforcing steel and capping plates. This foundation concept is adaptable to varying soil conditions and requires a minimum of site preparation. The 1/4 to 1/3 yard of soil drilled from each pile will be spread over an approximate six foot circle, requiring no removal of excess soil. After appropriate cure, the pilings are ready for heliostat installation.

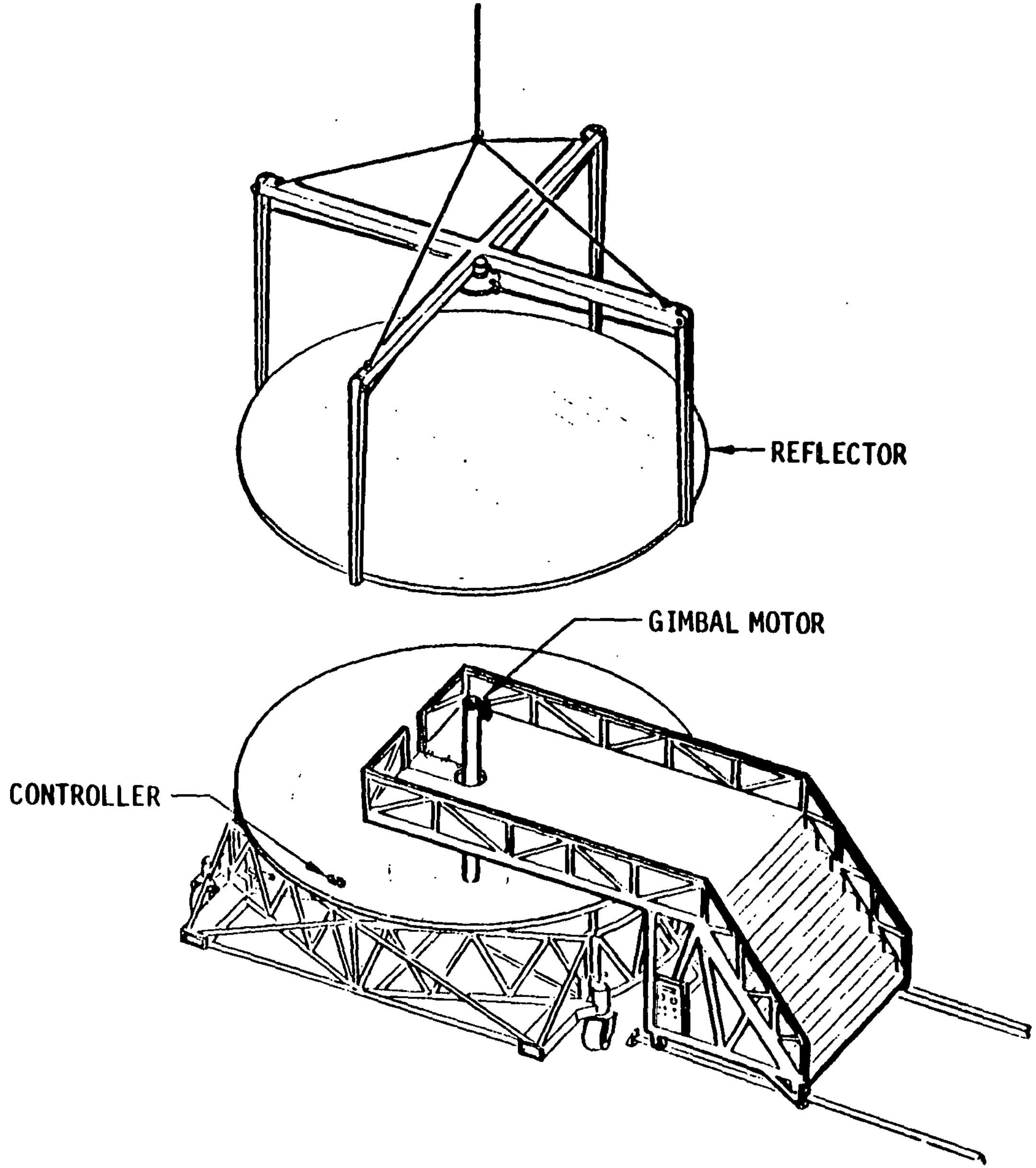

Figure 3.1-10 Reflector Installation

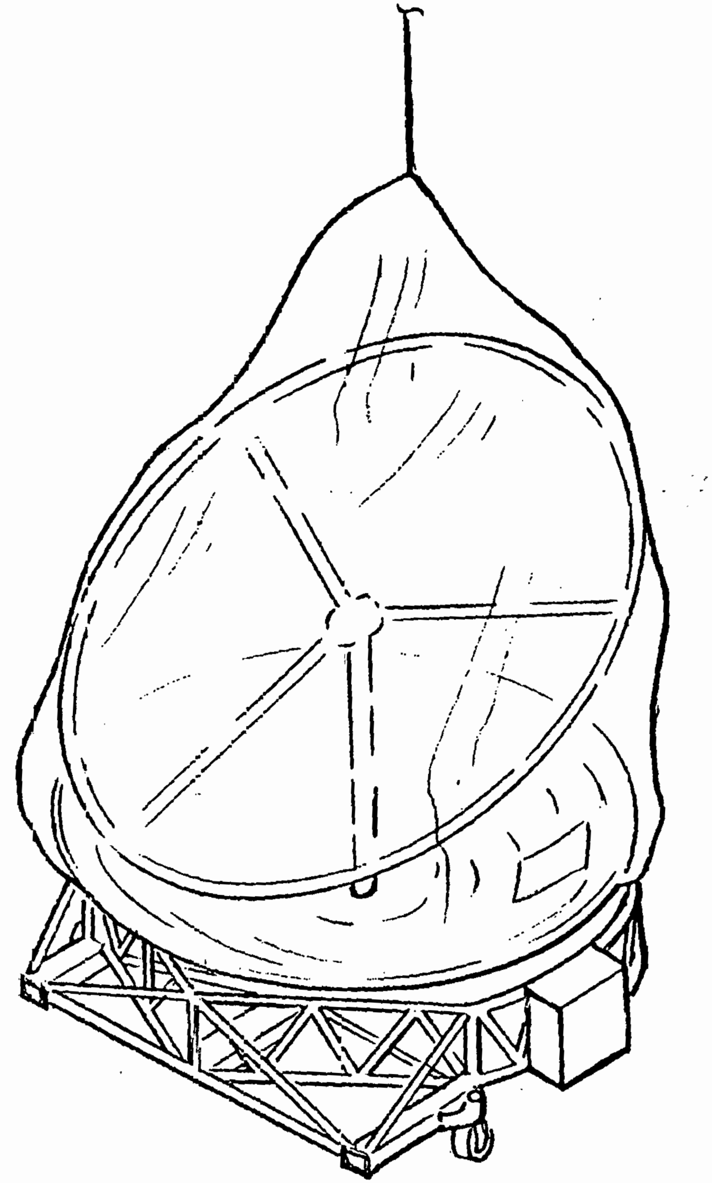

Figure 3.1-11 Enclosure Installation

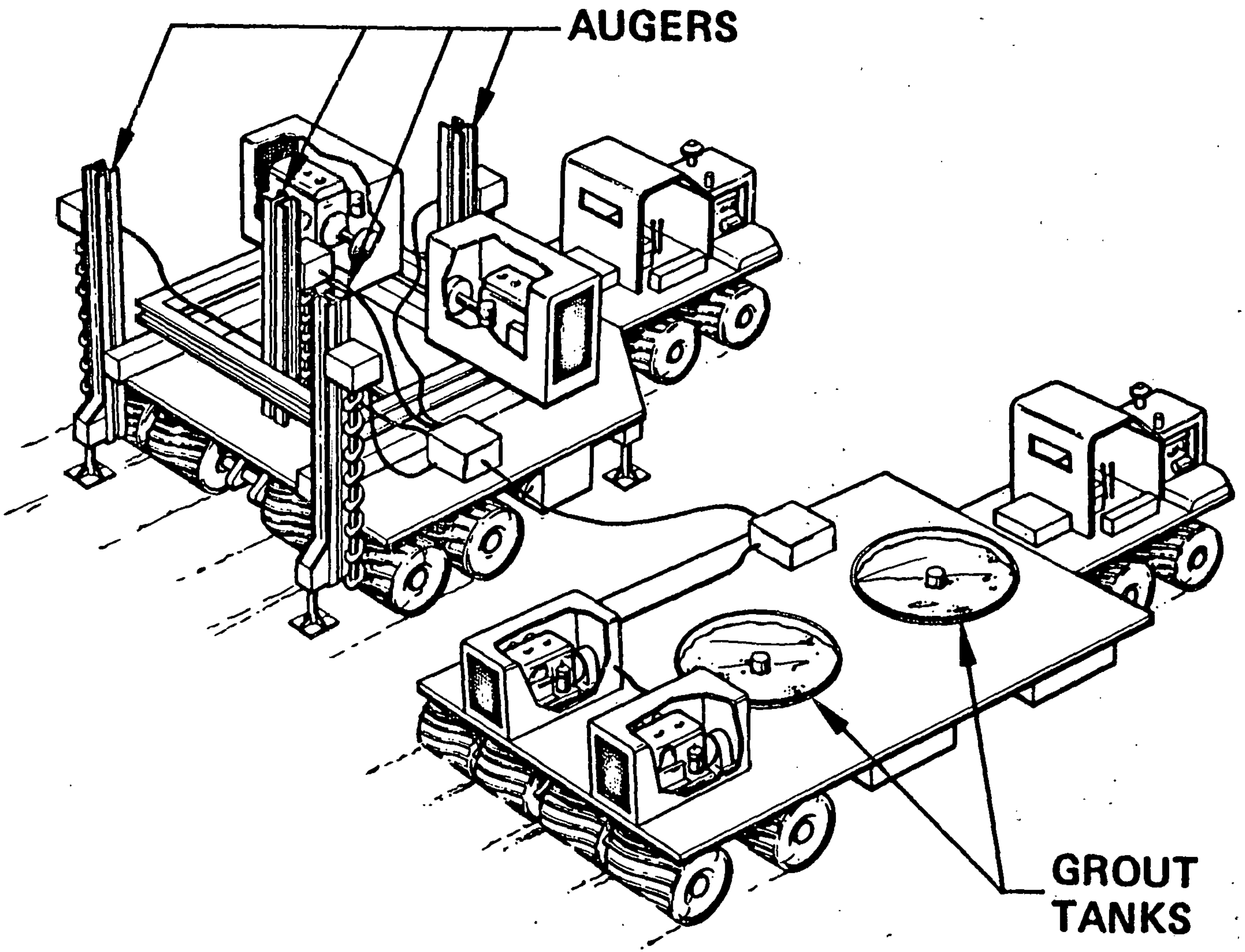

Figure 3.2-1 Auger cast Piling Installation Equipment

The factory assembled, functionally checked, and internally clean heliostat arrives at the site from the production/assembly facility over plant dedicated roads. This vehicle and transport fixture is shown in Figure 3.2-2. The fixture is that utilized in the plant assembly process. It provides a clamping support to the pedestal for support during transit and installation. The speed of this vehicle should be in excess of 20 mph on prepared interconnecting roads, and approximately 5 mph over the rough graded site. The transporter vehicle provides axial movement up to 18 inches in the horizontal plane to precisely interface the heliostat with the piling. A vernier control in the vertical plane will provide a shock free lift power capability. The heliostat and fixture is lowered until contact is made between the pedestal, stanchions, and the four steel piling caps. A verticality check is made to assure the pedestal is properly aligned before arc welding the pedestal to the piling cap plate. The three stanchions are now welded to their cap plates. The power connection to the blower is transferred from tractor power to field power. The assembly fixture is now removed from the heliostat, returned with the transporter vehicle to the factory, and recycled into the production line.

The power and signal wiring connection is now made to the heliostat controller, the ground connection made, and the heliostat is ready for functional checkout and alignment processes.

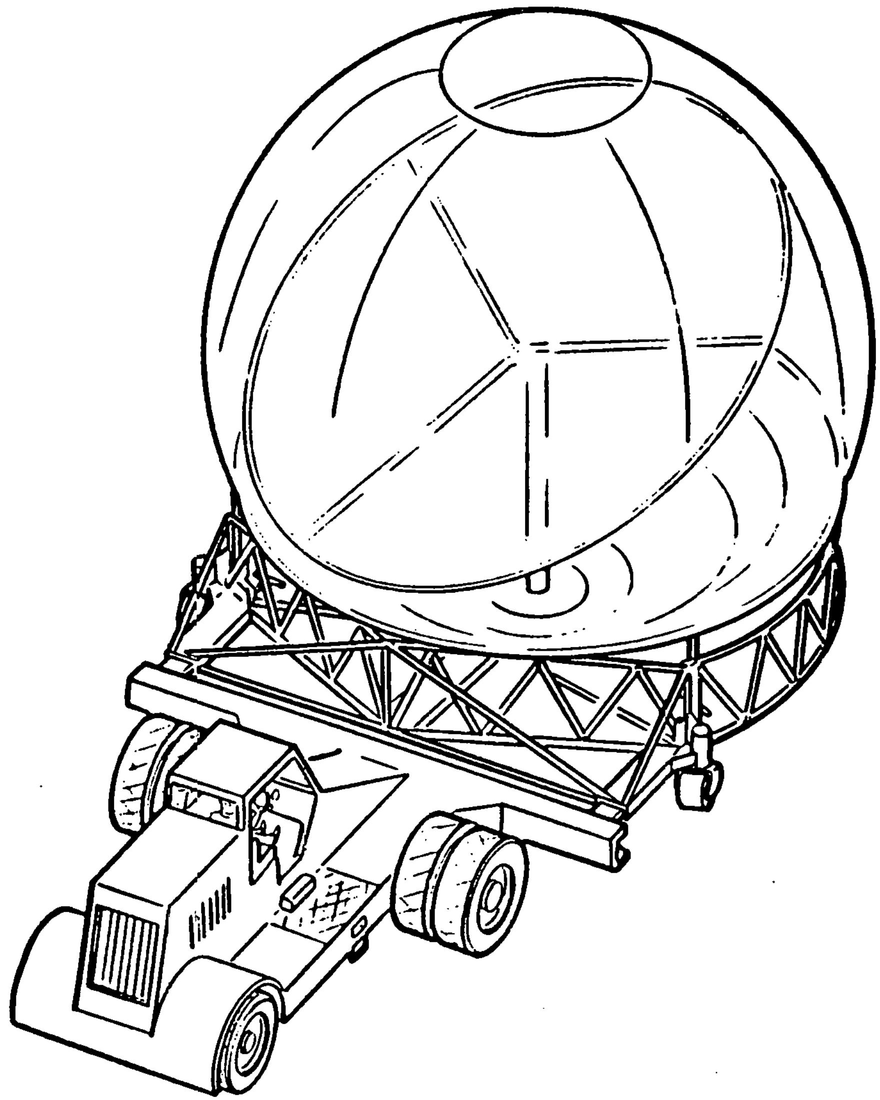

Figure 3.2-2 Heliostat Transporter

4.0 MAINTENANCE CONCEPTUAL DESIGN

Previous studies identified system areas which had high maintenance requirements. The following is a description and status of the maintenance conceptual design and analysis intended to reduce these maintenance requirements. Included are the concepts under technical and cost evaluation and descriptions of corresponding support equipment. Table 4.0-1 presents the analyses underway by major heliostat assembly.

4.1 PROTECTIVE ENCLOSURE CLEANING

Experience has shown that the external surface of the enclosure will gradually become contaminated to the extent that a reduction in specular transmittance will be realized. Analytical and experimental work has been performed by Boeing and others in an attempt to quantify the extent of reflectance loss with time and determine acceptable ways to clean the surface.

A literature search was conducted to seek out ways to clean plastic films utilizing techniques other than with water. No techniques were found that appeared applicable to the enclosure concept. New concepts will be sought-out on a continuing basis throughout the performance of the contract.

Four water cleaning concepts were selected for evaluation and are discussed below. These concepts are shown in Figure 4.1-1. Cost trade studies of labor and equipment are in progress and will be completed for the final report.

4.1.1 Self Contained Mobile Washing Machine

The mobile washing machine as shown in Figure 4.1-2 is considered for dome cleaning. When used for cleaning it would be equipped with hemispheric arms containing rows of nozzles which sweep around the dome and clean the surface. Self contained tanks would provide water and/or cleaning solution if required and recover residue for later filtering and reuse. Recent cleaning experiments at Boeing have shown that dome material (Tedlar) exposed at Albuquerque can be successfully cleaned using only a high pressure (550 psi) water spray. Post test

TABLE 4.0-1

ASSEMBLY	ANALYSIS
Enclosure	• Evaluation of cleaning approaches. No suitable alternate to water cleaning has been found to date. Four concepts in current trade study: (1) Self-contained mobile washing machine. (2) Centrally supplied mobile washing machine. (3) Overhead sprinkler system with central supply and recovery. (4) Individual enclosure wash units (flood type) with central supply and recovery. • Scheduled replacement. Time/motion analysis to estimate man and machine requirements based on a 15-24 year replacement cycle.
Reflector	• Analysis of dust accumulation over heliostat lifetime to determine need for cleaning. Near zero leakage heliostat. Evaluation of cleaning with air or water wash, if required.
Gimbal	• Cost/technical trade study to assess increasing encoder MTBF. Considering: (1) Use of synchro positional transducer, instead of optical encoder. (2) Elimination of encoder. (3) Derating voltage to encoder lamps thereby increasing MTBF. • Equipment concept for gimbal maintenance: (1) Van with airlock/ladder modifications. (2) Temporary reflector support used during gimbal replacement.
Controls	• Cost/technical trade to assess increasing high maintenance component MTBF's. • Study to determine location of heliostat controller (HC) outside or inside heliostat. • Equipment concept for replacement of HC, if located inside.
Air Supply	• Low leakage rate 0.006 m^3/min (.2CFM) heliostat design has been selected. • Ultra-high filtration system used to assure cleanliness of reflector has been studied. • Individual heliostat blower versus central air supply system is being evaluated for technical feasibility and cost benefits. • Air bearings and other long life bearings for blower are being considered to increase blower MTBF.

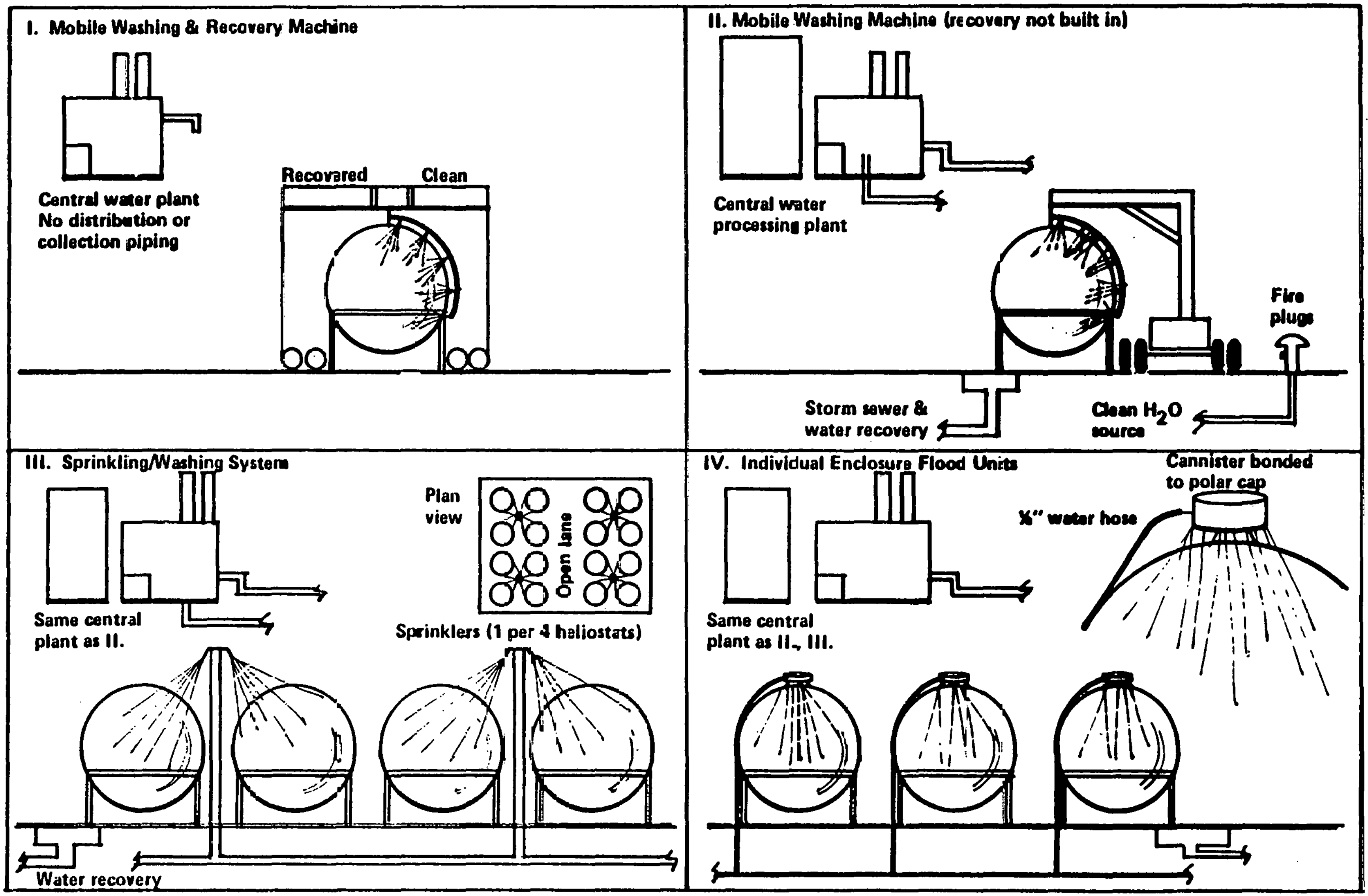

Figure 4.1-1 *Heliostat Washing Evaluation*

Figure 4.1-2 *Self-contained Mobile Cleaning Facility*

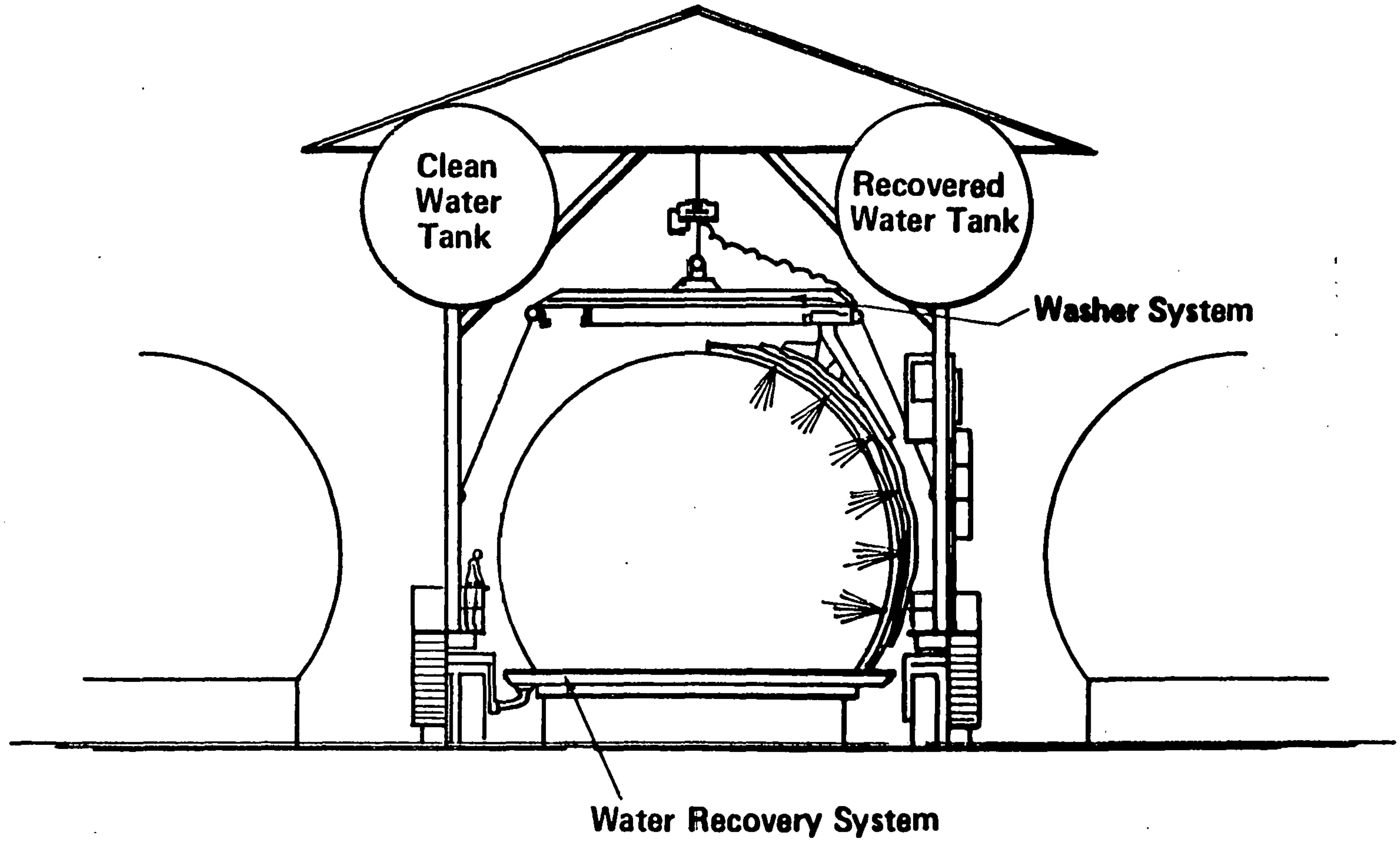

transmittance data showed complete recovery. In addition tests were conducted on a Boardman heliostat enclosure to obtain data relative to nozzle to enclosure configuration, nozzle sweep rate across dome surface and water consumption.

The preliminary analysis of the test data leads to the following:

3 minutes to wash and rinse one heliostat
5 minutes to move and set up between heliostats
2 minutes/heliostat for tank draining and filling

---

10 minutes/heliostat cleaning time.

For a field of 25,000 heliostats, a single machine operating 24 hours per day would require approximately 6 months to clean the field.

Although applicable washing frequency data is not yet available for domes, for purposes of this study a period of between four and six months has been assumed. Further analysis for costs associated with the washing machine is under way. A preliminary estimate of machine cost is $150,000/unit.

It is assumed that two operators per machine per shift would be required. This translates to the following labor costs per year for a 25,000 heliostat plant:

No. of Washes/Year	No. of Machines	Man-Years/Year
2	1	6
3	1.5	9

Assuming 3 washes per year, 270 man-years and $225,000 for machines would be required in the 30 year period. This translates to approximately $4 per sq. meter.

Preliminary estimates of wash and rinse water requirements based upon Boardman test site data are that up to 200 gallons per heliostat may be needed. Based on 25,000 heliostats, 5 million gallons of water would be required per wash. Further, the annual requirements would range from 10 to 15 million gallons of clean water. Because of these large quantity water requirements, the need to reclaim and reprocess is recognized. A central water treatment plant that would process the collected wash and rinse water will probably be required for most sites. The mobile washing machine would transfer dirty water to and receive clean water from such a facility. Approximate costs for this facility are being estimated.

4.1.2 Centrally supplied Mobile Washing Machine

This concept employs the same basic approach to cleaning; i.e., hemispherical rotating arm with pressure spray nozzles. However, a simpler basic chassis is involved and no water storage tanks are included (Figure 4.1-3). Wash water is supplied from a central water treatment plant through piping and hydrants in the heliostat field. Long hoses are used between the hydrant and washer. Water recovery is accomplished by a system of underground piping (storm sewer) or trench network running back to the central treatment plant.

The washing time per heliostat, hence annual labor cost of this machine is expected to be about the same as the self-contained unit. The cost per machine is expected to be about one-half. Water requirements would also be the same as described in 4.1.1.

4.1.3 Sprinkler Washing System

This concept is based upon experience and studies (Reference 4.1.3) that indicate more frequent rinsing, followed by infrequent washing, may provide satisfactory cleanliness. The approach employs a high standpipe located centrally between four heliostats. At the top of the standpipe is a set of four spray nozzles that direct rinse water onto the polar caps of the four enclosures. The water runs down the side walls of the enclosure carrying away dust contaminants. Because of the short duration between rinsing cycles, the bonding between dust particles and the enclosure is weak and easily overcome. The water is collected and returned to the central treatment plant via a water recovery system.

Figure 4.1-3 Alternate Washing Concept

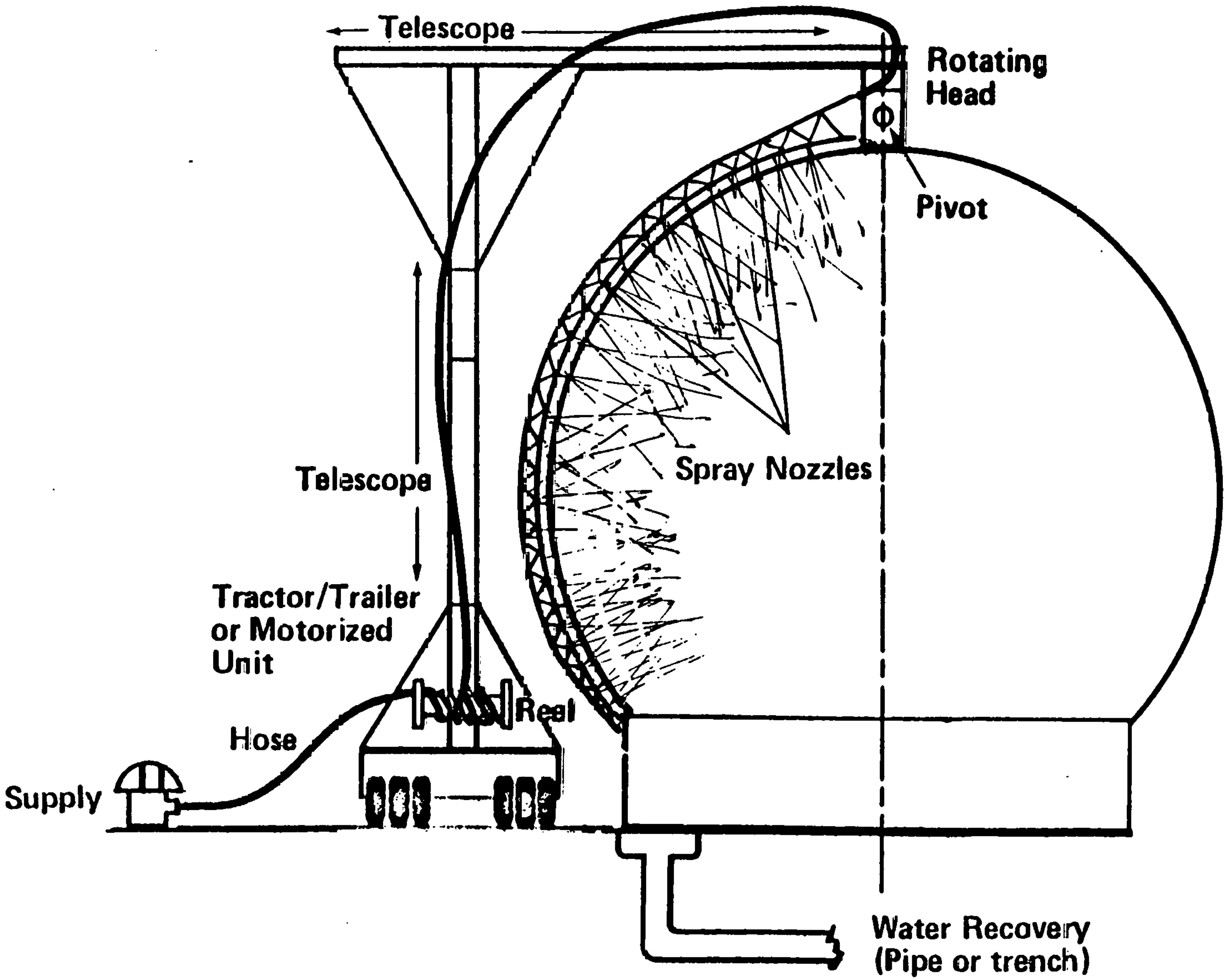

The rinsing frequency would probably be weekly on an annual average basis, as dictated by variable dust and humidity conditions. Since only top to bottom rinsing is being accomplished and no washing is involved the following applies:

> 50 - 100 gallons/rinse - assume 75 gallons/rinse
> 25,000 x 75 gal/rinse = 1.9×10^6 gallons/rinse
> 52 rinses per year = 98.8×10^6 gallons/year

If semi-annual washing with two machines is used in conjunction with the sprinkler system, an additional 10×10^6 gallons/year would be required. The water volume handled per year would be about ten times that of either of the mobile machine systems. However, the rinsing system is less labor intensive.

4.1.4 Individual Flood Units

The approach described here is quite similar in most respects to the sprinkler system of 4.1.3 except that the water is dispensed directly on the polar cap of each enclosure. The water and labor requirements are essentially the same. It would also employ the principle of frequent rinse and infrequent wash. Supply and recovery from a central treatment plant is assumed. The potential advantages over the sprinkler system are lower water makeup, due to over-spray losses and no access lane blockages for sprinkler risers.

4.2 PROTECTIVE ENCLOSURE REPLACEMENT

Previous analysis of enclosure material life indicated that enclosures would have to be replaced once in 30 years. The replacement would start near the 15th year and require completion by at least the 24th year.

Figure 4.2-1 is a conceptual schematic of the mobile facility required to move through the field, remove old enclosures and install new ones. The facility straddles a heliostat, encloses it for wind protection, while removal and installation operations proceed. Twenty to thirty new enclosures are stored folded in

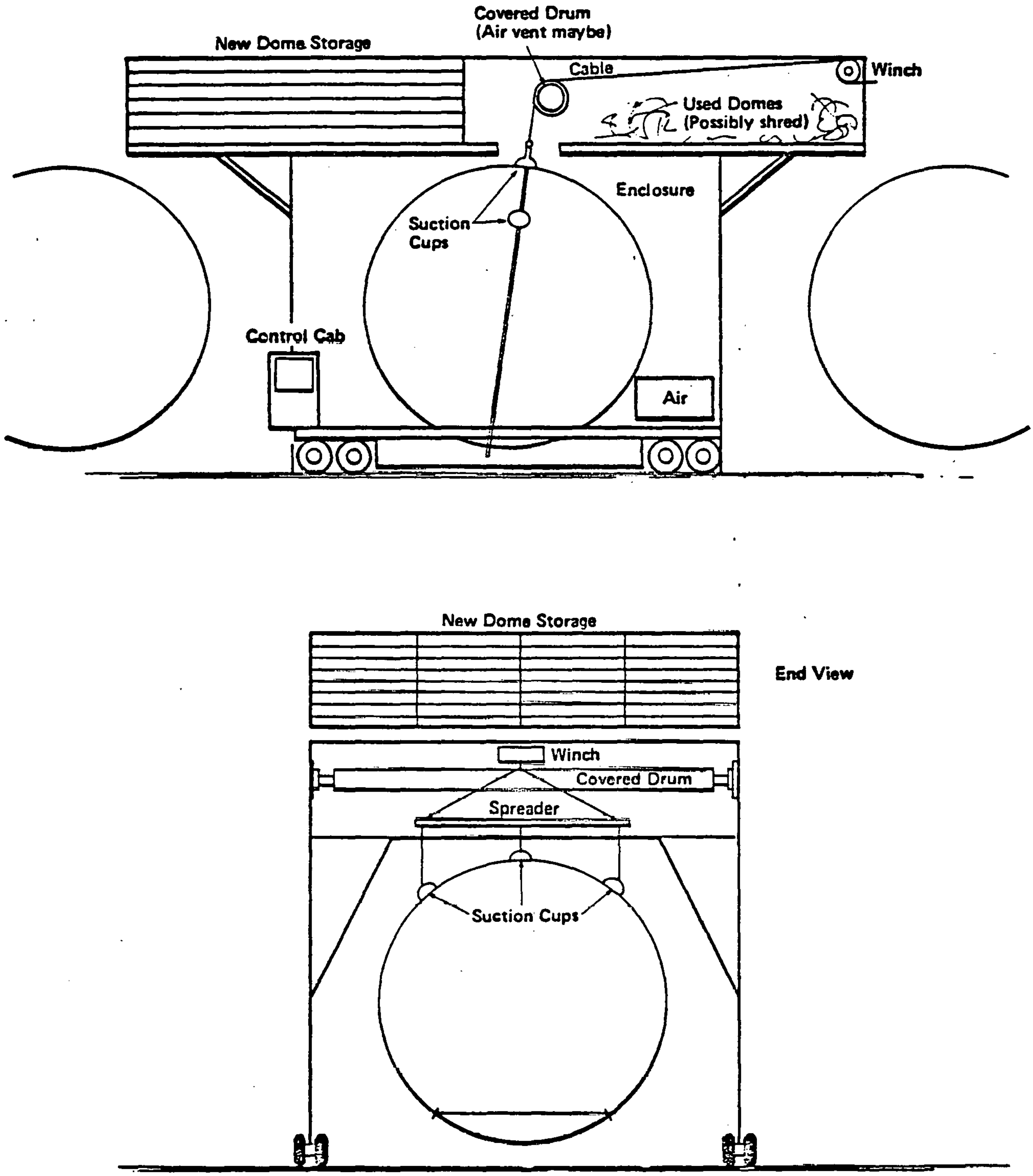

Figure 4.2-1 *Enclosure Replacement Facility*

a storage loft on top of the unit. A winch and roller system are used to move enclosures about. The enclosure is lifted with a multiple suction cup and spreader array attached to the winch cable. Used enclosures are compacted or shredded to minimize spacial requirements in the loft.

The time to position the mobile facility, remove old dome, install new dome and pressurize new dome are estimated to be 45 minutes with three men, or 2.25 manhours per dome. This leads to 56,250 manhours or about 30.6 manyears total for the replacement of 25,000 enclosures.

Analysis shows that two such machines with three men would complete the effort in about five years. Increasing the numbers of machines provides no particular advantage and does increase capital costs.

Cost estimation of machines is in progress and will be provided in the final report.

4.3 REFLECTOR CLEANING AND REPLACEMENT

The enclosure design provides for near zero air leakage. A flow rate of 0.0006 m^3/min (0.2 cfm) is predicted. An analysis of the particulate contamination transport into the enclosure and the subsequent selection of ultra-high quality filtration provides assurance that reflectance losses will remain $<5\%$ in 30 years. (See Reference 4.3-1). If the reflectance loss after 15 years has reached an unacceptable amount, cleaning of reflectors can be accomplished during enclosure replacement operations. Experience gained during the previous research showed that distilled water rinse, pressurized water spray and air wash all provided considerable cleaning effect. An approach that would require further research to resisting dust accumulation and repulsion of existing dust is the application of a high voltage bias of the proper polarity to the reflector.

4.4 GIMBAL ASSEMBLY MAINTENANCE

An ultimate design goal is to eliminate the requirement to enter the heliostat. Until a gimbal with sufficient MTBF has been designed, we have made provisions for access and a means for maintaining the gimbal.

Maintenance of the gimbal assembly will be performed by removal of the unit, replacement and then repair of the malfunctioning unit at the maintenance depot. Figure 4.4-1 shows the tool used to support the reflector while the exchange takes place. The tool simply grips the pedestal directly below the gimbal, supports the reflector by its spokes near the center hub and lifts the reflector upward a fraction of an inch when support arms are rotated to an off-center lock position. The fasteners at both interfaces have been loosened several turns prior to the lifting step. Removal and replacement of the gimbal is now accomplished.
Cost and technical trades toward increasing MTBF's are underway. Elimination of the shaft encoders or use of synchro positional transducers are being considered for potential improvements in both unit cost and failure rate.

Encoder lamps have been identified as low MTBF components and a scheme to increase life by derating lamp voltage is under investigation. The effect on the MTBF was not yet determined at the time of this report.

Access into the enclosure is anticipated to be minimal. This is expected to occur on cycles of several years and is for unscheduled maintenance. Access to the gimbal and the heliostat controllers for failures are the only required entries. Figure 4.4-2 illustrates the heliostat maintenance van. The van is equipped to assist during gimbal maintenance, heliostat controller replacement and enclosure repairs. The cargo section is sealed and equipped with a blower for pressurization. The rear entry is equipped with an air bag that can be extended and connected to the heliostat base door penetration. When the cargo section and air bag are pressurized to 0.067 N/cm^2 (0.1 psi) the door can be removed for access to the heliostat electronics mounted on the door or gimbal maintenance performed via the boom/ladder apparatus. The van is equipped with an extension boom and ladder as shown in Figure 4.4-2 that allows the worker to enter and climb up to the gimbal without any contact with the enclosure, base shell, or pedestal. The vehicle is a standard utility van with modifications to make it roughly airtight, blower unit w/filter, hydraulic controlled extension boom, 8-10 foot extension ladder with special attachment fittings, and possibly some ballasting and suspension stiffening. A preliminary estimate for two to three units, at a cost of $10,000 to $15,000 each, has been made.

Figure 4.4-1 *Gimbal Removal Tool*

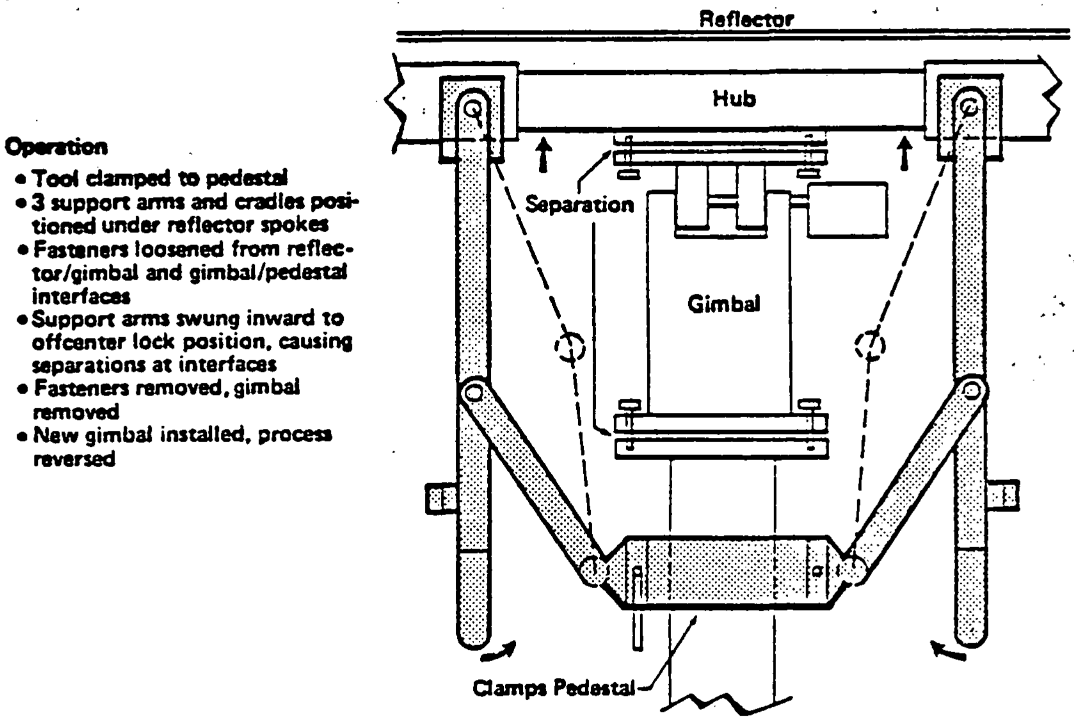

Figure 4.4-2 *Heliostat Maintenance Van*

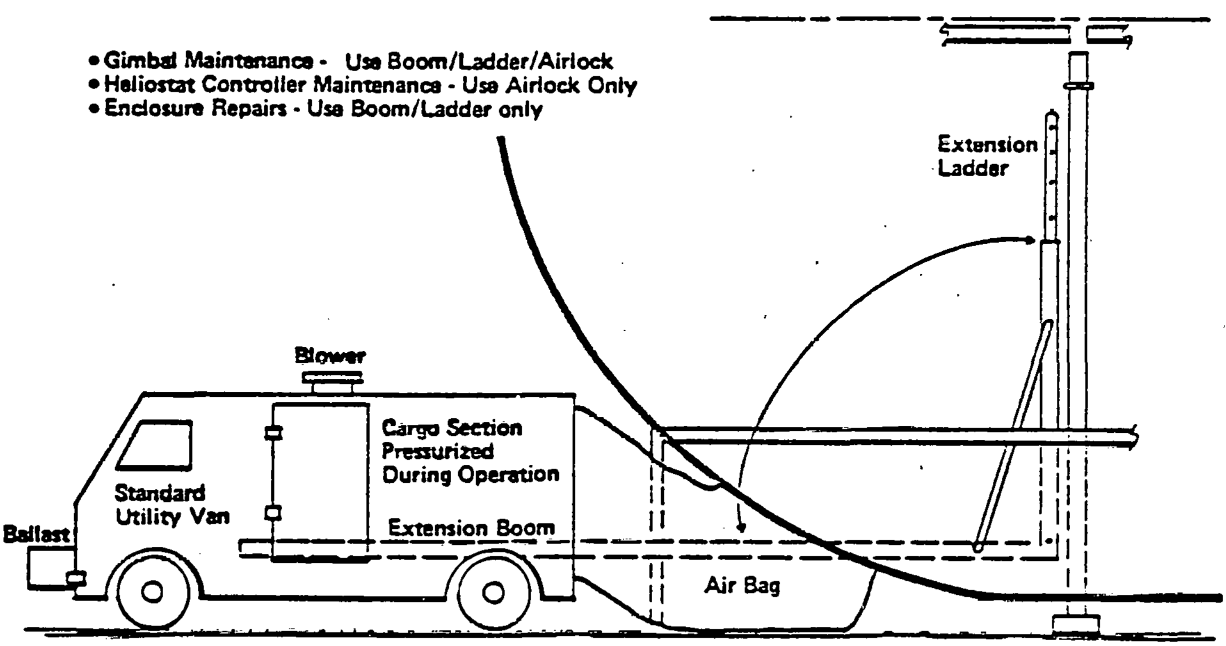

4.5 CONTROL SYSTEM MAINTENANCE

A cost trade study is being performed to assess the possibility of increasing electronic component MTBF's. The heliostat controllers are of particular interest by virtue of their large number. Table 4.5-1 lists components of the heliostat controller, the failure rates determined in previous work and failure rates recently determined for higher quality equivalent components. As can be seen, the net effect is an overall failure rate decrease of 26 failures per million operating hours (MTBF improvement of 16.2 yrs.) is realized. The improvement is at a cost which must be traded off against labor savings.

A study was made to determine whether the heliostat controller should be placed inside the enclosure with minimal packaging or outside the enclosure with weather-proof packaging and forced cooling provision. Inside placement would rely upon natural convection cooling. To perform this analysis, the costs associated with the outside packaging and cooling blower had to be traded against the added labor costs due to opening and entering the enclosure. By mounting the controller on the inside of the base door and utilizing the maintenance van airlock system described earlier, it was found that the time for removal was only slightly greater than for removing the components from an outside mounted weather-tight sealed box. The cost of the weather-tight sealed box would outweigh the few minutes labor savings, especially in view of the low number of replacement operations performed over the plant life (between 1 and 8 in 30 years).

4.6 AIR SUPPLY MAINTENANCE

Because of the near zero leakage enclosure design and the subsequent low filter loading, filter replacement is calculated to be required on an annual basis for the pre-filter and once during plant life for the primary filter. These filter replacement intervals are based upon the contamination analysis described in Appendix C.

Final selection of the pressurization blower will be made soon. Air bearings or other long life bearings have been proposed by suppliers to attain the

TABLE 4.5-1

FAILURE RATE/MTBF HELIOSTAT CONTROLLER

COMPONENT	NO. REQ.	COMMERCIAL PARTS: PART NUMBER	COMMERCIAL PARTS: FAILURE RATE X10^{-6} (F/MOH) EACH	COMMERCIAL PARTS: FAILURE RATE TOTAL RATE X10^{-6} (F/MOH)	HIGH RELIABILITY PARTS: PART #	HIGH RELIABILITY PARTS: FAILURE RATE X10^{-6} EACH	HIGH RELIABILITY PARTS: FAILURE RATE TOTAL	SOURCE OF INFORMATION
Integrated Circuits	12	CD4000 AD	.145	1.74	M98510/05503BEX	.036	.472	(1) B-1
Integrated Circuits	5	SN 5400	.145	.725	MS8510/00302BCB	.0185	.0925	(1) 206,B-1 Q
Capacitor-Ceramic	13	CK	.22	2.86	M39014/01-13--	.00013	.002	(1) 411,C-2-4
Capacitor-Electrolytic	2	CE	.41	.82	M39003/01-2977	.002	.004	(1) 401,C-2-6
Resistor	1	RN	.017	.017	-	-	.017	
Resistor	75	RC	.01	.75	-	-	.75	
Transformer	1	182-11380-2	.066	.066	-	-	.066	
Inductors - Filter	2	P53-4, -10	.063	.126	-	-	.126	
Zener - Diode	4	IN971B,IN746A	.8	3.2	Like JANTXIN78286	.03	.12	
Voltage Comparator	2	LM 111	.24	.48	-	-	.48	
Triac	1	T2300B	.8	.8	-	-	.8	
Diac	1	D32024	.8	.8	-	-	.8	
Transistor	8	B0278	.9	7.2	JANTX2N3741	.006	.048	(1) 309,C-5
Crystal OSC	1	20A0111	.2	.2	-	-	.2	
Relay	1	1A012	.6	.6	-	-	.6	
*Switch	1	PIP-8	.57	.57	-	-	.57	
Micro Processor	4	8000 Series	.2	.8	-	-	.8	
Power Supplies	2	-	5.0	10.0	-	-	-	
Fuse	1	-	.1	.1	-	-	.1	
Power Supply	-	-	-	-	-	-	-	
Transformer	1	-	-	-	Similar to B-1 C & D	.1	.1	
Capacitor-Electrolytic	-	-	-	-	M39006/01-3037	.064	.195	
Capacitor-Ceramic	3	-	-	-	M39014/01-13--	.00013	.00039	
Transistor	1	-	-	-	JANTX2N3741	.012	.012	
Zener	1	-			JANTXIN38286	.03	.03	
Diodes	6	-				.03	.12	
Resistors	5	-				.017	.085	
	TOTAL FAILURE RATES			31.854			5.77	
	MTBF			3.59 Yrs.			19.8 Yrs.	

desired high blower MTBF. The additional costs of the higher quality bearings will be traded against the labor savings realized.

A cost and technical evaluation of a central air supply system for comparison against the individualized blower system is underway and near completion. This system would employ a central compressor station (or stations) with filtration and humidity control also centralized. The clean, dry air would be fed to the individual heliostats through a system of piping laid in the same trenches provided for power and signal wiring for the drive and control system. The low flow rate requirements make possible the use of small diameter and low-cost piping, which is the primary capital cost driver of such a system. The attractiveness of this system lies in the maintenance of a single large blower and filter facility instead of 25,000 individual blower/filters.

5.0 PHASE II PLANS

.1 INTRODUCTION

The Phase I contract statement of work requires that the Phase I Final Report contain a Phase II Plan. The Final Report is due June 30, 1978, with a preliminary draft submitted on June 1, 1978. To expedite the DOE planning for transition into Phase II, the contractor has been requested to provide preliminary planning information in this Interim Technical Report. Accordingly, a Phase II scope and schedule plan (costs submitted under separate cover) is included herein. The Final Technical Report Draft of June 1 will provide the detailed Phase II plan including recommendations for additional R&D which could achieve a significant cost/performance benefit.

This Phase II plan is structured to achieve maximum benefit in furtherance of solar collector development. The plan includes the fabrication of full sized heliostats with installation at the STTF for demonstration and evaluation. DOE/Sandia recommendations relative to this plan are solicited such that they may be incorporated into the Final Technical Report.

5.2 STATEMENT OF WORK

Task 1 PROTOTYPE HELIOSTAT DEVELOPMENT

Design Prepare detailed manufacturing drawings of the prototype test heliostat design to be fabricated in Phase II. This will be based on the commercial plant preliminary design developed during Phase I study. The prototype test heliostat will be highly representative of the commercial plant design. However, the base dish will be a welded assembly rather than a one-piece stretch-formed dish, and the enclosure will be gore seamed rather than thermoformed. Analysis will be performed to design a cost effective control system and software for demonstrating beam pointing accuracy through continuous tracking. Alternate designs may be developed for evaluation of selected components such as the enclosure-to-base attachment. An alternate variable tension reflector design will be developed for evaluating and optimizing gravity focus. The commercial plant heliostat design will be updated at the end of Phase II to incorporate all experience gained from manufacture, installation, testing, and maintenance of the prototype heliostats.

Tooling Development Fabricate special tooling required for manufacture of three (3) prototype heliostats plus two spare enclosures and reflectors. Within constraints of cost effectiveness, it is the intent that the prototype tooling demonstrate and verify techniques and processes to be employed with automated high production rate tooling. The exceptions are that tooling will not include a press for stretch-forming the dish and the tooling will be for gore seaming rather than thermoforming the enclosure.

Prototype Fabrication Three prototype full size heliostats will be manufactured. Two spare enclosures and reflectors will be fabricated. In addition, several components of alternate design may be fabricated for comparative evaluation of performance and cost effectiveness (such as the enclosure to base ring attachment fittings, enclosures of different materials, etc.).

Prototype Installation One prototype will be installed at the Boeing Space Center facilities at Kent, Washington. Two prototypes will be installed at the STTF at Albuquerque, New Mexico. Boeing will install the complete heliostat including foundation on a site selected by the DOE. The DOE will provide power to the heliostats, power to the field controller electronics, and the signal distribution cabling from the controller electronics to the heliostat. A small facility space for assembly of the heliostat base and reflector will be required from DOE near the STTF. The DOE will provide hardware and support personnel for alignment of the heliostats.

Prototype Heliostat Testing Boeing will perform testing to the DOE approved test plan. The DOE (STTF) personnel will provide test support and monitoring of the heliostats during the test phase. The STTF will provide test support equipment such as the target, image beam scanner, data acquisition system, etc.

Task 2 MANUFACTURING, DEPLOYMENT AND OPERATING PROCESSES

Develop preliminary designs for the automated tooling, manufacturing/assembly facility, installation equipment, and maintenance equipment. Analyze the manufacture, assembly, installation, and maintenance processes to establish labor hours. Definition of equipment and processes will be developed to sufficient detail to support credibility of cost estimates. These preliminary designs will be updated at the end of Phase II to incorporate the experience gained from manufacture, installation, test and maintenance of the prototype heliostats.

Task 3 COST ESTIMATES

The cost estimates from the Phase I study will be refined to incorporate:

1) the experience gained during prototype fabrication, assembly and installation.
2) the experience gained from the maintenance tests on prototype heliostats.
3) the analysis of the preliminary designs of manufacturing, assembly, installation and maintenance processes.
4) possible design changes that are found necessary, or desired on the basis of cost effectiveness, as a result of the prototype test experience.

Costs will be provided for all elements of the CBS and defined as facility, equipment, material and labor for both capital cost of heliostats and operation and maintenance of heliostats over a 30-year plant life.

An updated estimate of heliostat thermal power performance will be provided based on results of prototype test experience.

Task 4 PROGRAM MANAGEMENT AND REPORTING

Effective program management and controls will be employed. The management plan and controls (to be documented in the Phase I final report) will be similar to that of Phase I. The Integrated Management System (IMS) will continue to provide high visibility of program status. Monthly reports to the DOE/Sandia will include:

- Milestone Plan and Management Report
- Contract Management Summary Report
- Manpower Management Report
- Cost Management Report, and
- Technical Status Report

A detailed test plan will be submitted for DOE approval one month following ATP. An interim Technical Report will be submitted at the end of the eighth month. A Final Report Draft will be submitted for approval at the end of the fifteenth month. The final report will be submitted at the end of the sixteenth month. Five oral presentations will be scheduled throughout the program as follows:

First Oral - 1 month following ATP (Sandia Laboratories)
Review of Program Plan and Detailed Test Plan.

Second Oral - 3 months following ATP (BEC - Kent, WA)
Detail Design Review (DDR) of commercial heliostat design and of prototype test hardware.

Third Oral - 8 months following ATP (BEC - Kent, WA)
Review of Technical Progress and of Installation Readiness.

Fourth Oral - 12 months following ATP (STTF - Albuquerque)
Review of Technical Progress and Test Results

Fifth Oral - 15 months following ATP (BEC - Kent, WA)
Summary Review of Phase II results.

5.3 TOOLING AND EQUIPMENT DEVELOPMENT PLAN

It is the objective of the tooling development plan to demonstrate process feasibility and tooling capability for selected most critical manufacturing assembly processes. Prototype tooling will be developed and utilized in the construction of three prototype heliostats plus two spare enclosures and reflectors.

Two fluorocarbon and three oriented polyester enclosures will be fabricated and tested for comparative evaluation. The fluorocarbon gores will be heat sealed and the polyester gores will be bonded, thus requiring minor tooling modifications.

A Phase II test goal is to evaluate and optimize the focusing capability of the membrane reflector due to gravity sag of the stretched membrane. The image quality and focal lengths are a function of the membrane tension applied during bonding of the membrane to the structural ring. Accordingly, one test reflector will be fabricated with the capability of varying tension during optical image tests to establish an optimum tension for various focal lengths. The other reflectors will be of standard design but with values of tension optimized for the STTF range.

At this time the only critical process that needs to be proven to enable preliminary design of automated tooling is one-piece dome thermoforming. Ram-forming of tubular rings and electro-magnetic swaging of joints are proven processes. All manufacturing processes appear feasible. Fabrication of the prototype heliostats will demonstrate the process feasibility in all areas other than thermoforming of one piece enclosures.* Studies will be continued on alternate processes to optimize for economics of high rate production. An example is a trade between stretch-forming or spinning the base dish. This trade will also involve consideration of other materials such as fiberglas or impregnated fabric or plastic.

With processes as known, the major study effort is to define the automated tooling. The production flow and assembly plant layout will be prepared. The analysis of tooling rates will define the quantities of tooling required and factory man-loading. Two items of specialized equipment are significant in defining heliostat costs. These are:

1) the equipment for installing piling foundations in the field, and
2) the transporter which delivers the assembled heliostat from the assembly building and installs the heliostat on its foundations.

A conceptual design (see Figure 5.3-1) and evaluation of the automated machine for installing piling has been developed by The Truzillo Company.

* Expected to be pursued under a related Sandia contract.

A Phase II pull and shear stability test of installed piling will verify piling diameter and depth requirement in a typical desert soil. Test results will support the preliminary equipment design and evaluation of foundation costs.

A conceptual sketch of the heliostat transporter is shown in Figure 5.3-2. It is envisioned that this tooling will be used as an assembly jig during manufacture. At the last assembly station, the mobile tractor is attached, transports the heliostat to the site, and positions the heliostat on the foundation where the tie-down is completed. The fixture is then recycled to the assembly line. A preliminary design of this equipment will be prepared and industry expertise will be enlisted for design and costing support.

Prototype equipment will be developed to support washing/cleaning experiments on the prototype heliostats. A preliminary design of automated equipment for heliostat washing will be developed.

A prototype airlock for maintenance access will be fabricated to support the prototype heliostat testing. A preliminary design for commercial plant maintenance access will be developed based on the prototype experience.

The end product of the critical tooling and equipment development will be:

1) Preliminary designs of automated tooling and equipment for manufacture, assembly, installation, and maintenance at commercial plant production/installation rates.

2) Firm basis for cost estimates.

5.4 TEST PLAN

This section describes the individual tests planned in support of Phase II. The purpose of the test program is to provide data for detail design early in the program, verify component performance later on, and demonstrate heliostat performance near the end of Phase II.

5.4.1 Materials Tests

Acceptance tests will be performed on the enclosure and reflector materials as they are received from suppliers. Included will be optical (specular transmittance and specular reflectance) and mechanical (yield, ultimate, elongation and thickness) measurements of the materials at various positions along the delivered roll stock.

Materials coupons will periodically be withdrawn from the real-time and accelerated desert exposure tests initiated in Phase I for optical and mechanical testing in the laboratory. These tests are intended to assist in the prediction of material life.

5.4.2 Foundation Pile Test

Tensile and compression tests on a single foundation pile will be performed early in the program. Test data will be used to support design analysis. Tensile loading will be performed using a crane with a load cell in series. Dead weights will be used for compression loading. As load is applied deflection will be monitored.

5.4.3 Enclosure/Basewall Attachment Test

Prior to final design completion a section of the enclosure to basewall attachment will be fabricated with representative materials and several configurations. This attachment will be subjected to tensile loading, leakage measurement and general handling evaluation.

5.4.4 Reflector Structural Joint Test

Prior to final design completion, full scale tests on reflector structural joints will be performed. Included will be tensile and torsional testing of the electromagnetic swaged joints used at rim-to-spoke and spoke-to-hub connections.

5.4.5 Gimbal Mechanical Test

Tests will be conducted to evaluate gear lash, the orthoganality of the elevation and azimuth axes, and the thermal performance and survivability of the gimbal assembly. The gear lash and axis orthoganality tests will be used in assessing mechanical contribution to system pointing error.

5.4.6 Reflector Structural Dynamic Test

The natural frequency, simple mode shapes, and dynamic response from drive motor inputs will be measured on the reflector assembly which includes the reflector, pedestal and gimbal drive assembly. The reflector and pedestal will be instrumented with accelerometers. This test will be performed with the reflector installed inside the protective enclosure.

5.4.7 Heliostat Integration

All assemblies of the prototype heliostat will be assembled indoors in a large high bay. The build-up will be accomplished in a stepwise fashion for fit and clearance verifications. Handling, assembly and disassembly operations will be formulated and demonstrated here. Functional operation of the drive and control and air supply system will be performed. After satisfactory functional performance demonstration the heliostat will be relocated outside in a field at the Kent site for further testing.

5.4.8 Pressure and Leak Rate Test

The enclosure will be pressurized to design pressure and inspected for conformity to design configuration. A flow meter will be installed on the blower/filter inlet to measure flow and determine heliostat leakage.

Next, the enclosure pressure will gradually be increased until stresses in the dome film have reached the maximum design condition (TBD). The intent of this test is to verify survival under combined pressurization and maximum wind loading.

5.4.9 Control System Testing

Control system software will be developed during the first seven months of the contract. Hardware will also be fabricated by the 7th month. Bench testing of the control system will follow. This involves end-to-end verification using the developed software, computers, heliostat controller and a gimbal assembly. All modes of operation (not requiring sun) will be exercised and verified prior to installation in the Kent Test Site heliostat.

5.4.10 Alignment and Tracking Tests

The Kent site heliostat will be aligned by laser geodolite. All drive and control system manual and automatic control modes will be demonstrated.

The STTF heliostats alignment will be coordinated with STTF personnel and equipment. All control modes will be demonstrated. One of the two heliostats will be dedicated to an extended period of continuous tracking. Image scans would be taken throughout the full day, for several days periodically spaced over a two month period.

5.4.11 Optical Performance Tests at Kent Site

An optical scanner, consisting of a radiometer capable of translation in two axes in the vertical plane will be used to map the reflected image. This scanner will be located on the top or side of a high building near the heliostat. The iso-solar map provided by the scanner will be used to evaluate non-uniformities and gravity focusing effects. The variable tension reflector will be installed in the Kent heliostat and the effect of membrane tension on focal length will be evaluated.

5.4.12 Environmental Tests

Environmental effects will be monitored and recorded periodically. Included will be:

1) Enclosure and base ring deflection due to wind loading.

2) Critical component temperatures.

3) Inside and outside relative humidity and temperature.

4) Internal and external dust accumulation material samples will be periodically removed for laboratory evaluation of reflectance and transmissivity.

5.4.13 Maintenance Requirements and Cleaning Tests

Methods for washing the dome will be tested. A small array of spray nozzles will be fabricated and used to further define washing techniques, procedures and cleaning water requirements for a full scale washing facility. Maintenance experience will be documented for future use in development of procedures.

5.5 PHASE II SCHEDULE

The schedule chart (Figure 5.5-1) is a master schedule for accomplishing the Phase II effort.

The major features indicated by this schedule are:

1) Immediate order of required materials and purchased components for prototype heliostat fabrication.

2) Immediate start on design of tooling for manufacture of prototype heliostats.

3) Earliest possible installation of test heliostat at the Boeing, Kent facility to verify compatibility of interfaces and to prove-out installation/maintenance processes and test equipment.

4) Earliest possible installation of demonstration/test heliostats at at the STTF.

5) Sufficient total program time to accomplish the significant critical testing which will then influence the design update of the commercial heliostat and allow update, where necessary, of the tooling and equipment preliminary design.

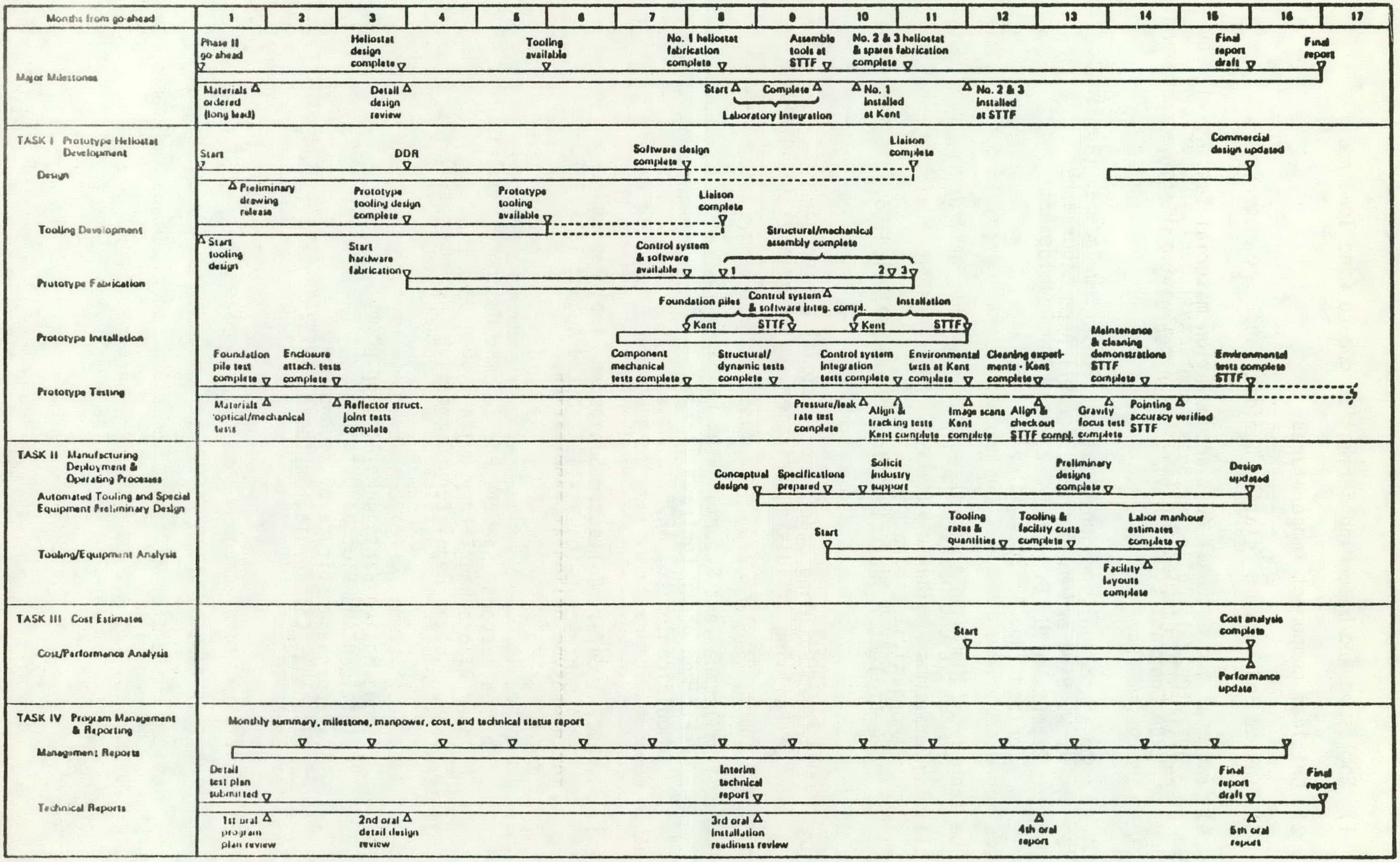

Figure 5.5-1. Phase II Master Schedule

6.0 REFERENCES

2.3.2.2-1 D277-10022-1, Collector Subsystem Detail Design Report, ERDA Contract E(04-3)-1111, Dated February 24, 1976.

2.3.2.3-1 Design Manual for Spherical Air Supported Radomes (Revised), W. W. Bird and M. Kamrass, Cornell Aero Laboratory Report No. U. B. - 909-D-2 Rome Air Development Contract No. AF 30 (602)-976.

2.3.2.3-2 Heliostat Enclosure Wind Tunnel Test Performed At The University Of Washington Aeronautical Laboratory (U.W.A.L.) See Collector Subsystem Final Report P.121.-135.

2.3.2.3-3 Uniform Building Code, International Conference Of Building Officials, Whittier, California, 1976 Edition.

2.3.2.3-4 Hailstone Test Report, dated February 15, 1978 Performed under Contract EY-76-C-03-1111 (Modification No. A006)

2.3.4.2-1 D277-10047-1, Collector Subsystem Final Report ERDA Contract E-(04-3)-1111, Dated August 15, 1977.

2.3.4.3-1 Design Response Spectra For Seismic Design Of Nuclear Power Plants Regulatory Guide 1.60 U. S. Nuclear Regulatory Commission, December 1973.

2.3.4.3-2 Strong Motion Earthquake Accelerograms; Digitized And Plotted Data; California Institute of Technology, Pasadena, California, September 197?.

APPENDIX A

GIMBAL ACTUATOR SPECIFICATIONS

APPLICATION

PART NUMBER	NEXT ASSY	USED ON	EFFECTIVITY	REV

SPECIFICATION CONTROL DRAWING

DIMENSIONS ARE IN INCHES EXCEPT AS NOTED	CONTR	THE BOEING COMPANY
	DR	CORPORATE OFFICES SEATTLE, WASHINGTON 98124
	CHK	
	STRUCT	GIMBAL/ACTUATOR ASSEMBLY
DWG ORIG BY	ENGR W S Davidson 1-24-78	
	GR	PROJ
CHANGE NO.		

SIZE	CODE IDENT NO.	
A	81205	277-10046
SCALE	REV	SHEET 1 of 16

D1 4600 3700 REV. 4/74

J16-047

1.0 SCOPE

1.1 Scope

This document delineates the design and performance requirements for a gimbal/drive mechanism to be used to support and orient a lightweight circular mirror assembly within a protective enclosure (see Figure 1.1-1). The entire assembly, called a heliostat, is an integral part of a Solar Electric Power Generation System, as shown in Figure 1.1-2.

1.2 Part Number

To Be Determined

2.0 APPLICABLE DOCUMENTS

The following documents form a part of this specification to the extent specified herein. Unless otherwise specified, the revision and issue in effect on date of invitation for bids or requests for proposals shall apply.

2.1 Specifications

None

Standards

None

Procedures

None

Drawings

277-10046 - Gimbal Actuator Interface 1/24/78

Publications

None

Copies of specifications, standards, procedures, and publications required by contractors in connection with specific procurement functions should be obtained from the procuring activity or as directed by the contracting officers.

USE FOR TYPEWRITTEN MATERIAL ONLY

SIZE	CODE IDENT. NO.	
A	81205	277-10046
SCALE	REV	SHEET 2

Elevation View

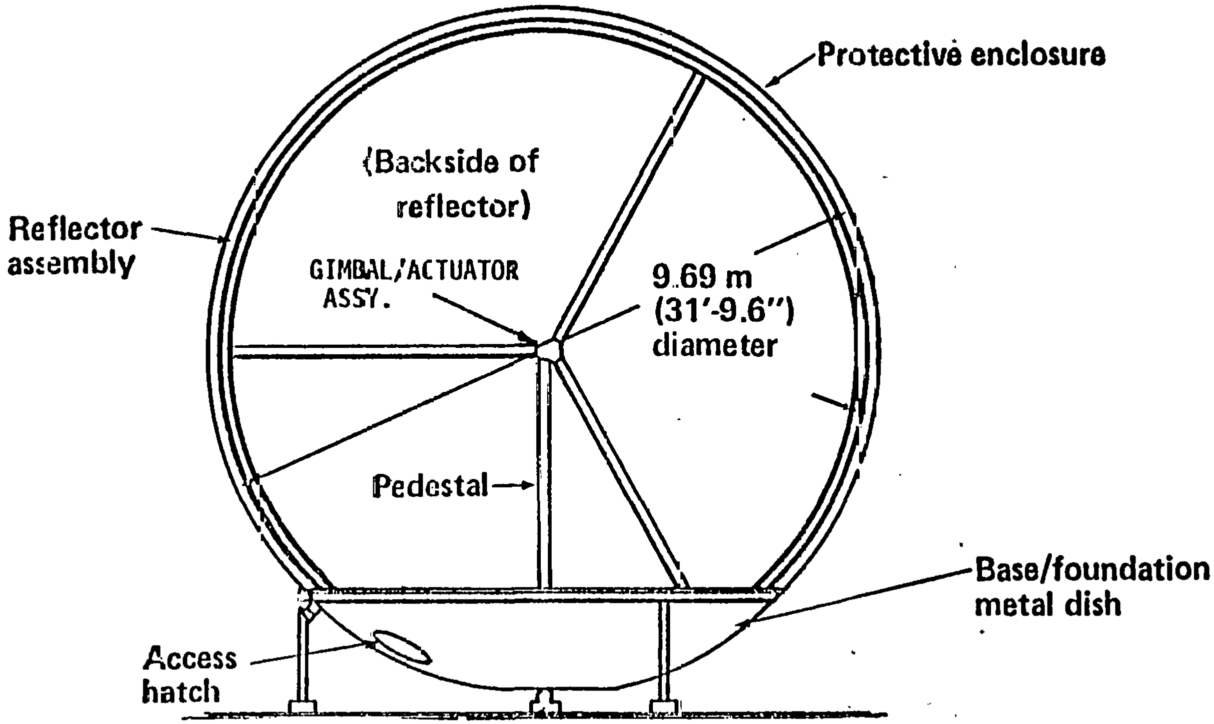

Figure 1.1-1 HELIOSTAT ASSEMBLY

USE FOR TYPEWRITTEN MATERIAL ONLY

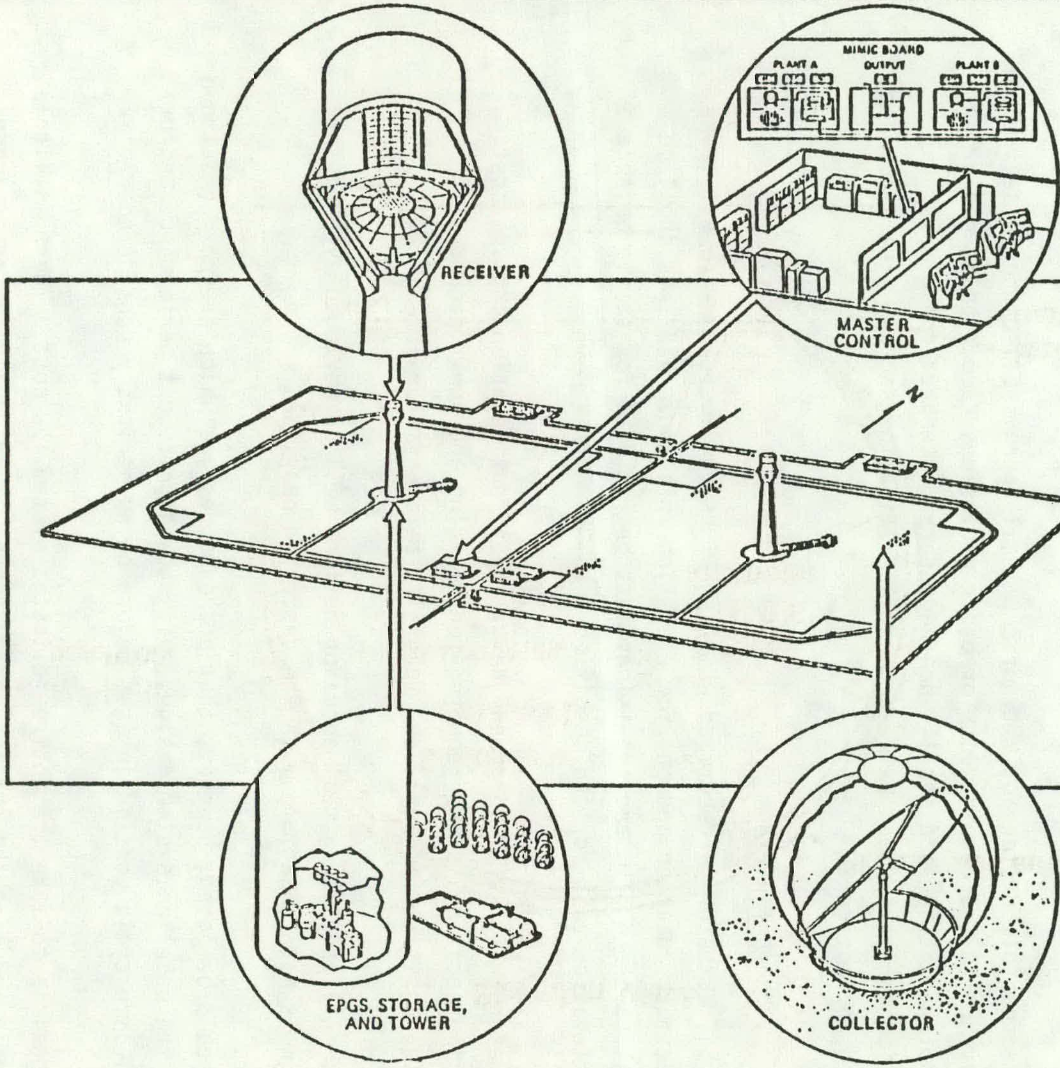

Figure 1.1-2 SOLAR ELECTRIC POWER PLANT (Typical)

SIZE A | CODE IDENT. NO. 81205 | 277-10046

SCALE | REV | SHEET 4

2.2 Other Publications

Occupational Safety & Health Administration Regulations

Metric Practice Guide, ASME Designation E380-74

Uniform Building Code

3.0 REQUIREMENTS

The responsible design activity of BEC shall approve all changes, deviations, or waivers to the requirements or other provisions specified herein prior to implementation, and shall, when necessary, interpret and clarify any conflicting requirement between their specification and any other document listed in Section 2.

3.1 Definition

A gimbal actuator is described which shall be configured in two axis, one for azimuth rotation and one for elevation rotation. One axis shall be normal to the other, and provisions must be included for static balance of the elevation axis for the specified load.

Parameters which will be given the greatest consideration include cost, pointing accuracy, power required for rotating and power required for holding position (if any), and mean time before failures.

Note: All proposed gimbal actuator designs will be reviewed even if the design is not compatible with the described baseline.

It should be noted, however, that proposed designs which are not compatible with the baseline system design, must show significant performance and/or total life cycle cost advantages before being seriously considered.

The goal is to make the entire heliostat system low cost. There is little value in reducing the cost of one component if an equal or greater amount must be spent on another part of the system to compensate.

3.1.1 Interface Definition

A baseline design has been developed for a heliostat/collector control system, including a gimbal/actuator assembly. The baseline design is described below and in Figure 3.1.1-1, so that prospective suppliers can understand in detail how the total system must function.

Orientation of each mirror is controlled by computer. Control signals are carried via data bus to an electronic assembly inside each protective enclosure, which then provides the necessary electrical signals to cause a multipole stepper motor with gear reduction to rotate (either direction). The stepper motor/gear reduction assembly (actuator) drives a 2 axis gimbal such that the reflected image from the sun falls on a pre-selected target.

The baseline heliostat control electronics interface is shown in Figure 3.1.1-2.

3.1.1.1 Load

As defined on 277-10046 Gimbal Actuator Interface Drawing

3.1.1.2 Pedestal Mount

Interface Optional

3.1.2 Major Component List

2 axis gimbal/actuator (end item)

1. gimbal assembly
2. actuator (2 required)
3. angular position inciding device (2 required)
4. cable assembly

3.2 Characteristics

3.2.1 Performance

3.2.1.1 Azimuth Rotation

Bi-directional, 360 degree maximum. See Figure 3.2.1.1-1

3.2.1.2 Elevation Rotation

Bi-directional, 182 degrees maximum. See Figure 3.2.1.2-1.

3.2.1.3 Angular Rate

Both axis, both directions. Minimum - zero degree per second.

Maximum - .14^{o} per second.

3.2.1.4 Pointing Angle Resolution *

Static and dynamic - equal to or better than .01125^{o}.

3.2.1.5 Pointing Angle Repeatability *

As required to meet requirements specified on 277-10046 Gimbal Actuator Interface Drawing.

3.2.1.6 Pointing Angle Accuracy (all position) *

Both axes - as defined on 277-10046 Gimbal Actuator Interface Drawing.

3.2.1.7 Backlash, both axes

As required to meet the requirements specified on 277-10046 Gimbal Actuator Interface Drawing.

3.2.1.8 Position Indicating Transducer

A position indicating device is required for each axis.

3.2.1.8.1 Total Angular Position

Total angular position - 360^{o}.

3.2.1.8.2 Pointing Angle Resolution

Equal to or better than .36^{o}.

* Assume base to be fixed (immovable).

3.2.1.8.3 Pointing Angle Repeatability

Equal to or better than ± .0167° (1σ).

3.2.1.8.4 Pointing Angle Accuracy

Static and dynamic equal to or better than .0167° (1σ).

3.2.1.8.5 Backlash

Must be less than .0017°.

3.2.1.8.6 Output

Optional - must interface with an electronic control assembly.

3.2.1.8.7 Reference Position

Each position indicating device shall provide for one reference position output.

NOTE: Reference output not required if the chosen position indicating device is an absolute shaft position encoder.

3.2.1.8.7.1 Location of Reference

Optional.

3.2.1.8.7.2 Resolution, Repeatability, Accuracy, Etc.

The requirements of paragraphs 3.2.1.8.2, .3, .4, .5, and .6 apply.

3.2.1.9 Limit Switches

Two limit switches are required for each axis. NOTE: Limit switches are not required if the chosen position indicating device is an absolute shaft position encoder.

USE FOR TYPEWRITTEN MATERIAL ONLY

SIZE	CODE IDENT. NO.	
A	81205	277-10046
SCALE	REV	SHEET 9

3.2.1.9.1 Limit Adjustment

Both limits on each axis shall be adjustable throughout the full range of gimbal travel as specified in paragraphs 3.2.1.1 and 3.2.1.2.

3.2.2 Physical Characteristics

3.2.2.1 Orthogonality (Baseline)

The two gimbal axes shall be orthogonal to within $.001^o$ for the entire rotational range of each axis. The azimuth axis shall be vertical and perpendicular to the plane of the pedestal interface within 0.1 degrees.

3.2.2.2 Stiffness

Reverse impedance of the reflector-gimbal assembly about either drive axis shall be such that under no circumstances will resonance be encountered when the gimbal drive rate is varied from 0 to 6 .01125 degree movements per second.

3.2.2.3 Electrical Cabling

An electrical cable "pigtail" including connectors shall be supplied with the gimbal/actuator assembly. Provisions shall be made for all electrical functions.

3.2.2.3.1 Length

Approximately 30 feet.

3.2.2.3.2 Connectors

"DIP" type connectors or an approved equivalent shall be installed on the cable pigtail.

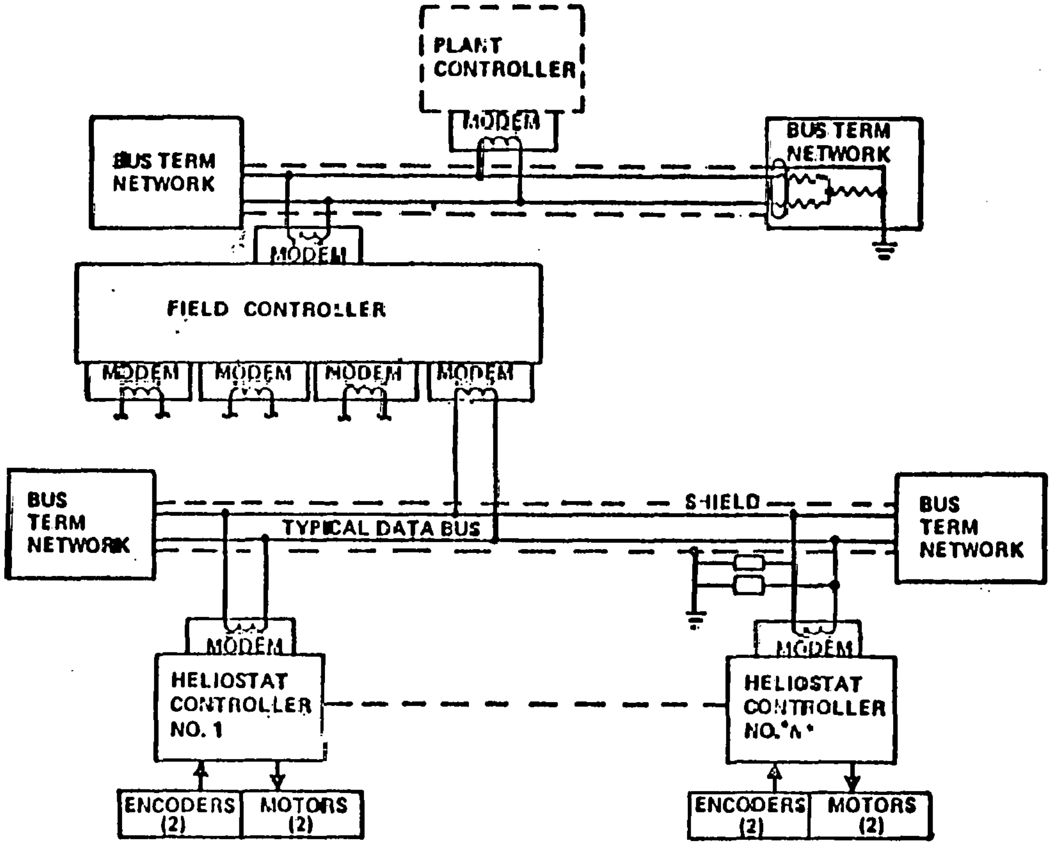

Figure 3.1.1-1 BLOCK DIAGRAM - BASELINE HELIOSTAT CONTROL SYSTEM

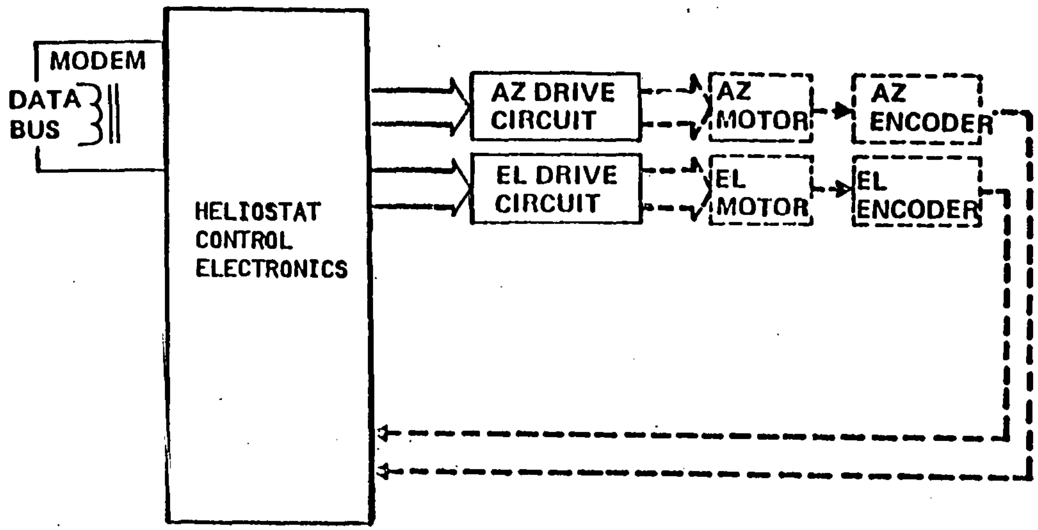

Figure 3.1.1-2 BASELINE INTERFACE DEFINITION

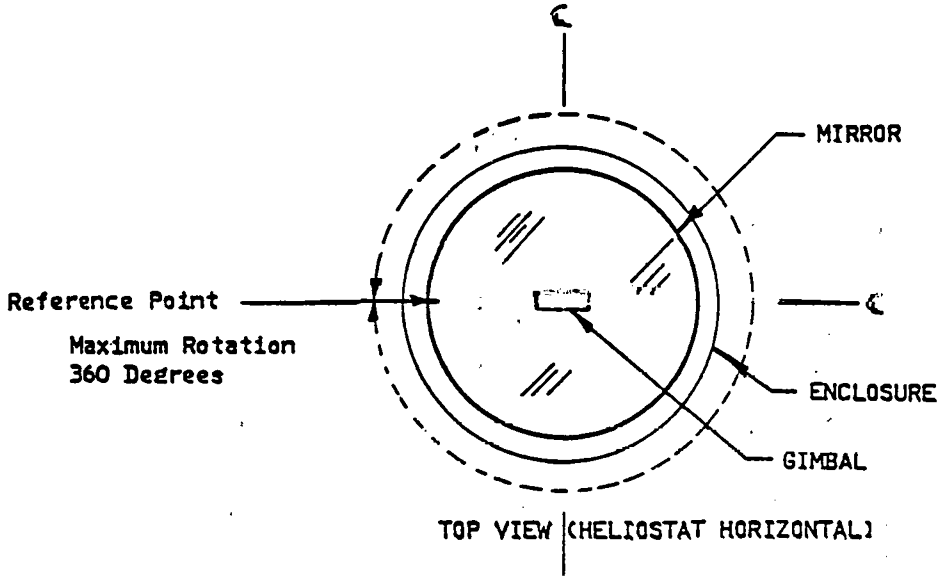

Figure 3.2.1.1-1 AZIMUTH ROTATION REQUIREMENTS

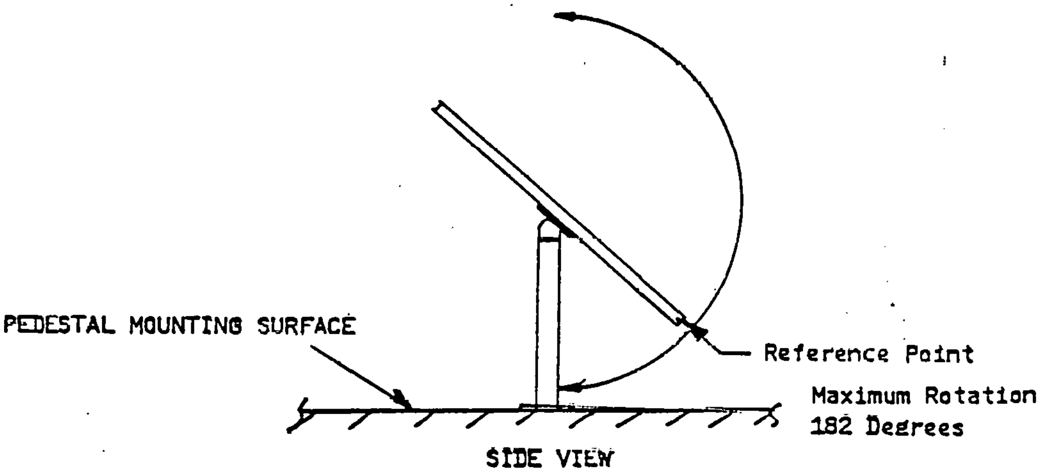

Figure 3.2.1.2-1 ELEVATION ROTATION REQUIREMENTS

SIZE	CODE IDENT. NO.	
A	81205	277-10046
SCALE NONE	REV	SHEET 13

3.2.2.3.3 Wire

Optional, providing all other requirements of this specification are met.

3.2.2.4 Lubricant Leakage

Leakage of lubricants, etc., from the assembly shall be less than that required to form drops.

3.2.3 Reliability/Lifetime

The useful lifetime of the assembly, with normal maintenance shall be equal to or greater than 30 years. Mean time before failure goal shall be 15 years when operated as described in Paragraphs 1.1 and 3.1.

3.2.4 Maintainability

A minimum of specialized tools and equipment shall be required for installation, alignment, and service of the gimbal actuator assembly unless it can be shown that total life cycle costs are reduced if special tools or equipment are used.

3.2.4.1 Actuator Replacement

The azimuth or elevation actuator shall be capable of being replaced in a minimum of time without removing the load from the gimbal assembly.

3.2.5 Environment

The assembly shall be installed within an air inflated plastic enclosure as described in paragraph 1.1, typically in a Southwestern U. S. location.

3.2.5.1 Ambient Temperature

3.2.5.1.1 Operating

-20° to $+150^{\circ}$F.

3.2.5.1.2 Non-Operating

-30° to $+150^{\circ}$F.

3.2.5.2 Temperature Cycling

The assembly shall not be damaged nor it's performance impaired by exposure to gradually applied temperatures as specified in Paragraph 3.2.5.1.1.

3.2.5.3 Moisture Resistance

The assembly shall not be damaged nor shall it's performance be impaired when subjected to a humidity of up to 95% relative.

3.2.5.4 Dust

The assembly shall not be damaged nor shall it's performance be impaired when operated in an enclosure as defined by paragraph 1.1. The pressurizing air is filtered in order to keep the dust to a minimum.

3.2.5.5 Earthquake

While operating with the load installed as specified 277-10046, Gimbal Actuator Interface Drawing, the assembly shall not be damaged as a result of earthquake activity as defined for seismic zone 3 in the Uniform Building Code.

3.3 Design & Construction

3.3.1 Materials

Optional

3.3.2 Workmanship

Shall be consistent with standard industry practices.

4.0 QUALITY ASSURANCE PROVISION

As required by the purchase order.

5.0 PROOF OF PERFORMANCE TESTING

As required by the purchase order.

USE FOR TYPEWRITTEN MATERIAL ONLY

1. THE ELEVATION AXIS AND AZIMUTH AXIS SHALL BE ORTHOGONAL WITHIN ±.001°
2. INTERFACE MOUNTING SHALL BE MUTUALLY AGREED UPON BETWEEN BOEING AND VENDOR.
3. POINTING AXIS IS NORMAL TO THE THEORETICAL PLANE OF THE REFLECTOR. 3
4. THE THEORETICAL PLANE OF THE REFLECTOR IS ESTABLISHED BY THE POINTING AXIS, ELEVATION AXIS AND A THIRD MUTUALLY PERPENDICULAR AXIS IN THE THEORETICAL REFLECTOR PLANE.

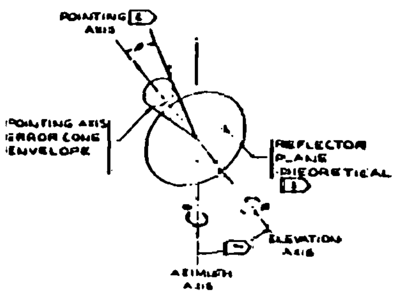

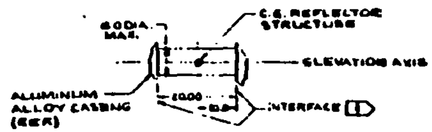

VIEW A-A

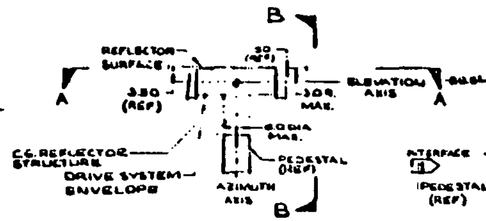

ELEV. VIEW
DRIVE SYSTEM ENVELOPE

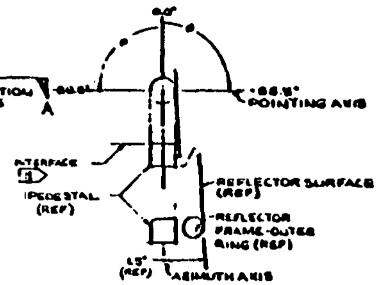

VIEW B-B

DRIVE SYSTEM ERROR ALLOWABLES			
OUTPUT ERROR SOURCE	ERROR CONE ANGLE "α" (deg)		
	3σ (99.73%)	2σ (95.4%)	1σ (68.27%)
"POINTING AXIS" *STATIC *DYNAMIC	.02 —	— —	— .02

[illegible] ≥ .14 [illegible]

* FOR ALL SPECIFIED ORIENTATIONS OF α AND β

TABLE 1

REFLECTOR STRUCTURE PARAMETERS	
WEIGHT: 240 POUNDS	
MOMENT OF INERTIA;	
ABOUT ELEVATION AXIS	I = 8,200. lb-sec²/in @ 0° ≤ α ≤ 360°
ABOUT AZIMUTH AXIS	I = 16,200. lb-sec²/in @ β = 0.0°
	I = 11,800. lb-sec²/in @ β = ±45°
	I = 8,200. lb-sec²/in @ β = ±89.5°
AIR MASS INERTIA	I = 3700. lb-sec²/in @ β = 180°[illegible]

TABLE 2

THE BOEING COMPANY

GIMBLE ACTUATOR INTERFACE

D 81205 277-10047

APPENDIX B

AUGERCAST PILE STUDY

Turzillo™
LEE TURZILLO CONTRACTING COMPANY
P. O. BOX 155 • BRECKSVILLE, OHIO 44141 • TELEPHONE 216/659-3141 • TWX 810-427-9101
"Our Experience Makes The Difference"™

February 22, 1978

Boeing Engineering and Construction
P.O. Box 3707
Seattle, Washington 98124

Attention: Mr. Doug McDonald

Subject: AUGERCAST® Piles, Heliostat Foundations

Gentlemen:

In accordance with your request at a meeting with Mr. L. J. Koss and the writer of the Lee Turzillo Contracting Company we are enclosing the following information, which I trust will answer the questions that you put forth regarding the above referenced job.

(1) We are enclosing copies of our design for required reinforcement to accommodate the design criteria that you furnished to us.

(2) We are enclosing conceptual drawings showing the grout plant for the automated equipment for the above referenced project and our drawing for the pile rig or drilling rig for the pile installation for an automated basis for the above referenced job.

(3) The time required to design, develop and fabricate these two prototype machines referenced above we estimate to be nine months.

(4) The cost of development and prototype demonstration for said equipment we estimate to be $500,000.

(5) The estimate of installation rate that could be achieved by the equipment is 40 pads per 8 hour day per rig unit.

(6) The quantity of automated equipment required to support the installation rate of 15 heliostats per hour is three rig units; the quantity of equipment required to support the installation rate of 70 heliostats per hour is 14 rig units; and the quantity of equipment required to support the installation rate of 450 heliostats per hour is 90 rig units. This is in accordance with the format of your Table I.

HOME OFFICE: 3351 BRECKSVILLE ROAD • RICHFIELD, OHIO 44286
ATLANTA • BALTIMORE • CHICAGO • DETROIT • FT LAUDERDALE • HOUSTON • JACKSONVILLE • MINNEAPOLIS • OMAHA • SEATTLE • TORONTO

LEE TURZILLO CONTRACTING COMPANY

The replacement life for the basis of 15 heliostats installed per hour over the life span of 30 years for the job would require the replacement of 18 rig units; the replacement life predicated on the installation rate of 70 heliostats per hour for a life span of 30 years would require 126 replacement units; and the life span of replacement predicated on the installation of 450 heliostats per hour over the 30 years period would require 1,080 replacement units.

(7) Our estimate of unit cost of equipment for quantities required at the three indicated installation rates, including spares and refurbishment is as follows:

> $8,460,000 would be required for the installation rate of 15 heliostats installed per hour; $59,220,000 would be required to maintain the installation rate of 70 heliostats per hour; $507,600,000 would be required to maintain the installation rate of 450 heliostats per hour, over the life span of 30 years.

(8) Our estimate of the current foundation costs, materials and labor, per heliostat, is $335.00 each. This estimate is predicated on a foundation of four piles per heliostat at present material and production costs.

I trust the information set forth will meet with your requirements and if you need any added refinement or additional assistance, kindly do not hesitate to contact the writer.

Very truly yours,

LEE TURZILLO CONTRACTING COMPANY

H. Bachmeier

H. Bachmeier, Regional Manager

HB:h
Enclosures

APPENDIX C

ANALYSIS OF AIR FILTRATION

THE BOEING COMPANY.

LABORATORY REPORT

NO. 2-4809-0001-048

Purpose ______ Model ______ Date 2-9-78

To: Roger Gillette M/S 8K-20 Org'n. K-6160 Part No. ______

Subject: Model for Predicted Light Scattering as a Result of Dust Accumulation

Source Heliostat Program Reinsp. Req. ______

Purchase Order ______ R.R. ______ Date Rec'd. ______ Quan. ______ Acc. ______ Rej. ______

Material ______ Spec. ______

☐ Chem. Lab. ______ ☐ Sonic ______ ☐ Met. Lab. ______ ☐ Mechanical ______

☐ X-Ray ______ ☐ Mag/Penetrant ______ ☒ Particle Identification Laboratory

Reference: C.C. to:

D277-10046-1, Volume #1, Technical Proposal
Solar Central Receiver Prototype Heliostat, July 15, 1977
(Other technical references at end of report)

SUMMARY: The task of this assignment was to determine make-up air filtration requirements for a heliostat unit in Arizona such that dust accumulated on the reflector surface over the proposed 15 year life cycle would not degrade reflective efficiency by more that 5%. There were three separate problems associated with this task:

1. A mathematical model of the dust accumulation rates for the reflector had to be prepared,

2. A model for relating dust accumulated on a surface to light scattering efficiency was needed, and

3. A filtration system which was inexpensive but could handle both the loading and the high efficiency requirements for the make-up air had to be selected.

A full mathematical model for the dust accumulation rates was outside the scope/budget requirements but a simplified model was constructed and used to determine essential system requirements. This model indicates that most of the airborne dust in the dome would sediment out in the first 24 hours of operation. Following that period, the dust in the air would be from the make-up air or resuspended dust from the lower part of the dome.

By minimizing air flow velecities the amount of resuspended dust can be minimized. Figure #1 in the following report indicates the areas of the dome that will deposit particles of a given size range on the reflector surface in eight hours.

The relationship between particle diameter and light scattering efficiencies is indicated by figure #2 in the following report. It can be seen that the critical size range is from 0.1μm to 1.0μm diameter particles. Most of these particles sediment from a height of not more than 128 cm above the surface of the reflector. (1σ from the mean radius of the small particle log normal mode of r = .2 um).

Prepared by E.R. Crutcher (signature) Approved by R. H. LeDoux (signature) Org'n. 2-4809

E.R. Crutcher R. H. LeDoux

DO 5000 2100 ORIG. 3/71

This reduced sedimentation volume was still large enough to collect particulate from the total volume, including all make-up air, over the 15 year life of the reflector. For these reasons it is important to keep the total airborne particulate levels low for the make-up air.

The filtration system recommended consists of a Gelman Type E/8" x 10" glass prefilter followed by a Gelman Acropor pore size 0.45 µm 8" x 10" filter or their equivalence. The Type E prefilter is a depth filter which will tolerate high loading (up to a gram of material). It is relatively efficient collecting approximately 99.7% of the total mass of airborne particulate. The acropor filter following the prefilter stops 99.99% of the particulate remaining. Assuming the filters were directly exposed to the atmosphere they would remove the particulate from 45,000 m^3 of air. Using the peak monthly average for Phoenix of 300 $\mu g/m^3$ as one extreme and the minimum monthly average for the Grand Canyon of 20 $\mu g/m^3$ for the other the following loadings would result:

Prefilter	Loading in 15 Years	Result
a. 300 $\mu g/m^3$	13.46 grams	Yearly change of filter
b. 20 $\mu g/m^3$	.9 grams	15 year life
Membrane		
300 $\mu g/m^3$	.04 grams	15 year life
20 $\mu g/m^3$	.003 grams	15 year life

With some intake air impingement both filters should last for the full 15 years.

Less than 5% loss of reflector efficiency can be expected due to external sources of particulate with this filtration system and a make-up flow rate not significantly exceeding 0.5 cfm. The interior of the dome, representing 1% of the total air exposure for the reflector will carry 99.99% of the particulate exposed to the reflector surface. An initial rest period after installing the reflector of 48 hours with the reflector stored in a vertical position should minimize the effect of this original particle burden.

(NOTE: Leaks will function as concave impactor orifices. This will result in a local accumulation of dust on the surface near the leak. The accumulation of dust at a point can be used to locate leaks and to act as a "typical" dust collection to evaluate the types of dust in the dome environment (i.e., wear metal from reflector rotation machinery, external dusts, etc.)

U.S. GOVERNMENT PRINTING OFFICE: 1980—640-258/1497